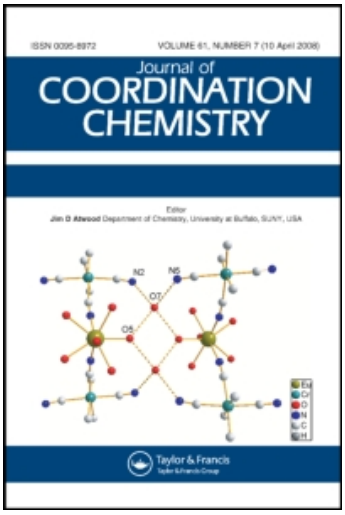

Journal of Coordination Chemistry
Publication details, including instructions for authors and subscription information:
http://www.informaworld.com/smpp/title~content=t713455674

THERMODYNAMIC AND STRUCTURAL STUDIES OF METAL COMPLEXES IN VARIOUS SOLVENTS

Shin-Ichi Ishiguro[a]; Hitoshi Ohtaki[a]
[a] Department of Electronic Chemistry, Tokyo Institute of Technology, Nagatsuta, Japan

To cite this Article Ishiguro, Shin-Ichi and Ohtaki, Hitoshi(1987) 'THERMODYNAMIC AND STRUCTURAL STUDIES OF METAL COMPLEXES IN VARIOUS SOLVENTS', Journal of Coordination Chemistry, 15: 3, 237 — 306
To link to this Article: DOI: 10.1080/00958978708081657
URL: http://dx.doi.org/10.1080/00958978708081657

J. Coord. Chem. 1987, Vol. 15. p. 237–306
Photocopying permitted by license only

THERMODYNAMIC AND STRUCTURAL STUDIES OF METAL COMPLEXES IN VARIOUS SOLVENTS

SHIN-ICHI ISHIGURO and HITOSHI OHTAKI†

Department of Electronic Chemistry, Tokyo Institute of Technology at Nagatsuta, Japan

Complexation of various metal-ligand systems has been discussed from the view-point of solute-solvent and solvent-solvent interactions in pure solvents and their mixtures on the basis of thermodynamic and structural measurements. In water and dioxane-water mixtures, it was suggested that the solvation structure in the secondary shell of ionic species significantly changes by adding dioxane to water due to the formation dioxane-water associates in the bulk. It was found that 1,10-phenanthroline formed its stacked species, such as $[H(phen)_2]^+$ and $(phen)_2$, in water, but the species hydrophobically associated disappeared in dioxane-water mixtures due to breaking of the hydrogen-bonded structure of water. Complexation of Zn(II), Cd(II) and Hg(II) ions with SCN^- ions in water was discussed in relation to the structures of the complexes determined by X-ray diffraction, and NMR and Raman spectral measurements. The solvent effect on the complexation of Cu(II) with chloride ions in acetonitrile, *N,N*-dimethylformamide and their mixtures was found to be remarkable, which was well explained in terms of preferential solvation of *N,N*-dimethylformamide, i.e., the formation of $[Cu(dmf^n)]^{2+}$ (n = 1–6), in acetonitrile.

Key words: Thermodynamics, structure of metal complexes, nonaqueous solvents, 1,10-phenanthroline, thiocyanato complexes, enthalpy of transfer on ions, copper(II) chloro complexes, solvation of ions, calorimetry potentiometry, spectrophotometry, x-ray diffraction, Raman spectroscopy.

INTRODUCTION

Complex formation reactions of metal ions in solution are significantly influenced by solvents employed, and solvent effects on complex formation reactions are caused by changes in solvation of metal ions, ligands and their complexes in different solvents. Therefore, solvation phenomena of relevant species must be thoroughly investigated when considering complex formation reactions in various solvents.

Knowledge of intrinsic solute-solute interactions as well as solute-solvent ones is greatly useful to elucidate roles of solvents on solvation and reactions of ions. With this point of view, protonation reactions of various organic compounds have been studied and acidities and basicities of various organic ligands have been determined in the gas phase in the last decade.[1] For example, the acidity of carboxylic acids increases with increasing number of methylene groups within the acids in the gas phase. However, it is well known that the acidity of carboxylic acids decreases with the length of the methylene chain in aqueous solution. The larger the aliphatic group of a deprotonated carboxylic acid, the more its alkyl group is polarized and thus the base is more stabilized in the gas phase, which leads to a higher acidity of the acid in this gas phase. On the contrary, a carboxylate anion with a larger aliphatic group that is polarizable is more weakly solvated with water and thus less stable in aqueous solution. Consequently, the larger the aliphatic group of an acid, the less the acidity of the acid in water. The fact clearly indicates the importance of solvation of substances on considering the nature of their acidity and basicity in a solution.

†Author for correspondence.

Among various physicochemical properties of solvents, donor and acceptor properties have been pointed out to play the most important role for solvation phenomena of ions.[2] Strengths of donor and acceptor properties of aprotic solvents are largely dependent on the structure of solvent molecules and interactions among them. An aprotic solvent with a higher donor property shows a higher affinity with metal ions. An example is seen in Gibbs energies (ΔG°_{solv}) and enthalpies (ΔH°_{solv}) of solvation of Hg^{2+} and Cd^{2+} in dimethyl sulfoxide and in water. These ions have more negative ΔG°_{solv} and ΔH°_{solv} values in the former solvent, which has a larger donor number (D_N), than in the latter,[3] although dimethyl sulfoxide has a lower dielectric constant than water. The reverse trend should be expected: solvents having a high acceptor property preferably solvate anions to cations.

Water has both relatively stronger donor and acceptor properties. Water molecules interact with each other to form a hydrogen-bonded structure.[4] Therefore, solvation of ions in water should be changed when the hydrogen-bonded structure would be broken.

In a mixed solvent consisting of two kinds of solvents with different donor and acceptor properties, ions are preferentially solvated with one solvent in the mixture.[5] The solvent composition in the vicinity of an ion is thus largely different from that in the bulk. The solvent composition in the solvation sphere of the ion varies in a complicated manner depending on the nature of the ion and solvents with varying composition of the solvents in the bulk. In aqueous organic mixtures, the hydrogen-bonded structure of water may be enhanced in a mixture with a hydrophobic solvent or weakened in a mixture with a hydrophilic solvent having a poor hydrogen-bonding property between them.

Recently ion-solvent and solvent-solvent interactions have been investigated by using thermodynamic, spectrophotometric and diffraction methods, and it becomes possible to discuss complex formation reactions of metal ions in relation to the structures of solvents, solvated metal ions and metal complexes in the liquid state.

Although it is impossible to obtain thermodynamic quantities for solvation of single ions by usual experimental methods, various attempts have been carried out to divide thermodynamic quantities of solvation of salts into those of each ionic component by employing conventional (extrathermodynamic) assumptions.[6] Gibbs energies, enthalpies and entropies of solution of salts have been determined in various solvents, the difference of these quantities in a solvent from those in a reference solvent being defined as the corresponding thermodynamic quantities of transfer of the salts. By using an extrathermodynamic assumption, thermodynamic quantities of transfer of salts were divided into each ionic component, and Gibbs energies, enthalpies and entropies of transfer of various cations and anions from water to a number of nonaqueous solvents have been evaluated,[7] which give us useful information about the difference in solvation of an ion between solvents.

X-ray and neutron diffraction and EXAFS methods provide useful information for the structure of metal ions and complexes in solution. A review of the structural investigation of ions and complexes in solution studied by X-ray diffraction method has been previously published.[8]

In the present paper, we discuss solvent effects on complex formation reactions of metal ions in aqueous solution, aqueous organic mixtures with dioxane, acetonitrile (AN), *N,N*-dimethylformamide (DMF) and AN–DMF mixtures. An on-line controlled calorimetry system newly developed has been employed to the investigation of complex formation reactions of metal ions, and of solvation phenomana of metal ions, ligands and metal complexes in these solvents. Thermodynamic quantities of formation and of transfer of metal complexes are discussed in connection with the structure of the metal complexes.

2. EXPERIMENTAL

2.1 *Potentiometric Measurements*

Potentiometric measurements were carried out to determine formation constants of metal complexes in aqueous and aqueous dioxane solutions. Potentiometric measurements were performed in a liquid paraffin bath controlled at (25.00 ± 0.02)°C, and pH of a test solution was determined by using a glass electrode in combination with an Ag–AgCl electrode as a reference. The measurements were carried out under an atmosphere of nitrogen gas equilibrated with solvent vapor. In each series of titrations the constant appearing in the Nernstian equation, E_0, was first determined by means of Gran plots by titrating 10 cm^3 of a perchloric acid solution of a known concentration with a standard lithium hydroxide solution. Then 10 cm^3 of a solution containing metal and hydrogen ions and a ligand of known concentrations was added to the solution and titrations were continued with the same lithium hydroxide solution as used for the Gran-plot procedure until pH of the test solution reached about 10. EMF's at each point of measurements were related to the concentration of free hydrogen ions h by the Nernstian equation, $E = E_0 + 59.154 \log h$, in the pH region where the liquid junction potential was negligible ($3 < \mathrm{pH} < 10$). The ionic medium of the test solutions was kept 3 mol dm^{-3} with $LiClO_4$ throughout the measurements.

At each point of titrations the total concentrations of metal (C_M) and hydrogen ions (C_H) and ligand (C_L) are related to concentrations of respective free species, m, h and l as follows:

$$C_M = \sum_p \sum_q \sum_r p\beta_{pqr}\, m^p\, h^q\, l^r + m \tag{1}$$

$$C_H = \sum_p \sum_q \sum_r g\beta_{pqr}\, m^p\, h^q\, l^r\, K_W/h + h \tag{2}$$

$$C_L = \sum_p \sum_q \sum_r r\beta_{pqr}\, m^p\, h^q\, l^r + l \tag{3}$$

where β_{pqr} and K_W stand for the overall formation constant of the $[M_qH_qL_r]$ (charge is omitted) complex and the autoprotolysis constant of the solvent, respectively. The formation constants were determined by the least-squares method, where the error square sum, $U = \Sigma\{(C_{M,exp} - C_{M,calcd})^2 + (C_{H,exp} - C_{H,calcd})^2 + (C_{L,exp} - C_{L,calcd})^2\}$, was minimized by using the program MINIQUAD.[9]. The protonation constants of the ligand used had been determined in advance of equilibrium measurements of the complexes by separate experiments, and they were kept constant in the courst of the least-squares refinement of the formation constant of metal complexes.

2.2 *Calorimetric Measurements*

2.2.1 *Titration calorimetry.* Measurements were carried out in a thermostated bath controlled at (25.000 ± 0.007)°C. 100 cm^3 of a test solution was first placed in a Dewar vessel and was immersed in the thermostated bath for more than 10 hours to attain the thermal equilibrium of the test solution.

In aqueous and aqueous dioxane solutions, initial test solutions contained a kind of metal ions and of ligands, the concentration of the latter being slightly larger than three times the concentration of the former. The concentration of hydrogen ions in the solutions was kept so low that the predominant complex species was $[ML_3]$ at the initial stage of the titration. Then a perchloric acid solution of *ca.* 0.4 mol dm^{-3} was used for

the calorimetric titrations. At each step of calorimetric titrations was added the perchloric acid solution of 0.6–1.6 cm^3 with the certainty of $\pm$ 0.001 cm^3 to the test solution by using an automatic piston buret (Dosimat E535, Metrohm, Switzerland).

On the basis on the formation constants of the $[M_pH_qL_r]$ complexes thus obtained by potentiometric measurements, the calorimetric data were analyzed by using the program KOLARI.[10] Concentrations of all species involved at each point of calorimetric titrations were calculated by using the formation constants determined. The total heat accompanying the formation of species involved in a solution of volume V is given as follows:

$$Q = -V\left(\sum_p\sum_q\sum_r \beta_{pqr}\Delta H^\circ_{\beta pqr}\, m^p h^q l^r - K_w\Delta H^\circ_{kw} h^{-1}\right) \tag{4}$$

where $\Delta H^\circ_{\beta pqr}$ and ΔH°_{kw} denote the enthalpies pertaining to the reaction, $pM + qH + rL = M_pH_qL_r$ (charge is omitted) and $H^+ + OH^- = H_2O$, respectively. The values of K_w and ΔH°_{kw} had been determined in the solvent mixtures in separate works.[11,12] Heat evolved (q) at the i-th titration point was compared with the calculated one, $q_{i,calcd} = Q_{i,calcd} - Q_{i-1,calcd}$, by taking into account suitable values of $\Delta H^\circ_{\beta pqr}$ for each species. The enthalpies of formation were optimized by minimizing the error square sum, $U = \Sigma(q_{i,obsd} - q_{i,calcd})^2$. Enthalpies for the protonation reactions of ligands were determined in advance by separate experiments.

In acetonitrile, *N,N*-dimethylformamide and in their mixtures, formation constants and enthalpies of formation of chloro complexes of copper(II) have been obtained by calorimetric measurements, because suitable electrodes which respond to Cu^{2+} or Cl^- in the solvents were not available and thus potentiometric measurements for the metal-ligand system could not be carried out. Throughout the calorimetric titrations, and ionic medium was kept constant (0.1 and 0.2 mol dm^{-3}) by using $(C_2H_5)_4NCl$ solutions.

A heat q_i evolved at a titration point i is represented by Eq. (5) by using formation constants β_n and overall enthalpies $\Delta H^\circ_{\beta n}$ of formation of the $[CuCl_n]^{(2-n)+}$ complexes.

$$q_i = -\left(V_i \sum_n \beta_n\Delta H^\circ_{\beta n}\, m_i x_i^n - V_{i-1}\left|\sum_n \beta_n\Delta H^\circ_{\beta n}\, m_{i-1}x_{i-1}^n\right.\right) \tag{5}$$

where V denotes the volume of test solution, and m and x stand for concentrations of free copper(II) and chloride ions, respectively, which related to their total concentrations C_M and C_X according to the mass-balance equations (6) and (7):

$$C_M = \sum_n \beta_n\, m_i x_i^n + m_i \tag{6}$$

$$C_X = \sum_n n\beta_n\, m_i x_i^n + x_i \tag{7}$$

The formation constants and enthalpies were determined by minimizing the error square sum, $U = \Sigma(q_{i,obsd} - q_{i,calcd})^2$ by using the program KALORI.[10]

In all the systems examined, heats of dilution of titrant solutions were separately determined by titrating a test solution without metal ions with the relevant titrant solutions, and heats evolved in the course of complex formation reactions of metal ions were corrected for the heats of dilution of the relevant titrant solutions. The on-line calorimetric system fully automatically controlled by an electronic computer was

employed throughout the titrations, details of the procedure will be described in Chapter 3.

2.2.2 *Solution calorimetry.* Enthalpies of solution were measured in a room thermostated at (25.0 ± 0.2)°C by using an MPS-11 calorimeter (Tokyo Riko, Tokyo). A Teflon vessel was placed in an aluminium block controlled at (25.000 ± 0.003)°C in an air bath. All parts inserted in the vessel were made of Teflon. A standard heater and a thermal sensor were sandwiched between the bottom of the vessel and the aluminium block. Powder of a sample salt was placed in a glass ampoule in a dry box over P_2O_5, and the ampoule was weighed and then sealed. The ampoule containing a given amount of a sample salt was immersed in a solvent of 50 cm^3 in the Teflon vessel.

The measurement of heat of solution of a sample consisted of two stages I and II. A typical chart for a heat measurement of a sample salt is shown in Figure 1. A vessel equipped with an ampoule in a solvent was installed in an aluminium block. At the begining of measurement, the vessel was thermally equilibrated with the aluminium block (temperature θ_0). Then the vessel was heated with a standard heater for a given period of time from $t = 0$ to $t = t_h$. Thus temperature of the vessel rose during the heating period then spontaneously fell and became to the initial temperature (θ_0) within a few hours (stage I). Then the ampoule was mechanically broken and the temperature increased or decreased depending on the exothermic and endothermic dissolution of a salt. In Figure 1 an endothermic dissolution of a salt (NaCl in this case) is depicted

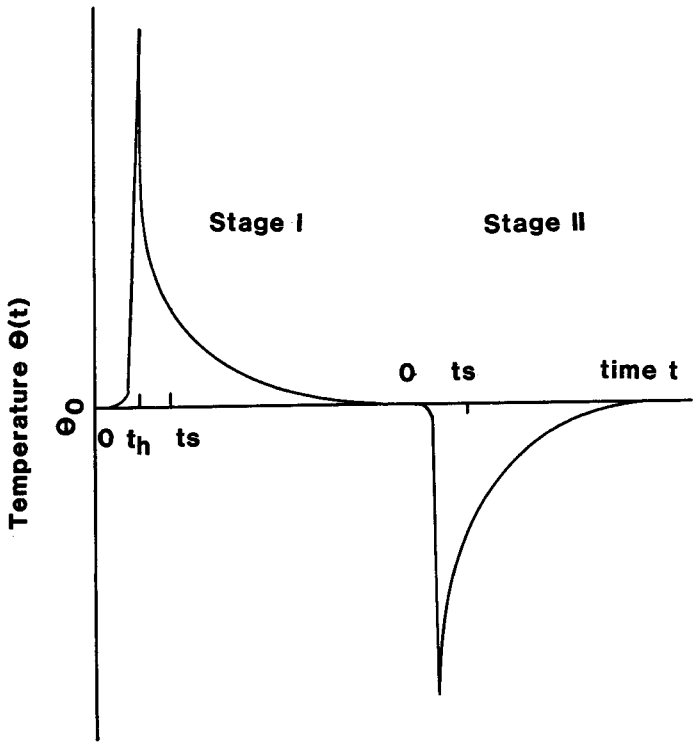

FIGURE 1. A typical example for the calorimetric determination of heat of solution of a salt.

(stage II). The temperature change detected by using a thermal sensor was recorded in a PC-8801 (NEC) computer every second through a 12-bit AD converter. Measurements were performed with the aid of the on-line system for solution calorimetry developed in our laboratory.

Total heat q evolved (or absorbed) in the vessel was obtained by integrating measured temperature changes from $t = 0$ to $t = \infty$ as follows:

$$q = \lambda \int_0^\infty \{\theta(t) - \theta_0\}dt \tag{8}$$

where λ stands for the heat transfer coefficient of the vessel. C_p and λ values were measured in the region of time $0 < t < t_s$ and those in the region $t_s < t < \infty$ were estimated by Eq. (9) according to Newton's law of cooling:

$$\theta(t) - \theta_0 = \{\theta(t_s) - \theta_0\} \exp\{-(\lambda/C_p)(t - t_s)\} \tag{9}$$

where C_p denotes the heat capacity of solution in the vessel. C_p and λ values were determined by heating the vessel with a standard heater at stage I in advance of dissolution of a salt at stage II. Details of the procedure will be described in Chapter 3.

2.3 *Spectrophotometric Measurements*

Since formation constants of copper(II) chloride complexes in acetonitrile and *N,N*-dimethylformamide could not be determined by potentiometry, formation constants of the complexes in the solvents have been determined by spectrophotometry and the values were compared with those obtained by calorimetry. A flow cell with a light-pass length of 0.5 cm was connected with a titration vessel through Teflon and glass tubes. Electronic spectra were measured with a HITACHI 340 spectrophotometer (HITACHI) equipped with a JEC 6 electronic computer (JEOL, Tokyo) which recorded data at selected wavelengths.

Electronic spectra of copper(II) chloride solutions were measured in the solutions of various C_X/C_M. The absorbance A_{ij} at a selected wavelength λ_j in the solution i is represented by Eq. (10) by using the formation constant β_n and molar extinction coefficient $\varepsilon_n(\lambda_j)$ of the $[CuCl_n]^{(2-n)+}$ complex:

$$A_{ij} = \sum_n \varepsilon_n(\lambda_j)\beta_n m_i x_i^n + \varepsilon_{Cu}(\lambda_j)m_i + \varepsilon_{Cl}(\lambda_j)x_i \tag{10}$$

The formation constants and molar extinction coefficients of the complexes were determined by minimizing the error square sum, $U = \Sigma\Sigma(A_{ii\ \mathrm{obsd}} - A_{ij,\mathrm{calcd}})^2$ by using the program SPEC.

2.4 *X-Ray Diffraction Measurements*

X-Ray scattering data were obtained at 25°C with a JEOL θ-θ type diffractometer equipped with a Philips Mo X-ray tube ($\lambda = 71.07$ pm). The method of measurements and data treatments were described elsewhere.[8]

2.5 *Raman Spectral Measurements*

Raman spectra were recorded on a JEOL JRS-S1 spectrometer using 514.5 nm line of NEC GLG3200 argon ion laser in a room at (25 ± 0.2)°C.

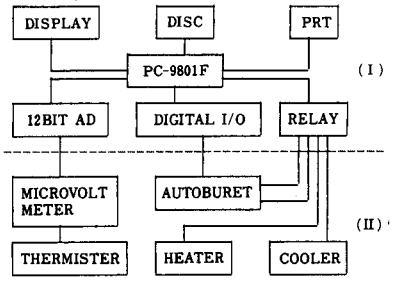

FIGURE 2. The on-line controlled titration calorimetry system.

3. ON-LINE CONTROLLED CALORIMETRY SYSTEM

A fully automatically controlled on-line system for calorimetry has been developed in our laboratory.[13,14] The on-line controlled system for titration calorimetry consists of computer (I) and calorimeter (II) parts as illustrated in Figure 2. A thermister, a heater, a cooler and the tip of an autoburet were inserted into the titration vessel as shown in Figure 3. A heater and a cooler were used for adjusting temperature in the titration vessel to a thermal equilibrium temperature. The heater was also used for evaluation of cell constants C_p and λ of the vessel. A given volume of titrant was automatically added from an autoburet (Dosimat E535, Metrohm, Switzerland) controlled by a computer. A computer employed in the present study was PC-9801 (NEC, Tokyo) or JEC-6 (JEOL, Tokyo) computer.

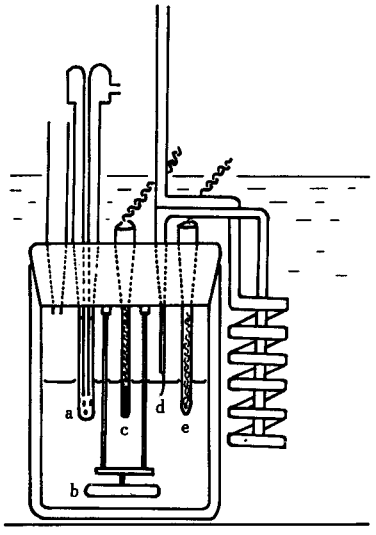

FIGURE 3. The cell arrangement used for titration calorimetry. a: cooler which is filled with water and is connected with an air pump, b: stirring bar, c: heater, d: the tip of buret, e: thermister.

3.1 *Determinaton of Heat of Reaction*

Under nonadiabatic conditions, a change in temperature $\theta(t)$ as a function of time t relative to a thermal equilibrium temperature of a reaction vessel is represented as follows:

$$C_pV\{d\theta(t)/dt\} = q(t) - \lambda\theta(t) \tag{11}$$

where V denotes a volume of a test solution and $q(t)$ stands for a heat evolved or absorbed per unit time at t. Since $\theta(t) = 0$ at $t = 0$ and $t = \infty$, the total heat evolved or absorbed in the vessel at each addition of a titrant is thus obtained by integrating a relative temperature measured in the range $t = 0$ to ∞ as follows:

$$q = \int_0^\infty q(t)dt = \lambda \int_0^\infty \theta(t)dt \tag{12}$$

Temperature in a test solution increases or decreases during a reaction, but it spontaneously approaches the thermal equilibrium temperature after the reaction in the vessel is finished. In the spontaneous temperature-increasing (or decreasing) region of the solution where no more heat evolution occurs ($q(t) = 0$ in Eq. (11)), a temperature variation after a certain time $t = t_s$ can be expressed according to Eq. (13):

$$\theta(t) = \theta(t_s)\exp\{-\mu(t - t_s)\} \tag{13}$$

where $\mu = \lambda/C_pV$. Therefore, the right hand side of Eq. (12) can be separated into two terms as follows:

$$q = \lambda \int_0^{t_s} \theta(t)dt + \int_{t_s}^\infty \theta(t)dt$$

$$= \lambda\left[\int_0^{t_s} \theta(t)dt + \theta(t_s) \int_{t_s}^\infty \exp\{-\mu(t - t_s)\}dt\right] \tag{14}$$

By replacing μ with λ/C_pV, we obtain

$$q = \lambda \int_0^{t_s} \theta(t)dt + C_pV\theta(t_s) \tag{15}$$

Therefore, by knowing the constants λ and C_p of the test solution in the reaction vessel, we can determine heat evolved or absorbed in a reaction by measuring $\theta(t)$ in the region from $t = 0$ to $t = t_s$.

A relation between a temperature variation curve and a heat evolved by a reaction is illustrated in Figure 4. Total heat evolved q is given from the area under the curve from $t = 0$ to $t = \infty$, which is divided into two regions at $t = t_s$. The heat q_1 given by the first term in Eq. (15) corresponds to the heat released from the vessel in the region $0 < t < t_s$. On the other hand, the heat q_2 given by the second term in Eq. (15) corresponds to the heat remaining in the vessel at $t = t_s$, which will be released spontaneously from the vessel over the range of time $t_s < t < \infty$.

The constants λ and C_p are determined by heating the solution with a standard heater at the beginning of titrations. A standard heater is operated for a given period of

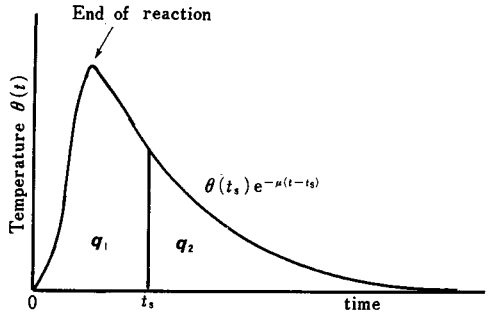

FIGURE 4. Relation between heat evolved and temperature variation curve at the addition of a portion of a titrant.

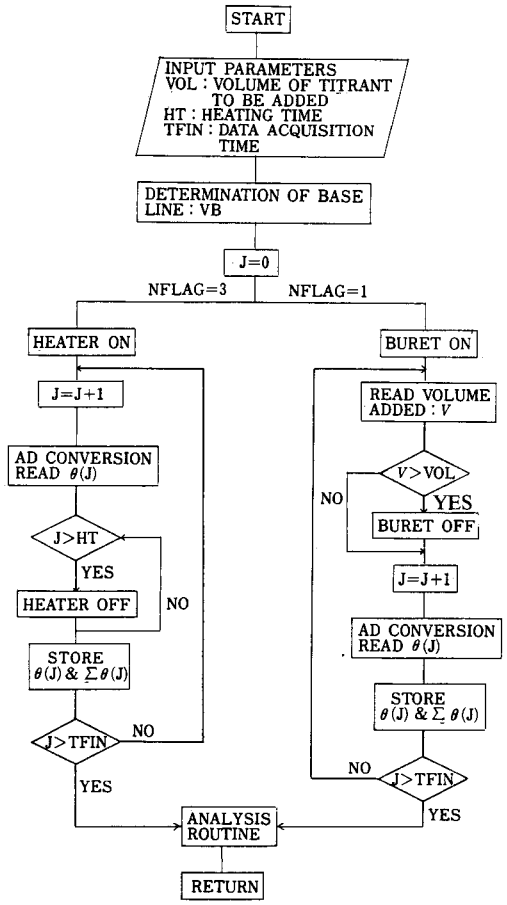

FIGURE 5. Flow chart for acquisition of temperature data at the processes of heating with a standard heater (NFLAT = 3) and of titration of a titrant from an autoburet (NFLAG = 1).

time and thus a given amount of heat q_{ev} is evolved. After the heating, temperature of the solution spontaneously falls. The μ value in Eq. (13) is determined from the slope of plots in ln $\theta(t)$ *vs.* t by the least-squares method. Since the quantities $\theta(t)$ and $\int_0^t \theta(\tau)d\tau$ are recorded in a computer, the values of λ and C_p are obtained by Eqs. (16) and (17).

$$\lambda = q_{ev} \Big/ \left[\int_0^{t_s} \theta(t)dt + \mu\theta(t_s) \right] \tag{16}$$

$$C_p = \lambda / \mu V_{init} \tag{17}$$

where V_{init} stands for the initial volume of the test solution. The λ and C_p are determined at various t_s of successive 300 points measured every second in the spontaneously decreasing (or increasing) region of temperature, and the final values were obtained by averaging the λ and C_p values at 300 t_s's.

The flow chart for determination of heat evolved or absorbed at the addition of a titrant is shown in Figure 5. In the flow chart, the symbol J signifies time, and the iteration cycle time used in the measurement was one second. The values of $\theta(t)$ and $\Sigma\theta(t)$ data of successive 150 points starting from 50 seconds after the end of the addition of a titrant in the region where temperature in the vessel gradually increased or decreased after an endothermic or an exothermic reaction, respectively, in the titration vessel. The final q value was obtained by averaging the q values estimated at various points of time.

4. COMPLEX FORMATION REACTIONS IN AQUEOUS DIOXANE SOLUTIONS

4.1 *Introduction*

Dioxane is a nonpolar basic solvent. Some typical physicochemical properties of dioxane are summarized in Table I. Although intermolecular interactions between dioxane molecules are weak, interactions between dioxane molecules and acidic or

TABLE I
Physicochemical properties of dioxane.

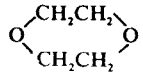

: $C_4H_8O_2$

Molecule weight	88.107
Boiling point	101.32° (1.0132×10^5 Pa)
Freezing point	11.80°C
Density	1.02797 g cm^{-3} (25°C)
Viscosity	0.001087 Pa s (30°C)
Heat of vaporization	35.6 J mol^{-1} (at b.p.)
Heat capacity	153.0 J K^{-1} g^{-1} (18°C)
Conductivity	5×10^{-15} S cm^{-1} (25°C)
Dipole moment	1.50×10^{-30} C m (0.45 D[a])
Relative dielectric constant	2.209 (25°C)
Donor number	14.8
Acceptor number	10.8

[a]The Debye unit.

amphiprotic solvents are rather strong due to the basicity of the etherial oxygen atoms of dioxane. Therefore, dioxane can form hydrogen-bonds with water and is missible at any composition of dioxane-water mixtures. As dioxane forms associates with water molecules in an aqueous dioxane solution, hydrogen bonds between water molecules originally existing in water are partly replaced with those between dioxane and water molecules in the mixture. On the other hand, since dioxane has very poor acidity, dioxane molecules cannot interact with the oxygen atom of a water molecule. As the result, dioxane acts as a breaker of the water structure.

The donicity of dioxane is rather weak (it is sometimes even classified into an aprotic solvent instead of a basic one) and the donor number ($D_N = 14.8$) of dioxane is smaller than that of water (18.0). Therefore, metal ions (Lewis acids) in aqueous dioxane solutions may be preferentially solvated with water molecules. Especially in a water-rich region of aqueous dioxane mixtures, metal ions may be fully solvated with water molecules in their first coordination sphere.[15] The acceptor number ($A_N = 10.8$) of dioxane is much smaller than that of water (54.8), and thus, anionic ligands may also be preferentially solvated with water. The preferential solvation of water may be more remarkable in anions than in cations.

In this chapter, we discuss about protonation reactions of ligands and complex formation reactions of metal ions in water and in aqueous dioxane solutions. Such reactions are strongly influenced by the hydrogen-bonded water structure in the bulk in aqueous dioxane solutions in comparison with those in aprotic solvents. Most of organic ligands have more or less both hydrophobic and hydrophilic natures in aqueous solutions. Since hydrophobicity of a ligand molecule is originated from the fact that water molecules are hydrogen bonded in the bulk and thus the network structure among water molecules is constructed in aqueous solution, solvation and protonation reactions of a hydrophobic molecule in aqueous dioxane solutions may largely change depending on the solvent composition of the solvent mixtures because the extent of structuredness of water in the bulk aqueous dioxane solutions is strongly affected by the solvent composition. 1,10-Phenanthroline has both hydrophobic (aromatic rings) and hydrophilic (nitrogen atoms) moieties within the molecule, therefore, the solvation and protonation of 1,10-phenanthroline were investigated over the whole range of the solvent composition of the dioxane-water mixtures.

Enthalpies of solution of 1,10-phenanthroline in acidic and neutral dioxane-water mixtures of a given solvent composition are found to significantly differ in the range 0–0.2 mole fraction of the dioxane content. The $[H(phen)_2]^+$ species was only found to form in the same range of the dioxane content in the mixtures, and was suggested to be a stacked species which form in a highly structured solvent. These facts indicate that the hydrogen-bonded structure of water is broken in the dioxane-water mixtures compared to water, but is still partially constructed in the mixture of 0.2 mole fraction dioxane. Protonation reactions of ethylenediamine and amino carboxylic acid, and complex formation equilibria of some metal ions with the ligands were then studied in water and in the 0.2 mole fraction dioxane mixture. In all the systems examined, formation constants of metal complexes in the mixture became larger than those in water. Further discussion of the solvent effect on the complex formation equilibria is made in Chapter 6 in relation to the ethalpies of transfer of single species involved in the complex formation reactions from water to the 0.2 mole fraction dioxane mixture.

In a given solvent, the change in thermodynamic quantities of formation of a series of mononuclear complexes of a metal ion reflects the changes in the metal-ligand and metal-solvent interactions within the complexes with the introduction of ligands into the coordination sphere of the metal ion in the course of complex formation reactions. Thus, equilibrium enthalpies and entropies, and rate constants of formation of metal complexes were discussed in connection with the changes in the metal-ligand and metal-solvent bond distances with increasing number of ligands within the complexes.

As to the thiocyanato complexes of zinc(II), cadmium(II) and mercury(II) in water, formation equilibria of the complexes were calorimetrically studies and the coordination structures of the tetrathiocyanato complexes of the metal ions were determined by X-ray diffraction, Raman and NMR measurements. These results will be discussed in Chapter 5.

4.2 *Solvation and Protonation of 1,10-Phenanthroline*

Protonation reactions of 1,10-phenanthroline (phen) in aqueous solutions have so far been studied by potentiometry and calorimetry, and it has been reported that $[Hphen]^+$ and $[H(phen)_2]^+$ were formed in the range $-\log[H^+] = 2$-7 and $[H_2phen]^{2+}$ was also found in a solution of $[H^+] > 1$ mol dm^{-3}.[16-20] A proton NMR study of 1,10-phenanthroline solutions containing various concentrations of hydrochloric acid also suggested the formation of $[Hphen]^+$ and $[H(phen)_2]^+$ and, in fact, the $Hphen \cdot ClO_4$ and $H(phen)_2 \cdot ClO_4$ crystals were isolated.[21]

Due to the hydrophobicity of aromatic rings of 1,10-phenanthroline, the solubility of the neutral species is low in water, but remarkably increases in organic solvents and also in aqueous organic mixtures. With this point of view, protonation reactions of 1,10-phenanthroline have been studied in various aqueous alcohol solutions.[22]

Solvent effects on protonation reactions of 1,10-phenanthroline is very different from those of amines and amino acids. The protonation constant of $Hphen^+$ decreases with increasing concentration of an organic component in aqueous organic solutions, in contrast to protonation constants of amino groups which are practically invariable and those of carboxylate groups which increase in the solutions.

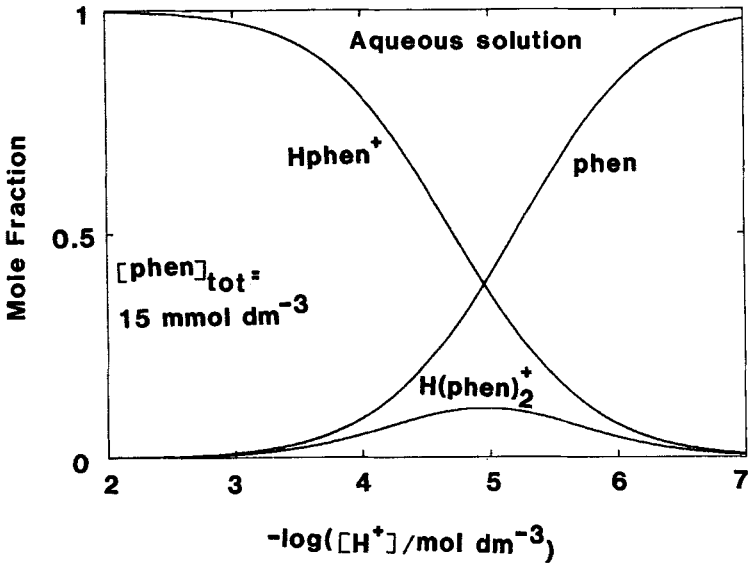

FIGURE 6. Distribution curves of protonated and unprotonated 1,10-phenanthroline in aqueous solution containing 0.3 mol dm^{-3} NaCl as a constant ionic medium at 25°C. Total concentration of 1,10-phenanthroline in solution: $[phen]_{tot} = 0.015$ mol dm^{-3}.

TABLE II

Thermodynamic quantities, $\log(K_n/\text{mol}^{-1}\ \text{dm}^3)$, ΔG_n°/kJ mol^{-1}, ΔH_n°/kJ mol^{-1} and ΔS_n°/J K^{-1} mol^{-1}, for the stepwise reaction, $[\text{H(phen)}_{n-1}]^+ + \text{phen} = [\text{H(phen)}_n]^+$ ($n = 1$ and 2) in dioxane-water mixtures containing 0.3 mol dm^{-3} NaCl as a constant ionic medium at various mole fractions x of dioxane.

	$[\text{Hphen}]^+$				$[\text{H(phen)}_2]^+$			
x	$\log K_1$	ΔG_1°	ΔH_1°	ΔS_1°	$\log K_2$	ΔG_2°	ΔH_2°	ΔS_2°
0.0	4.96	−28.3	−16.6	39	1.69	−9.6	−17.7	−27
0.0125	4.83	−27.6	−	−	1.69	−9.6	−	−
0.025	4.71	−26.9	−19.7	24	1.45	−8.3	−16.2	−27
0.05	4.57	−26.1	−20.7	18	1.45	−8.3	−9.9	−5
0.1	4.33	−24.7	−18.7	20	1.38	−7.4	−6.6	4
0.2	4.01	−22.9	−13.9	30				
0.3	3.86	−22.0	−10.7	38				
0.4	3.86	−22.0	−10.2	40				

The formation of $[\text{H(phen)}_2]^+$ and different solvent effects on the formation of $[\text{Hphen}]^+$ from those on the formation of protonated amines or amino carboxylic acids suggested an importance of solvation at aromatic rings of 1,10-phenanthroline in the course of protonation reactions of 1,10-phenanthroline. In order to elucidate the solvation phenomena of 1,10-phenanthroline, enthalpies of solution of anhydrous 1,10-phenanthroline were determined both in neutral aqueous dioxane solutions (dioxane content $x = 0$ - 1 mole fractions) and in acidic ones containing 0.1 mol dm^{-3} HCL ($x = 0$–0.4). Thermodynamic quantities, ΔG_n°, ΔH_n° and ΔS_n°, for protonation reactions of 1,10-phenanthroline in various aqueous dioxane solutions are discussed in connection with changes in solvation of the neutral and protonated species. Thermodynamic quantities, $\log(K_n/\text{mol}^{-1}\ \text{dm}^3)$, ΔG_n°/kJ mol^{-1}, ΔH_n°/kJ mol^{-1} and ΔS_n°/J K^{-1} mol^{-1}, for the stepwise reactions, $[\text{H(phen)}_{n-1}]^+ + \text{phen} = [\text{H(phen)}_n]^+$ ($n = 1$ and 2), in various aqueous dioxane solutions are summarized in Table II. Distribution curves of protonated and unprotonated 1,10-phenanthroline in water is depicted in Figure 6, which are calculated using protonation constants of 1,10-phenanthroline in water listed in Table II.

Enthalpies of solution of anhydrous 1,10-phenanthroline were determined in both neutral ($\Delta H_{\text{s,neutral}}^\circ$, $x = 0$ - 1) and acidic ($\Delta H_{\text{s,acid}}^\circ$, $x = 0$ - 0.4) aqueous dioxane solutions. In the neutral solvents, the formation of protonated species of 1,10-phenanthroline was negligible. In solutions involving 0.1 mol dm^{-3} HCl, 1,10-phenanthroline was fully converted into $[\text{Hphen}]^+$, but not into $[\text{H(phen)}_2]^+$ in such a highly acidic solution. Thus, the enthalpies of solution measured in an acidic solution at a given solvent composition was given as the sum of enthalpies of solution of 1,10-phenanthroline (ΔH_s°(phen)) and of formation of $[\text{Hphen}]^+$(ΔH_1°), the latter value having been determined in the calorimetric titration experiment and being given in Table II. Thus ΔH_s°(phen) was calculated according to Eq. (18):

$$\Delta H_s^\circ(\text{phen}) = \Delta H_{\text{s,acid}}^\circ - \Delta H_1^\circ \tag{18}$$

Values of ΔH_s°(phen), $\Delta H_{\text{s,acid}}^\circ$ and $\Delta H_{\text{s,neutral}}^\circ$ obtained in various aqueous dioxane solutions are summarized in Table III.

4.2.1 *Enthalpies of solution of 1,10-phenanthroline.* If only monomeric 1,10-phenanthroline molecules were present in a neutral solution, $\Delta H_{\text{s,neutral}}^\circ$ should be equal to ΔH_s°(phen). However, as seen in Figure 7, ΔH_s°(phen) was appreciably different from $\Delta H_{\text{s,neutral}}^\circ$ in the dioxane-water mixture of $x < 0.3$. The difference may be ascribed to the formation of stacked neutral species of 1,10-phenanthroline, $(\text{phen})_n$, in the

Table III

Enthalpies of solution of 1,10-phenanthroline measured in acidic ($\Delta H^{\circ}_{s,acid}$/kJ mol^{-1}) and neutral ($\Delta H^{\circ}_{s,neutral}$/kJ mol^{-1}) aqueous dioxane solutions, and calculated enthalpies of solution of monomeric 1,10-phenanthroline (ΔH°_{s}(phen)/kJ mol^{-1}) in the mixtures.

dioxane content mole fraction	$\Delta H^{\circ}_{s,acid}$	$\Delta H^{\circ}_{s,neutral}$	ΔH°_{t}	ΔH°_{s}(phen)	$\Delta\Delta H^{\circ a}_{s}$
0.0	−11.6	−0.3	−16.6	5.0	−5.3
0.025	−10.2	–	−19.7	9.5	–
0.05	−9.4	3.9	−20.7	11.3	−7.4
0.1	−5.0	5.7	−18.7	13.7	−8.0
0.2	−0.6	11.3	−13.9	13.3	−2.0
0.3	−1.2	10.0	−10.7	9.5	0.5
0.4	0.2	10.8	−10.2	10.4	0.4
0.6		11.9			
0.7		11.4			
0.8		11.7			
0.9		13.4			
1.0		17.7			

[a] $\Delta\Delta H^{\circ}_{s} = \Delta H^{\circ}_{s,neutral} - \Delta H^{\circ}_{s}$(phen).

neutral solvent mixtures, as suggested by an NMR study in water.[23] The value of $\Delta H^{\circ}_{s,neutral}$ was always positive but smaller than ΔH°_{s}(phen) in the mixture of $x < 0.3$, which suggested that the enthalpy of formation of the stacks should be negative if such stacks of 1,10-phenanthroline are formed in the mixtures. Negative enthalpies for the formation of stacked species were also reported for Methylene Blue in aqueous mixtures of various alcohols.[24]

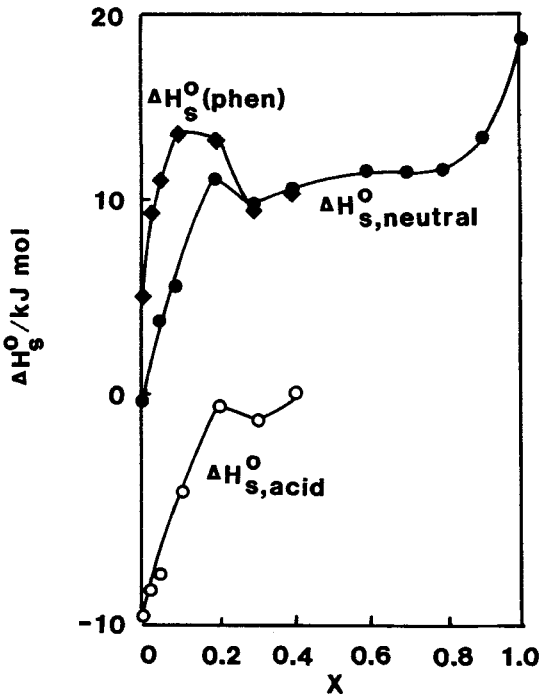

FIGURE 7. Enthalpies of solution of 1,10-phenanthroline in neutral ($\Delta H^{\circ}_{s,neutral}$) and acidic ($\Delta H^{\circ}_{s,acid}$) solutions and ΔH°_{s}(phen) plotted against x.

The value of ΔH_s°(phen) was practically the same as $\Delta H_{s,neutral}^\circ$ in the dioxane-water mixtures at $x = 0.3$ and 0.4, and the results suggested that the stacks did not form in the solutions due, probably, to destruction of the hydrogen-bonded structure of water in the bulk, which led to the decomposition of the hydrophobic hydration sphere around the aromatic rings of 1,10-phenanthroline. Observations by X-ray diffraction[25] suggested the destruction of the hydrogen-bonded structure of bulk water at $x > 0.3$.

Values of ΔH_s°(phen) were obtained in aqueous dioxane solutions at $x = 0$–0.4, but not in solutions at $x > 0.4$ due to experimental difficulties for determination of ΔH_i° and $\Delta H_{s,acid}^\circ$. However, since self-stacking of 1,10-phenanthroline molecules was hardly expected in aqueous dioxane solutions at $x > 0.4$ and, in fact, practically the same values of ΔH_s°(phen) as those of $\Delta H_{s,neutral}^\circ$ were found in the mixtures at $x = 0.3$ and 0.4. we can reasonably assume that $\Delta H_s^\circ(\text{phen}) = \Delta H_{s,neutral}^\circ$ in aqueous dioxane solutions at $x > 0.4$.

The value of ΔH_s°(phen) steeply increased with increasing x up to 0.1, and then slightly decreased in the range $x = 0.1$–0.3. The sharp increase in ΔH_s° was also reported for the solution of 2,2′-bipyridyl in aqueous alcohol solutions with increasing alcohol content.[26] A further increase in x did not appreciably affect the ΔH_s°(phen) value until $x = 0.8$. In the range $x > 0.8$, ΔH_s°(phen) again steeply increased with x, and ΔH_s°(phen) in pure dioxane was more positive by about 13 kJ mol^{-1} than that in pure water. It is well known that the solubility of 1,10-phenanthroline markedly increases in organic solvents. Therefore, the result that ΔH_s°(phen) was more endothermic in pure dioxane than in pure water indicated that the high solubility of 1,10-phenanthroline in dioxane was essentially owing to the contribution of a large entropy of solution of the species.

The variation of ΔH_s°(phen) in the range $x = 0$–0.1 may be explained in terms of enhanced solvation of dioxane due to the breaking of the hydrophobic hydration structure around the aromatic rings of 1,10-phenanthroline molecules. A slight decrease of ΔH_s°(phen) in the range $x = 0.1$–0.3 may be ascribed to the enhanced hydration of hydrophilic nitrogen atoms within 1,10-phenanthroline due to the breaking of the hydrogen-bonded water structure in the bulk. The enhancement of hydration of cations in aqueous dioxane solutions than in water is suggested as will be discussed in Chapter 6. The solvation structure of 1,10-phenanthroline with water at the sites of nitrogen atoms and with dioxane at the aromatic part probably remained unchanged in the range $x = 0.3$–0.8, so that ΔH_s°(phen) was almost independent of solvent composition. In solutions of the highest dioxane content $x > 0.8$, water molecules solvating the nitrogen atoms within 1,10-phenanthroline should be replaced with dioxane molecules.

4.2.2 *Solvent effects on the formation of [Hphen]$^+$.* The solvent effect on thermodynamic quantities for the formation of [Hphen]$^+$ was shown in Figure 8, where the increments of ΔG_1°, ΔH_1° and $T\Delta S_1^\circ$ in an aqueous dioxane solution from those in water, $\Delta\Delta G_1^\circ = \Delta G_1^\circ(\text{mix}) - \Delta G_1^\circ(\text{w})$, $\Delta\Delta H_1^\circ = \Delta H_1^\circ(\text{mix}) - \Delta H_1^\circ(\text{w})$ and $T\Delta\Delta S_1^\circ(\text{mix}) - T\Delta S_1^\circ(\text{w})$, are plotted against x in the range $x < 0.4$.

$\Delta\Delta G_1^\circ$ monotonously increased with increasing x, while $\Delta\Delta H_1^\circ$ and $T\Delta\Delta S_1^\circ$ first decreased and then increased after passing through minima at $x = 0.05$ with increasing x. The change in $\Delta\Delta H_1^\circ$ can be expressed in terms of enthalpies of transfer, $\Delta H_t^\circ = \Delta H_s^\circ(\text{mix}) - \Delta H_s^\circ(\text{w})$, of the related species from water to the dioxane-water mixtures as follows:

$$\Delta\Delta H_1^\circ = \Delta H_t^\circ(\text{Hphen}^+) - \Delta H_t^\circ(\text{H}^+) - \Delta H_t^\circ(\text{phen}) \tag{19}$$

By knowing values of $\Delta\Delta H_1^\circ$ and ΔH_t°(phen), the value of $\Delta H_t^\circ(\text{Hphen}^+) - \Delta H_t^\circ(\text{H}^+)$ was calculated according to Eq. (19) and the values of ΔH_1°, ΔH_t°(phen) and $\Delta H_t^\circ(\text{Hphen}^+) - \Delta H_t^\circ(\text{H}^+)$ thus calculated are summarized in Table IV. Since the enthalpy of transfer of

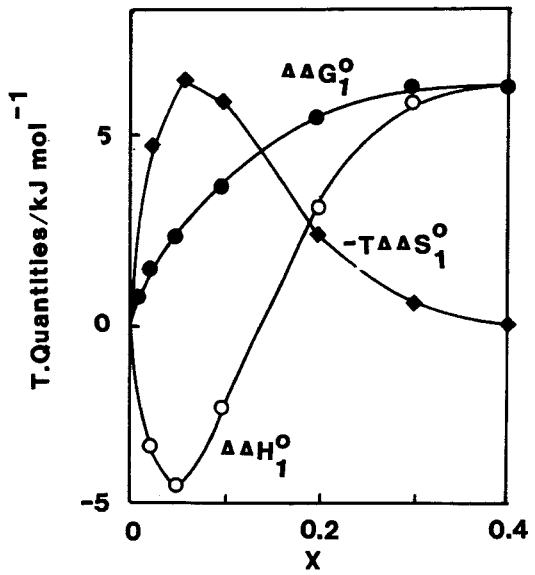

FIGURE 8. Gibbs energies, enthalpies and entropies of formation $[Hphen]^+$ in aqueous dioxane solutions relative to those in water.

proton $\Delta H_t^\circ(H^+)$ from water to the 0.2 mole fraction dioxane-water mixture was known (see Chapter 6), $\Delta H_t^\circ(Hphen^+)$ from water to the mixture was calculated and the values are also listed in Table IV.

$[Hphen]^+$ involves a hydrophilic $\rangle NH^+$ group solvated with water and hydrophobic aromatic rings preferentially solvated with dioxane in aqueous dioxane solutions. The enthalpy of transfer of $[Hphen]^+$ from water to an aqueous dioxane solution should thus involve contributions of those of $\rangle NH^+$ ($\Delta H_t^\circ(\rangle NH^+)$) and aromatic rings ($\Delta H_t^\circ(Ar)$) within $[Hphen]^+$. The enthalpy of transfer of the $\rangle NH^+$ group may be assumed to be similar to that of H^+, because it has been found that the enthalpy of transfer of the protonated ethylenediamine($[Hen]^+$) from water to the 0.2 mole fraction dioxane-water mixture was very close to that of proton, *i.e.*, $\Delta H_t^\circ(H^+)$ and $\Delta H_t^\circ(Hen^+) \cong \Delta H_t^\circ(H^+)$ (see Chapter 6).

If we assume that solvation of the protonated nitrogen atom $\rangle NH^+$ within $[Hphen]^+$ with water varies in a similar manner to that of H^+ in the range $x = 0$–0.4, $\Delta H_t^\circ(phen)$-$\Delta H_t^\circ(H)$ should approximately reflect the change in solvation of the aromatic rings within $[Hphen]^+$. Variations of $\Delta H_t^\circ(Hphen^+)$-$\Delta H_t^\circ(H^+)$ and $\Delta H_t^\circ(phen)$ with x show that they have a similar trend in the range $x = 0$–0.2. In the range $x = 0.2$–0.3, $\Delta H_t^\circ(phen)$ more steeply decreased with x than $\Delta H_t^\circ(Hphen^+)$-$\Delta H_t^\circ(H^+)$, which may be

TABLE IV

Changes in enthalpy of formation of $[Hphen]^+$ relative to that in water and enthalpies of transfer ΔH_t°/kJ mol^{-1} of relevant species from water to aqueous dioxane solutions at 25°C

x	ΔH_t°	$\Delta H_t^\circ(phen)$	$\Delta H_t^\circ(Hphen^+)$-$\Delta H_t^\circ(H^+)$	$\Delta H_t^\circ(Hphen^+)$	$\Delta H_t^\circ(H^+)$
0.025	−3.1	4.5	1.4		
0.05	−4.1	6.3	2.2		
0.1	−2.1	8.7	6.6		
0.2	2.7	8.3	11.0	−11.7	−22.7
0.3	5.9	4.5	10.4		
0.4	6.4	5.4	11.8		

caused by enhanced hydration at the sites of nitrogen atoms within 1,10-phenanthroline as discussed in a previous section.

The value $\Delta H_t^\circ(\text{Hphen}^+)$ from water to the 0.2 mole fraction dioxane-water mixture was −11.7 kJ mol^{-1}, which should be represented as the sum of $\Delta H_t^\circ(\text{>NH}^+)$ and $\Delta H_t^\circ(\text{Ar})$. If we simply assume that $\Delta H_t^\circ(\text{>NH}^+) = \Delta H_t^\circ(\text{H}^+)$ in the range $x = 0$–0.2, the value of $\Delta H_t^\circ(\text{Ar})$ from water to the 0.2 mole fraction dioxane-water mixture was estimated to be about 11 kJ mol^{-1}, which was slightly larger than $\Delta H_t^\circ(\text{phen})$ (8.3 kJ mol^{-1}). The slightly larger value of $\Delta H_t^\circ(\text{phen})$ suggests that the hydration at the sites of nitrogen atoms within 1,10-phenanthroline was enhanced in the 0.2 mole fraction dioxane-water mixture relative to water.

4.2.3 *Solvent effects on the formation of* $[H(phen)_2]^+$ The formation of $[\text{H(phen)}_2]^+$ could be detected only in aqueous dioxane solutions of $x < 0.1$, where the hydrogen-bonded structure of water in the bulk might still significantly remain and the stacks of 1,10-phenanthroline were expected to form.

Mitchell[27] suggested from measurements of the concentration dependence of the proton NMR spectrum of 1,10-phenanthroline molecules to form $[\text{H(phen)}_2]^+$. Considering that the $[\text{H(phen)}_2]^+$ species was not formed in aqueous dioxane solutions of relatively high dioxane content in which the hydrogen-bonded structure of water in the bulk may be almost destructed, we concluded that 1,10-phenanthroline molecules within $[\text{H(phen)}_2]^+$ should not be a planar structure, but a stacked one.

The values of ΔH_2° pertaining to the reaction, $[\text{Hphen}]^+ + \text{phen} = [\text{H(phen)}_2]^+$, were negative in all aqueous dioxane solutions examined. The result can be expected because of negative enthalpies of formation of stacked oligomers of 1,10-phenanthroline $(\text{phen})_n$.

4.3 *Protonation Reactions of Ligands*

Protonation reactions of ethylenediamine (en), glycinate (gly^-) and β-alaninate (ala^-) ions have been investigated by potentiometry and calorimetry in aqueous and aqueous

TABLE V

Thermodynamic quantities, $\log(K_n/\text{mol}^{-1}\ \text{dm}^3)$, ΔG_n°/kJ mol^{-1}, ΔH_n°/kJ mol^{-1} and ΔS_n°/J K^{-1} mol^{-1}, for the protonation reaction, $[\text{HL}_{n-1}] + \text{H} = [\text{H}_n\text{L}]$ (L = en, gly^- and β-ala^-, charges are omitted), in water and in a dioxane-water mixture (dioxane content: 0.2 mole fraction) containing 3 mol dm^{-3} $LiClO_4$ as a constant ionic medium at 25°C.

		H + L = HL			HL + H = H_2L		
L	$\Delta\chi_n^\circ$	aq	mix	$\Delta\Delta\chi_1^\circ$	aq	mix	$\Delta\Delta\chi_2^\circ$
	$\log K_n$	10.56	10.66	0.1	7.94	7.97	0.03
en	ΔG_n°	−60.3	−60.9	−0.6	−45.5	−45.5	0.0
	ΔH_n°	−65.2	−62.2	3.0	−58.5	−57.5	1.0
	ΔS_n°	−17	−5	12	−44	−40	4
	$\log K_n$	9.94	10.22	0.28	2.66	3.59	0.93
gly^-	ΔG_n°	−56.6	−58.3	−1.7	−15.3	−20.5	−5.2
	ΔH_n°	−57.9	−62.7	−4.8	−5.5	−10.3	−4.8
	ΔS_n°	−3	−15	−12	33	34	1
	$\log K_n$	10.65	10.86	0.21	4.03	4.98	0.95
β-ala^-	ΔG_n°	−60.8	−62.0	−1.2	−23.0	−28.4	−5.4
	ΔH_n°	−63.8	−64.5	−0.7	−9.2	−14.3	−5.1
	ΔS_n°	−10	−8	2	46	47	1

$\Delta\Delta\chi_n^\circ = \Delta\chi_n^\circ(\text{mix}) - \Delta\chi_n^\circ(\text{aq})$ ($\chi = G$, H or S).

dioxane (dioxane content: 0.2 mole fraction) solutions containing 3 mol dm^{-3} $LiClO_4$ as a constant ionic medium at 25°C. Thermodynamic quantities for protonation reactions of these ligands in the solvents are summarized in Table V.

Compared with the protonation reactions of 1,10-phenanthroline, those of ethylenediamine, glycinate and β-alaninate ions exhibited different solvent effects in the aqueous dioxane solution. As seen in Table II, the formation of $[Hphen]^+$ became less favorable as the concentration of dioxane increased in the mixture. On the other hand, the formation constants of $[Hen]^+$ and $[H_2en]^+$ practically remained unchanged in water and in aqueous dioxane solutions of 0.1 and 0.2 mole fraction dioxane. The formation of [Hgly] and [Hala] became slightly more favorable in the 0.2 mole fraction dioxane-water mixture than in water, and the formation of $[H_2gly]^+$ and $[H_2ala]^+$ was significantly favourable in the mixture compared with that in water. The solvent effects on the protonation reactions of the ligands will be discussed in connection with enthalpies of transfer of each species pertaining to the reactions from water to the dioxane-water mixture in Chapter 6.

4.4 *Relationship between Reactivities and Structures of Metal Complexes in Water*

Complex formation reactions of nickel(II), copper(II) and zinc(II) ions with ethylenediamine and glycine have been investigated by potentiometry and calorimetry in aqueous solutions.[28–33] These metal ions form a series of mononuclear complexes with the ligands and thermodynamic quantities thus determined are summarized in Table VI. Those of some complexes are not obtained in the present study but are quoted from the literature. The number of water molecules within the complexes is determined by the X-ray diffraction method as will be described later. For monoethylenediamine complexes of nickel(II), copper(II) and zinc(II) ions, the structure has not been determined, and thus numbers of water molecules within the coordination shell of the complexes are not determined.

In all the systems examined here, the stepwise enthalpies of formation ΔH_n° became more negative in the sequence mono- > bis- > tris-complex, while the reverse was the case for ΔG_n°. The stepwise entropies of formation ΔS_n° steeply decreased in the order mono- > bis- > tris-complex.

The structure of ethylenediamine and glycinato complexes of these metal ions in aqueous solution has been determined by the X-ray diffraction method.[34–39] For some cases in which the solubility of the relevant species is so low that the X-ray diffraction method is not applicable, the EXAFS method has been used.[40] The results are summarized in Table VII. Since the structure of the bis(glycinato)nickel(II) complex has been determined by the X-ray crystallographic method,[41] the structural data are also given in the table.

Nickel(II) ion is coordinated with six water molecules in water,[42] and the mono- and bis(ethylenediamine)nickel(II) complexes,[34] as well as the mono- and bis-(glycinato)-nickel(II) ones,[35] are coordinated with four and two water molecules, respectively, in water. The tris(ethylenediamine)nickel(II) and tris(glycinato)nickelate(II) complexes are not primarily coordinated with water molecules. Therefore, two water molecules are replaced with the ligands at each consecutive step of formation of the complexes according to the following reaction:

$$[NiL_{n-1}(H_2O)_{6-2(n-1)}] + L = [NiL_n(H_2O)_{6-2n}] + 2H_2O \qquad (20)$$

The Ni–OH_2 bond length increased from 204 pm within $[Ni(H_2O)_6]^{2+}$ to 210 pm within $[Ni(en)_2(H_2O)_2]^{2+}$ and to 208 and 210 pm within $[Ni(gly)(H_2O)_4]^+$ and $[Ni(gly)_2(H_2O)_2]$, respectively, with the increase in the number of ligand molecules coordinated. The lengthening of the Ni–OH_2 bond indicated weakening of the bond due, perhaps, to the

TABLE VI
Thermodynamic quantities, log (K_n/mol^{-1} dm^3), ΔG_n°/kJ mol^{-1}, ΔH_n°/kJ mol^{-1}, and ΔS_n°/J K^{-1} mol^{-1}, for the reaction $ML_{n-1} + L = ML_n$ (charges are omitted), in water at 25°C.

Complex[a]	Medium	log K_n	ΔG_n°	ΔH_n°	ΔS_n°	Ref
$[Ni(en)(H_2O)_m]^{2+}$	3 $LiClO_4$	7.87	−44.9	−45.4	−2	30
$[Ni(en)_2(H_2O)_2]^{2+}$		6.66	−38.0	−50.2	−41	
$[Ni(en)_3]^{2+}$		4.65	−26.5	−53.6	−91	
$[Ni(gly)(H_2O)_4]^{+}$	3 $LiClO_4$	5.74	−32.8	−27.3	18	31
$[Ni(gly)_2(H_2O)_2]$		4.96	−28.3	−32.2	−13	
$[Ni(gly)_3]^{-}$		3.74	−21.3	−35.5	−48	
$[Cu(en)(H_2O)_m]^{2+}$	3 $LiClO_4$	11.38	−65.0	−67.7	−9	32
$[Cu(en)_2(H_2O)_2]^{2+}$		9.97	−56.9	−71.0	−47	
$[Cu(gly)(H_2O)_4]^{+}$	0.1 $NaClO_4$	8.27	−47.2	−28.3	69.5	28
$[Cu(gly)_2(H_2O)_2]$		6.92	−39.5	−28.8	36.4	
$[Zn(en)_2(H_2O)_m]^{2+}$	3 $LiClO_4$	6.30	−36.0	−32.1	12.9	33
$[Zn(en)_2]^{2+}$		6.18	−35.3	−38.1	−9.5	
$[Zn(en)_3]^{2+}$		2.24	−12.8	−21.6	−29.6	
$[Zn(gly)(H_2O)_4]^{+}$	0.1	4.96	−28.3	−11	60	29
$[Zn(gly)_2(H_2O)_2]$		4.2	−24	−13	30	
$[Zn(gly)_3]^{-}$		2.4	−14	−10	−10	

[a]Number of water molecules in the first coordination shell of the complexes is determined by the X-ray diffraction method in solution. m is an undetermined quantity.

electron donation from the nitrogen and oxygen atoms within the ligands to the central metal ion by which the fractional charge on the nickel(II) atom might decrease. Although no structural data have been reported for the $[Ni(en)(H_2O)_4]^{2+}$ complex, we can expect such an elongation of the Ni-OH_2 bond within the complex when an ethylenediamine molecule coordinates to an aquanickel(II) ion. Therefore, the replacement of water molecules within the $[NiL_n(H_2O)_{6-n}]$ (L = en or gly^- and n = 0–2, charge is omitted) needs less and less energies with an increase in the number of ligands n within the complexes.

The same conclusion might be drawn for the copper(II)-ethylenediamine complexes. The Cu-OH_2(ax) bond length increased from 243 pm[43] within $[Cu(H_2O)_6]^{2+}$ to 292 pm[36] within $[Cu(en)_2(H_2O)_2]^{2+}$.

Since the Ni-N bond length also increases in the ethylenediamine and glycinato complexes of nickel(II) ion with the increase in the ligand number, the Ni-N bond may be weaker in the $[NiL_3]$ complexes than in the relevant $[NiL_2(H_2O)_2]$ complexes. Thus, we can expect that both Ni-OH_2 and Ni-N bonds are more and more weakened with the introduction of the ligand to the coordination sphere of the metal ion.

In spite of the weakening of the Ni-N bond in the $[NiL_n(H_2O)_{6-n}]$ complex with an increase in n, ΔH_n° in the aqueous solution became more negative. This suggests that the decrease in the Ni-OH_2 bond energy within the $[NiL_n(H_2O)_{6-n}]$ complex may be more enhanced than that of the Ni-N bond energy by the ligand substitution of two moles of H_2O with one mole of the ligand.

In the course of reaction (20), water molecules are liberated from solvation shells of nickel(II) ion and ligand, which results in an increase in the entropy of the reaction, while the bond formation between the metal ion and ligand leads to a decrease in the entropy. If the entropy loss due to coordination of ligands to the metal ion is not significantly different at each consecutive step of formation of the complexes, the difference in the entropies of formation ΔS_n° of the complexes with n may be mainly ascribed to that in the entropies of desolvation of water from the central metal ion,

TABLE VII

M-OH_2, M-O and M-N bond lengths within $[M(en)_n(H_2O)_m]^{2+}$ and $[M(gly)_n(H_2O)_m]^{(2-n)+}$ complexes of nickel(II), copper(II) and zinc(II) ions in aqueous solution at 25°C.

Complex	Bond Length/pm			Ref.
	M-OH_2	M-O	M-N	
$[Ni(H_2O)_6]^{2+}$	204	—	—	42
$[Ni(en)_2(H_2O)_2]^{2+}$	210	—	210	34
$[Ni(en)_3]^{2+}$	—	—	220	
$[Ni(gly)(H_2O)_4]^{+}$	208	209	209	35
$[Ni(gly)_2(H_2O)_2]$	206[a]	206[a]	206[a]	40
	210[b]	206[b]	208[b]	41
$[Ni(gly)_3]^{-}$	—	203	214	35
	—	203[c]	212[c]	40
$[Cu(H_2O)_6]^{2+}$	194(eq), 243(ax)	—	—	42
$[Cu(en)_2(H_2O)_2]^{2+}$	292(ax)	—	193(eq)	36
$[Cu(en)_3]^{2+}$	—	—	192(eq), 222(ax)	
$[Cu(gly)(H_2O)_4]^{+}$	198(eq), 227(ax)	199	199	37
$[Cu(gly)_3]^{-}$	—	202	202	
$[Zn(H_2O)_6]^{2+}$	208	—	—	42
$[Zn(en)_2]^{2+}$	—	—	213	38
$[Zn(en)_3]^{2+}$	—	—	228	
$[Zn(gly)(H_2O)_4]^{+}$	212	212	212	39
$[Zn(gly)_2(H_2O)_2]$	208[a]	208[a]	208[a]	40
$[Zn(gly)_3]^{-}$	—	212	212	39
	—	214[a]	214[a]	40

[a]EXAFS method; the bond lengths are not separable into each one. [b]Crystallographic data. [c]EXAFS method.

because the increase in the entropies of desolvation of water from the ligand may be the same at each consecutive step of formation of the complexes. The stepwise entropies of formation ΔS_n° of the $[NiL_n]$ ($n = 1$-3) complexes steeply decreased with increasing n. The larger entropy loss at higher consecutive step might be attributable to the more weakened Ni-OH_2 bond in the higher complex, because the number of water molecules removed from the first coordination sphere of the metal ion was the same at each consecutive step as indicated by reaction (20).

The Cu-OH_2 bond length at the axial position remarkably increases by the introduction of two ethylenediamine molecules at the equatorial positions of the hexaaquacopper(II) complex, so that the bis(ethylenediamine)copper(II) complexes, practically be regarded as a square-planar one. Although the structure of the monoethylenediamine complex has not been determined, the result suggests that the Cu-OH_2(ax) distance may have a value between 243 and 292 pm within the hexaaqua and bis(ethylenediamine)copper(II) complexes, respectively. The length of the Cu-N(eq) bond within the monoethylenediamine complex may be 192–194 pm, and the Cu-OH_2 bond length at the equatorial position of the monoethylenediamine complex may be longer than that of the hexaaqua complex. If the above consideration

is accepted, we may say that the strength of the Cu–N(eq) bond is practically invariable, while that of the Cu–OH_2(eq) markedly decreases with the number of ethylenediamine molecules within the coordination shell of copper(II) ion, and thus, it may need less energy for rupture of the Cu–OH_2(eq) bonds at the formation of a higher complex. Therefore, water molecules at the equatorial position may be replaced more exothermically with one ethylenediamine molecule at a higher consecutive step of the reaction. Since the water molecules within the coordination shell of a higher complex become more laibile due to weakening of the Cu–OH_2 bonds, liberation of the water molecules by the replacement of ethylenediamine molecules results in an entropy gain. Although we have not sufficient data for the structure of the glycinato complexes of copper(II), the same consideration may be applied to the system.

The structure of the mono(ethylenediamine)zinc(II) complex has not been determined yet, but the thermodynamic data suggest that the complex has a tetrahedral structure with two water molecules. The structure change occurs at the step of the formation of the tris(ethylenediamine)zinc(II) complex from tetrahedral to octahedral and accompanies a large decrease in ΔG° and an increase in ΔH°. The Zn–N bond elongates with the number of ethylenediamine molecules within the coordination shell, as seen in Table VII.

The structure of all the glycinato complexes of zinc(II) ion is octahedral and the lengths of Zn–OH_2, Zn–O and Zn–N bonds are practically independent of the number of glycinato ions. Enthalpies of the stepwise formation of the complexes are thus almost the same at each step ($-10 \sim -13$ kJ mol^{-1}) but the entropy steeply decreases at the third step.

The rate constants of stepwise formation of the glycinato complexes of nickel(II) ion change in the following order (Figure 9)[43]:

$$k_f(\mathrm{Ni(gly)^+}) < k_f(\mathrm{Ni(gly)_2}) > k_f(\mathrm{Ni(gly)_3^-}) \tag{21}$$

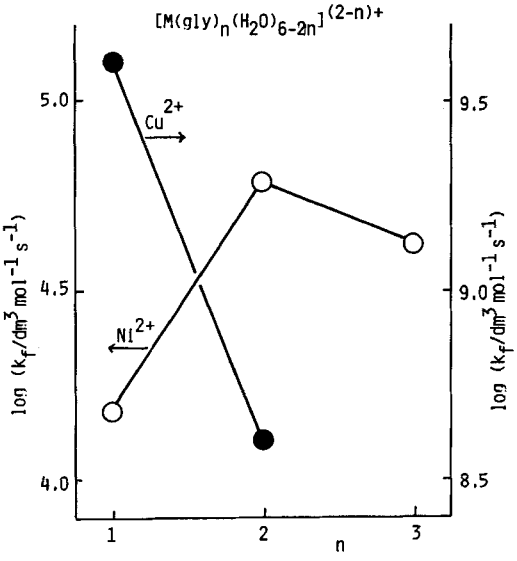

FIGURE 9. Rate constants of stepwise formation of glycinato complexes of nickel(II) and copper(II) ions.

If the water substitution reactions with entering glycinate ion have the dissociative mechanism in all the cases of the stepwise formation reactions, the rate constant k_f may be given as

$$k_f = K_{os} \cdot k_n \tag{22}$$

where K_{os} and k_n denote the formation constant of the outer-sphere complex $[ML_{n-1}^{(3-n)+} \cdot L^-]$ and the rate constant of the exchange of water molecules bound to the $[ML_{n-1}]^{(3-n)+}$ species within the outer sphere complex with L^-, respectively. K_{os} may decrease in the order

$$K_{os}(Ni(gly)^+) > K_{os}(Ni(gly)_2) > K_{os}(Ni(gly)_3^-) \tag{23}$$

due to the decrease in the positive charge on the $[ML_n]^{(2-n)+}$ complex, while k_n may increase with n:[44]

$$k_1(Ni(gly)^+) < k_2(Ni(gly)_2) < k_3(Ni(gly)_3^-) \tag{24}$$

because the lability of bound water molecules within the complexes may increase in this order. The two factors overlap to make the maximum value of k_f at $n = 2$.

The rate constants k_f of glycinato complexes of copper(II) ion steeply decrease with n. The K_{os} values may decrease in the same order as that shown in the case of the nickel(II)-glycinato complexes. However, the rate determining step at the substitution of water molecules with an entering glycinate ion may be at the step of replacement of one of the axial water molecules with a coordination site of a glycinate ion within an outer-sphere complex, and thus, the $k_2(Cu(gly)^+)$ may be larger than $k_1(Cu(gly)_2)$, because the $Cu\text{-}OH_2(ax)$ bond within $[Cu(H_2O)_6]^{2+}$ is longer and therefore weaker than that within $[Cu(gly)(H_2O)_4]^+$.

4.5 *Complex Formation of Metal Ions in an Aqueous Dioxane Solutions*

As described in section 4.2, the hydrogen-bonded structure of water may be significantly destroyed in the 0.2 mole fraction (55.0 w/w% of dioxane) dioxane-water mixture. The destruction of the water structure may influence physico-chemical properties of components of the mixed solvents, especially donor-acceptor properties of water molecules. The change in the solvent properties affects chemical equilibria between Lewis acids and bases. The solvent effects on complex formation reactions have been studied for $[Ni(en)_n]^{2+}$ ($n = 1$-3), $[Cu(en)_n]^{2+}$ ($n = 1$-2), $[Ni(gly)_n]^{(2-n)+}$ ($n = 1$-3), $[Ag(gly)_n]^{(1-n)+}$ ($n = 1$-2) and $[Ag(ala)_n]^{(1-n)+}$ ($n = 1$-2) in aqueous and aqueous dioxane (dioxane content: 0.2 mole fraction) solutions containing 3 mol dm^{-3} $LiClO_4$ as a constant ionic medium at 25°C. Thermodynamic quantities for the formation of the complexes are summarized in Table VIII.

In all the systems examined, the formation constants of the complexes increased in the dioxane-water mixture. However, enthalpies of formation ΔH_n° of the ethylenediamine complexes of nickel(II) and copper(II) ions became less negative in the mixture, and thus, the formation of the complexes was unfavorable in the mixture from the enthalpic point of view. Entropies of formation ΔS_n° of the complexes were larger by 16–32 J K^{-1} mol^{-1} in the mixture than in water, which led to the more negative ΔG_n° values of the complexes in the mixture than in water. As for glycinato and β-alaninato complexes of nickel(II) and silver(I) ions, ΔH_n° values were all more negative in the dioxane-water mixture than in water. Entropies of formation of the glycinatonickel(II) complexes increased, while those of the glycinato- and β-alaninatosilver(I) complexes decreased in the mixture.

TABLE VIII

Thermodynamic quantities, $\log(K_n/\text{mol}^{-1}\text{dm}^3)$, $\Delta G_n^\circ/\text{kJ mol}^{-1}$, $\Delta H_n^\circ/\text{kJ mol}^{-1}$ and $\Delta S_n^\circ/\text{J K}^{-1}\text{ mol}^{-1}$, for the reaction, $[ML_{n-1}] + L = [ML_n]$ ($M = Ni^{2+}$, Cu^{2+} or Ag^+, L = en, gly^- or β-ala^-, charges are omitted), in water and in a dioxane-water mixture (dioxane content: 0.2 mole fraction) containing 3 mol dm^{-3} $LiClO_4$ at 25°C, and their differences, $\Delta\log K_n$, $\Delta\Delta G_n^\circ$, $\Delta\Delta H_n^\circ$ and $\Delta\Delta S_n^\circ$ between the solvents.

	Water				Mixture				Difference			
Complex	$\log K_n$	ΔG_n°	ΔH_n°	ΔS_n°	$\log K_n$	ΔG_n°	ΔH_n°	ΔS_n°	$\log K_n$	ΔG_n°	ΔH_n°	ΔS_n°
$[Ni(en)]^{2+}$	7.87	−44.9	−45.4	−2	8.54	−48.7	−42.9	20	0.67	−3.8	2.5	22
$[Ni(en)_2]^{2+}$	6.66	−38.0	−50.2	−41	7.35	−41.9	−46.2	−14	0.69	−3.9	4.0	27
$[Ni(en)_3]^{2+}$	4.65	−26.5	−53.6	−91	5.38	−30.7	−48.3	−59	0.73	−4.2	5.3	32
$[Cu(en)]^{2+}$	11.38	−65.0	−67.7	−9	12.05	−68.8	−66.7	0.67	−3.8	1.0	16	1
$[Cu(en)_2]^{2+}$	9.97	−56.9	−71.0	−47	10.71	−61.1	−68.8	−26	0.74	−4.2	2.2	21
$[Ni(gly)]^+$	5.74	−32.8	−27.3	18	6.47	−36.9	−27.6	31	0.73	−4.1	−0.3	13
$[Ni(gly)_2]$	4.96	−28.3	−32.2	−13	5.73	−32.7	−35.9	−11	0.77	−4.4	−3.7	2
$[Ni(gly)_3]^-$	3.74	−21.3	−35.5	−48	4.65	−26.7	−36.7	−34	0.91	−5.4	−1.2	14
$[Ag(gly)]$	3.28	−18.7	−25.7	−23	3.79	−21.6	−30.1	−29	0.51	−2.9	−4.4	−6
$[Ag(gly)_2]^-$	3.68	−21.0	−36.5	−52	4.04	−23.1	−39.0	−53	0.36	−2.1	−2.5	−1
$[Ag(ala)_2]$	3.58	−20.4	−28.2	−26	4.02	−22.9	−34.5	−39	0.44	−2.5	−6.3	−13
$[Ag(ala)_2]^-$	3.88	−22.2	−38.9	−56	4.29	−24.5	−40.1	−52	0.41	−2.3	−1.2	4

$\Delta\log K_n = \log K_n(\text{mix}) - \log K_n(\text{w})$, $\Delta\Delta G_n^\circ = \Delta G_n^\circ(\text{mix}) - \Delta G_n^\circ(\text{w})$, $\Delta\Delta H_n^\circ = \Delta H_n^\circ(\text{mix}) - \Delta H_n^\circ(\text{w})$, $\Delta\Delta S_n^\circ = \Delta S_n^\circ(\text{mix}) - \Delta S_n^\circ(\text{w})$.

Although the formation of all complexes examined was more favorable in the mixture than in water, contributions of ΔH_n° and ΔS_n° to ΔG_n° were different among the metal-ligand systems as described above. The results can hardly be explained without taking into account variations of solvation of ions, molecules and metal complexes involved in the complex formation reactions. Solvent effects on the complex formation reactions will be discussed in connection with enthalpies of transfer of species involved in the reactions from water to the dioxane-water mixture in Chapter 6.

5. FORMATION OF THIOCYANATO COMPLEXES OF THE GROUP 2B METAL IONS AND THEIR STRUCTURES IN WATER

5.1 *Introduction*

Complex formation equilibria between thiocyanate and metal ions have widely been investigated from the interesting ambident nature of SCN^- ion, which can bind with metal ions through either the nitrogen or the sulfur atom depending on the central metal ions within their complexes. Among these studies, thiocyanato complexes of the Group 2B metal ions are of particular interest,[45–65] since mercury(II) and zinc(II) ions behave as soft and relatively hard acids, respectively, and cadmium(II) ion has an intermediate character. From recent X-ray diffraction and Raman spectral studies[65] on the thiocyanato complexes of zinc(II), cadmium(II) and mercury(II) in combination with the thermodynamic data[51] in dimethyl sulfoxide (DMSO), it has been found that thiocyanate ions coordinate to both mercury(II) and cadmium(II) ions through the sulfur atom, but to zinc(II) ion through the nitrogen atom.

Formation of the thiocyanato complexes of zinc(II), cadmium(II) and mercury(II) in aqueous solution has also been studied by thermodynamic,[45–49] Raman and infrared methods.[52–58] The results obtained from these studies are consistent with the conclusion that thiocyanate ions binds with mercury(II) ion through the sulfur atom, but to zinc(II) ion through the nitrogen atom within all the mononuclear species up to the tetra-complex. However, the coordination sites of SCN^- ions to cadmium(II) ion within the complexes are still not conclusive in aqueous solution.

Fronaeus and Larsson[53] interpreted two C-N absorption bands in the infrared spectrum at 2098 and 2132 cm^{-1} in terms of the presence of mononuclear and polynuclear species, respectively, in aqueous solution having lower molar ratios of thiocyanate to cadmium(II) ions. Taylor *et al.*[55] measured Raman spectra of the tetrathiocyanato complex of cadmium(II) in aqueous solutions, suggested that some SCN^- ions bound to cadmium(II) ion through the N atom and some through the S atom within the complex. In a recent Raman spectral measurement of cadium(II) thiocyanate aqueous solutions, Antić-Jovanović *et al.*[58] assigned the band at 2132 cm^{-1} to the $[Cd(SCN)]^+$ complex, while the bands appearing at 2102 and 784 cm^{-1} were attributed to higher $[Cd(NCS)_n]^{(2-n)+}$ complexes. Their conclusion for the binding type of SCN^- to cadmium(II) ions is consistent with that obtained by Taylor *et al.*[55]

In crystal of $Cd(SCN)_2$,[62] a cadmium(II) ion is octahedrally surrounded by four sulfur atoms and by two *trans*-nitrogen atoms with a slightly distorted geometry. In β-$Zn(NCS)_2$ crystal,[63] there are two crystallographically different zinc(II) ions, the one surrounded tetrahedrally by four N atoms and the other by four S atoms.

We determined thermodynamic quantities of formation of thiocyanato complexes of zinc(II) and cadmium(II) by calorimetry in aqueous solution at 25°C. Structures of the tetrathiocyanato complexes of zinc(II), cadmium(II) and mercury(II) have also been determined in aqueous solution. As to cadmium(II) thiocyanato complexes, it was indicated that SCN^- ions linked to cadmium(II) ion with both the N and S atoms in the series of mononuclear complexes, and thus, the probable bonding type of SCN^- ion within each complex was suggested on the basis of the thermodynamic and spectroscopic results.

5.2 *Formation of Thiocyanato Complexes of Zn(II) and Cd(II) in Water*

Thermodynamic quantities of formation of the thiocyanato complexes of zinc(II)[14] and cadmium(II)[66] have been calorimetrically determined in aqueous solutions containing 5 and 3 mol dm^{-3} $NaClO_4$, respectively, as a constant ionic medium at 25°C. Typical examples of calorimetric titration curves obtained for zinc(II) and cadmium(II) thiocyanate solutions are depicted in Figures 10 and 11, respectively. Enthalpies ΔH° calculated by $\Delta H^\circ = -q_{corr}/(\delta v C_{X,tit})$, where q_{corr} denotes heat corrected for dilution obtained at each titration point, δv denotes the volume of a portion of the titrant added at each titration point and $C_{X,tit}$ stands for the total concentration of NaSCN in the titrant solution, were plotted against the ratio C_X/C_M at each titration point where C_X and C_M represent total concentrations of SCN^- and metal ions, respectively, in a solution.

The calorimetric data thus obtained were analyzed by assuming the formation of a series of mononuclear thiocyanato complexes of each metal ion. The calorimetric data for the zinc(II) thiocyanato system were well explained in terms of formation of $[ZnX_n]^{(2-n)+}$ (X = SCN and n = 1-4). As to the cadmium(II) thiocyanate system, as seen in Figure 11, the experimental points deviated from the theoretical curves (the broken lines) calculated by assuming the only mononuclear complexes at relatively higher concentrations of cadmium(II) ion in the range $C_X/C_M < 1$. The deviation suggested the formation of polynuclear thiocyanato complexes of cadmium(II) in aqueous solution. Therefore, the analysis of the calorimetric data for the cadmium(II) thiocyanate system was carried out by taking into account the formation of polynuclear complexes. The results obtained by the least-squares method are summarized in Table IX. Theoretical curves calculated by using the constants finally optimized well reproduced the experimental points over the whole range of C_X/C_M for both the zinc(II) and cadmium(II) thiocyanate systems as drawn by the solid lines in Figures 10 and 11, respectively.

Distribution of the thiocyanato complexes of zinc(II) and cadmium(II) in aqueous solution is illustrated in Figures 12 and 13, respectively. Since the dinuclear $[Cd_2(SCN)]^{3+}$ complex is formed in aqueous cadmium(II) thiocyanate solutions, and thus, the distribution of species changes depending on the concentration of cadmium(II) ion in a solution, the concentration of cadmium(II) ion of 0.1 mol dm^{-3} was used to calculate the distribution of species in cadmium(II) thiocyanate solutions.

TABLE IX

The least-squares refinements of formation constants β_{pq} and enthalpies $\Delta H^\circ_{\beta pq}$/kJ mol^{-1}, of the reaction, $qM^{z+} + pX^- = M_qX_p^{(zq-p)+}$ (M = Zn or Cd, and X = SCN0 in aqueous solution at 25°C.

	Zn(II)	Cd(II)
β_{11}	8.3 ± 0.33	23.48 ± 0.01
β_{21}	39 ± 3	58.52 ± 0.01
β_{31}	147 ± 11	65.97 ± 0.01
β_{41}	327 ± 22	100 ± 4
β_{12}	–	17.83 ± 0.01
$\Delta H^\circ_{\beta 11}$	−5.04 ± 0.07	−10.19 ± 0.06
$\Delta H^\circ_{\beta 21}$	−2.1 ± 0.14	−30.3 ± 0.3
$\Delta H^\circ_{\beta 31}$	−8.4 ± 0.4	−7.7 ± 0.6
$\Delta H^\circ_{\beta 41}$	−12.8 ± 0.2	−30.5 ± 0.2
$\Delta H^\circ_{\beta 12}$	–	−14.8 ± 0.4

Uncertainties of constants refer to standard deviations.

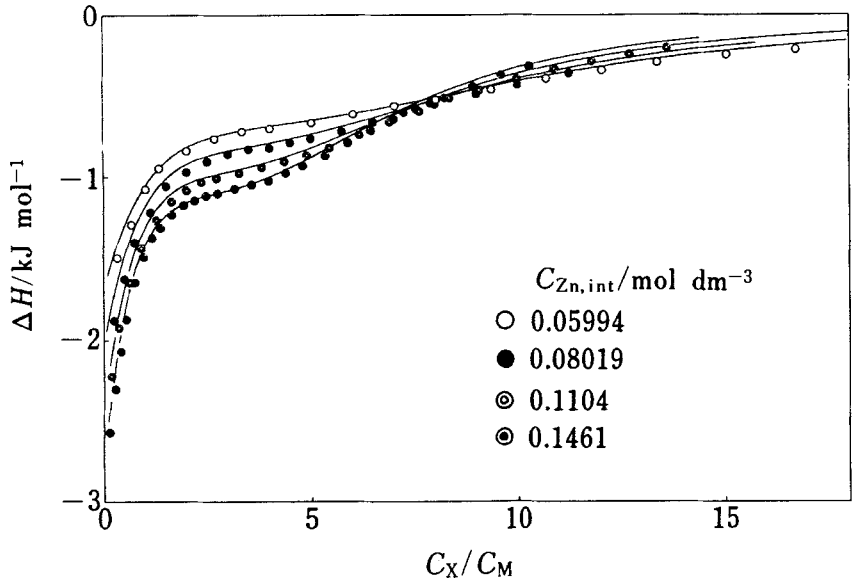

FIGURE 10. Calorimetric titration curves of the zinc(II) thiocyanate aqueous solutions containing 5 mol dm^{-3} $NaClO_4$ at 25°C. The solid lines show the curves calculated by using the constants in Table IX.

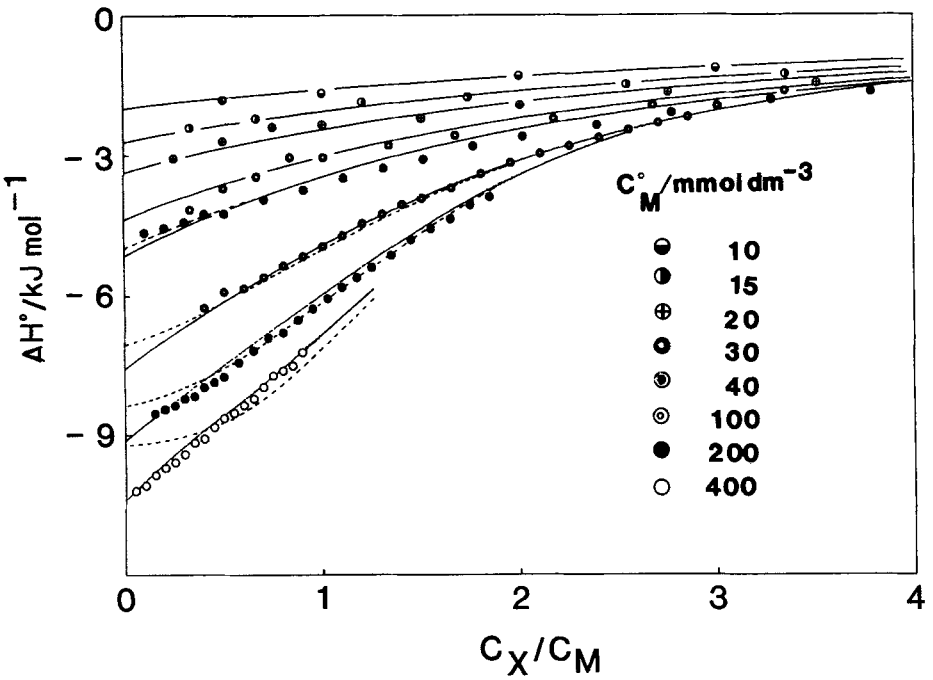

FIGURE 11. Calorimetric titration curves of the cadmium(II) thiocyanate aqueous solutions containing 3 mol dm^{-3} $NaClO_4$ at 25°C. The solid lines show the curves calculated by using the constants in Table IX.

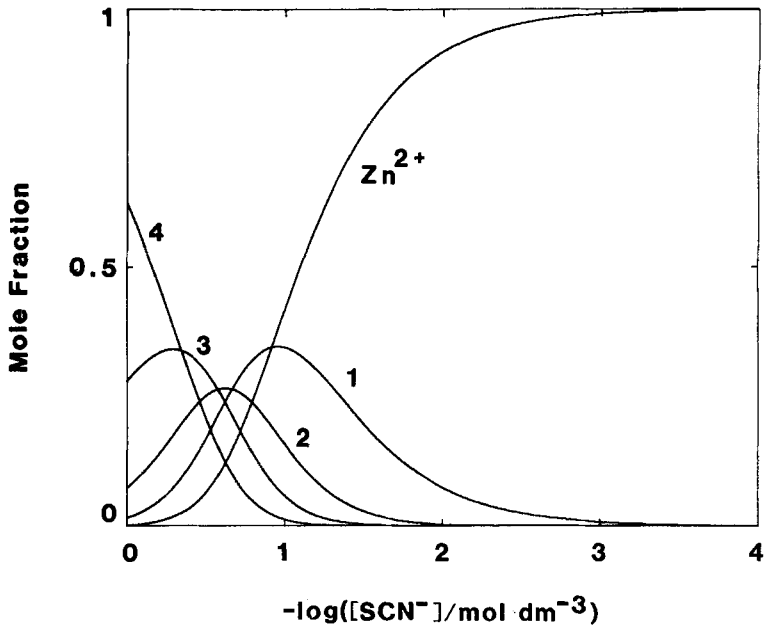

FIGURE 12. Distribution of zinc(II) thiocyanato complexes in 5 mol dm^{-3} $NaClO_4$ aqueous solution at 25°C.

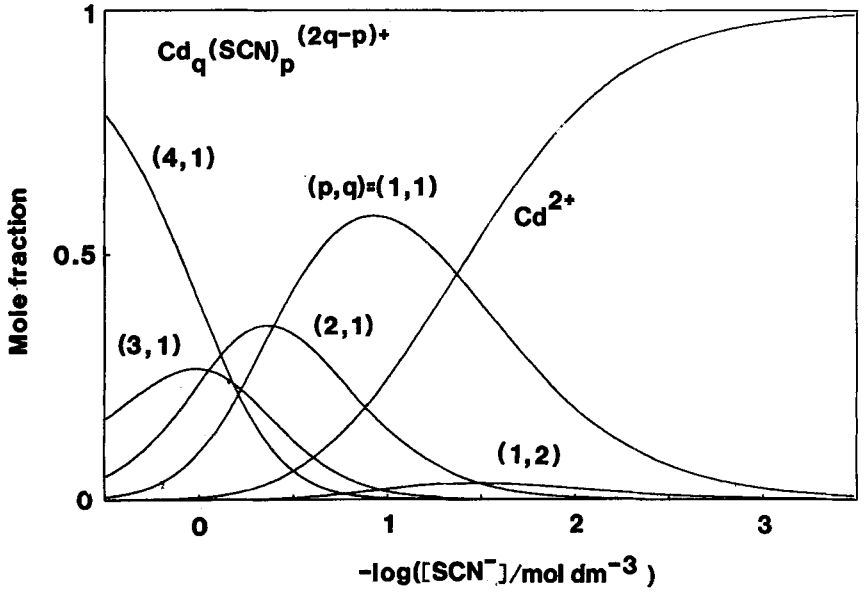

FIGURE 13. Distribution of cadmium(II) thiocyanato complexes in 3 mol dm^{-3} $NaClO_4$ aqueous solution at 25°C. $[Cd^{2+}]_{tot}$ = 0.1 mol dm^{-3}.

5.3 *Structures of* $[MX_4]^{2-}$ *(X = SCN⁻ and M = Zn, Cd and Hg) in Water*[67]

X-ray scattering measurements were carried out for zinc(II), cadmium(II) and mercury(II) thiocyanate aqueous solutions at 23°C, each solution contained 1 mol dm^{-3} metal ions and 7 mol dm^{-3} SCN^- ions, and thus, excess amounts of SCN^- ions were added to the solutions in the form of NH_4SCN. In all the metal thiocyanate solutions, the tetrathiocyanato complex was formed as a predominant species, and thus, the X-ray scattering data obtained reflected the structure of the complex in each metal thiocyanate solution. The measurements were also carried out for the 7 mol dm^{-3} ammonium thiocyanate solution as reference as will be discussed later. By analyzing the X-ray scattering data, the total radial distribution function (RDF) in the form of $(D(r) - 4\pi r^2\rho_0)$ was obtained.

In order to extract the peaks originating from zinc(II), cadmium(II) and mercury(II) thiocyanato complexes in the solutions, the RDF of NH_4SCN solution was subtracted from the RDFs of the metal thiocyanate solutions. The difference RDFs thus obtained for the mercury(II), zinc(II) and cadmium(II) thiocyanate solutions are shown in Figures 14, 15 and 16 (the thick solid line, the lower figure), respectively. Since an ammonium ion has a similar size to that of a water molecule and all the sample solutions contained an almost equal amount of SCN^- ions as well as the sum of $([NH_4^+] + [H_2O])$, the bulk structure and the hydration structure of SCN^- ion may be similar in all the solutions as the first approximation. Thus, in the difference RDFs, the contribution of the bulk water and the SCN^- hydration structures is mostly eliminated and hence the peaks due to the metal thiocyanato complexes in the solutions are emphasized.

In the difference RDF of the mercury(II) thiocyanate solution there are two peaks centered at 254 and 415 pm. From the sum of the covalent radii of Hg and S (148 and 104 pm,[68] respectively) and the mean Hg–S bond length of 255 pm reported in a structure determination of $[Hg(SCN)_4][Cu(en)_2]$ crystal,[64] the first peak at 254 pm can

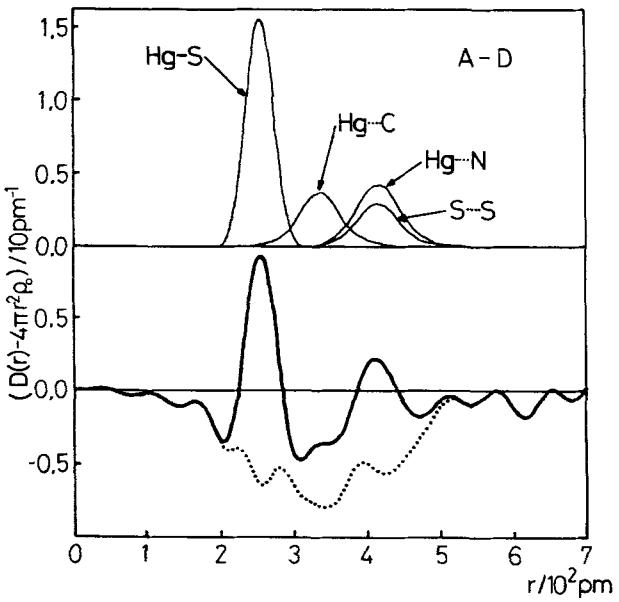

FIGURE 14. Difference RDF of aqueous mercury(II) thiocyanate solution (the thick solid line, the lower figure) and the residue (the dotted line, the lower one) obtained after subtraction of the peak shapes (the thin solid lines, the upper one).

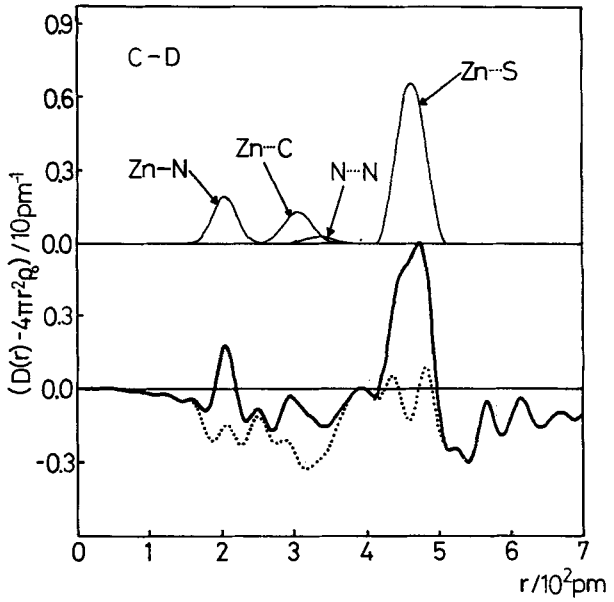

FIGURE 15. Difference RDF of aqueous zinc(II) thiocyanate solution (the thick solid line, the lower figure) and the residue (the solid line, the lower one) obtained after subtraction of the peak shapes (the thin solid lines, the upper one).

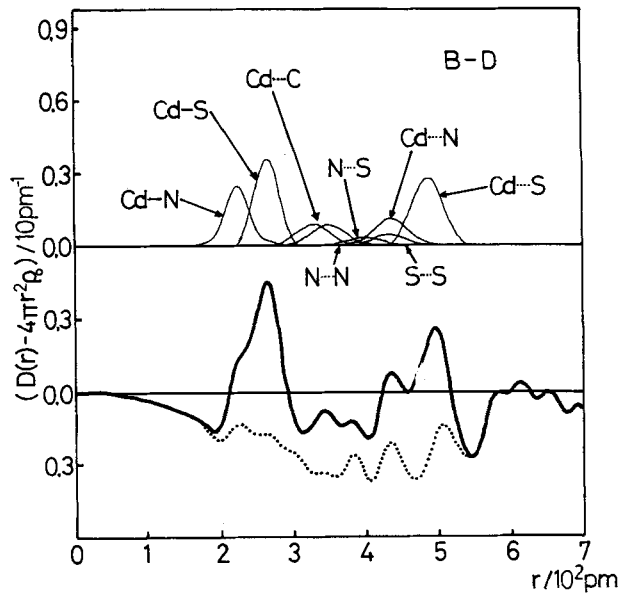

FIGURE 16. Difference RDF of aqueous cadmium(II) thiocyanate solution (the thick solid line, the lower figure) and the residue (the dotted line, the lower one) obtained after subtraction of the peak shapes (the thin solid lines, the upper one).

be assigned to the Hg-S bonds within $[Hg(SCN)_4]^{2-}$. In the crystal structure of $[Hg(SCN)_4][Cu(en)_2]$, nonbonding Hg-N and interligand S-S interactions appear around 400 and 420 pm, respectively, and hence they are possibly responsible for the peak at 415 pm in the difference RDF of the mercury(II) thiocyanate solution.

In the case of the zinc(II) thiocyanate solution, the difference RDF shows distinct peaks at 204 and 462 pm. On the basis of the effective ionic radii of Zn and N atoms (60 and 146 pm,[69] respectively) and the knowledge of the mean Zn-N (200 pm) and nonbonding Zn-S (470 pm) lengths within the $[Zn(NCS)_4]^{2-}$ moiety in β-$Zn(SCN)_2$ crystal,[63] the peaks around 204 and 462 pm are assignable to the Zn-N and Zn-S interactions, respectively, within $[Zn(NCS)_4]^{2-}$.

The difference RDF of the Cd(II) thiocyanate solution is more complex with peaks at 265, 435 and 490 pm and with a shoulder at 225 pm. The bond lengths of 225 and 265 pm well coincide, respectively, with the sum of the effective ionic radii of Cd and N, and of Cd and S (Cd: 78 pm, N: 146 pm and S: 184 pm[69]). In the crystal structure of $Cd(SCN)_2$ having two Cd-N and four Cd-S bonds,[62] the Cd-N and Cd-S distances have been reported to be 224 - 225 and 271 - 280 pm, respectively. On the basis of these facts, it can be concluded that the peak at 265 pm with the shoulder at 225 pm consists of both Cd-S and Cd-N bonds within the cadmium(II) tetrathiocyanato complex in aqueous solution.

A quantitative analysis of the X-ray scattering data was performed by comparing experimental values with theoretical ones calculated by a model both in the difference RDFs and in the difference structure functions.

A theoretical structure function of atom pairs 'i-j' was calculated by the Debye equation,

$$i(s)_{calc} = \sum n_{ij} f_i(s)[\sin(sr_{ij})/(sr_{ij})]\exp(-b_{ij}s^2) \qquad (25)$$

where r_{ij}, b_{ij} and n_{ij} represent the interatomic distance, the temperature factor and the number of interactions, respectively. The corresponding peak shape is obtained by the Fourier transform of the $s \cdot i(s)_{calc}$ values.

Finally, the difference RDFs of the zinc(II), cadmium(II) and mercury(II) thiocyanate solutions were analyzed. In the difference RDF of the Hg(II) system, the peak shape calculated for four Hg-S interactions were compared reasonably with the contour of the first peak at 254 pm, suggesting the tetrahedral coordination of four SCN^- ions to mercury(II) ion. On the basis of the tetrahedral geometry of $[Hg(SCN)_4]^{2-}$, the interligand S-S interaction was estimated to be 415 pm, a corresponding peak appearing at 417 pm in the difference RDF. The nonbonding Hg-N interaction should also appear around 417 pm according to the crystal structure of $[Hg(SCN)_4][Cu(en)_2]$. The distance of the Hg-C interaction within $[Hg(SCN)_4]^{2-}$ was also estimated to be 330 pm from the crystal structure data.[64] The peak shapes calculated for these atom pairs are shown in Figure 14 (upper). Subtraction of the sum of the peak shapes from the difference RDF gave the residue shown by the dotted line in Figure 14 (lower). Thus, the difference RDF of the mercury(II) thiocyanate solution was satisfactorily explained by the tetrahedral coordination model of four SCN^- ions to mercury(II) ion through the S atom.

A similar analysis applied to the difference RDF of the zinc(II) thiocyanate solution resulted in four Zn-N bonds from the area of the peak at 204 pm. Four Zn-S interactions also satisfactorily explained the distinct peak at 460 pm. On the basis of the Zn-N and Zn-S distances and a linear SCN^- ion, the Zn-C interaction was expected to appear at 310 pm, consistent well with the peak at 310 pm in the difference RDF. The theoretical peak shapes due to the Zn-N, Zn-S, Zn-C and N-N interactions were calculated for the theoretical model of the $[Zn(NCS)_4]^{2-}$ complex and subtracted from the difference RDF. In the resulting residue shown by dots in Figure 15, a small and broad peak still

remains at 350 - 500 pm, which may be physically insignificant features judging from uncertainties in the difference RDF.

In the case of the cadmium(II) thiocyanato complex, the first peak at 200 - 300 pm was analyzed by a trial-and-error method assuming various combinations of Cd-N and Cd-S interactions, and the most likely model attained was the one with two Cd-N and two Cd-S bonds per Cd(II). Nonbonding Cd-N and Cd-S interactions were assigned to the peaks at 440 and 490 pm, respectively, from the structural data of $Cd(SCN)_2$ crystal.[62] The Cd-C and interligand N-N, S-S and N-S distances were calculated from the tetrahedral geometry of the tetrathiocyanato complex with the linear SCN^- ion coordinated and their peaks are shown in Figure 16. Small peaks at 380 - 500 pm left after subtraction of the sum of the peak shapes from the difference RDF are probably related to other interligand interactions which were not taken into consideration.

A direct comparison between experimental and theoretical difference structure functions were also performed by minimizing the error square sum,

$$U = \sum_{s_{min}}^{s_{max}} s^2\{\Delta i(s)_{obsd} - \Delta i(s)_{calcd}\}^2 \qquad (26)$$

where $\Delta i(s)_{obsd}$ denotes the difference structure functions experimentally obtained by subtraction of the total $i(s)$ values of NH_4SCN solution from those of metal thiocyanate solutions, s_{min} and s_{max} the lower and upper limits of the s-range used in the calculations, respectively.

The model considered had the following characteristics:

a) Four SCN^- ions coordinate to zinc(II) ion through the N atom, and to mercury(II) ion through the S atom. Cadmium(II) ion is bound with two SCN^- ions through the N atom and the other two through the S atom.

TABLE X

Distances r/pm, temperature factors b/(10^2pm^2), number of interactions n and the bond angles θ/° used in the model calculations described in the text. The estimated standard deviations are given in parentheses.

		$[Hg(SCN)_4]^{2-}$	$[Cd(NCS)_2(SCN)_2]^{2-}$		$[Zn(NCS)_4]^{2-}$
M-N	r	415(4)	224.6(6)	435(2)	204.1(3)
	b	2.5[a]	0.25(8)	1.4(4)	0.30(5)
	n	4[a]	2[a]	2[a]	4[a]
M-C	r	335(4)	328(2)	349(3)	305[a]
	b	2.0[a]	1.5[a]	1.5[a]	1.0[a]
	n	4[a]	2[a]	2[a]	4[a]
M-S	r	253.5(5)	486.7(3)	264.9(3)	462(1)
	b	0.86(8)	1.8(2)	0.77(5)	1.5[a]
	n	4[a]	2[a]	2[a]	4[a]
N-N	r		367[b]		333[b]
	b		0.8[a]		1.0[a]
	n		1[a]		6[a]
S-S	r	414[b]	433[b]		414[b]
	b	2.5[a]	1.7[a]		2.5[a]
	n	6[a]	1[a]		6[a]
N-S	r		400[b]		
	b		1.5[a]		
	n		4[a]		
θ(M-N-C)			149(1)		145(1)
θ(M-S-C)		102(2)		106(1)	

[a]Fixed. [b]Assumed that θ(N-M-N) = θ(N-M-S) = 109.5°.

b) The interactions between atoms directly bound to metal ion were taken into account by assuming the tetrahedral coordination of the atoms around the metal ion.

c) The interactions between metal ion and the N and/or S atoms of SCN^- ion were defined by their interatomic distances, temperature factors, and the number of interactions (= 4), and the corresponding parameters r_{ij} and b_{ij} were allowed to vary independently with the coordination number fixed to the value of four. Parameters (r and b) due to the nonbonding M-C interaction were also allowed to vary in order to examine the deviation from the linearity of the SCN^- ion.

The final results of important parameters are summarized in Table X. On the basis of the M-N, M-C and M-S distances within the tetrathiocyanato complexes of the metal ions, we see that the SCN^- ion within the complex has an almost linear structure.

5.4 *Raman Spectra of the Thiocyanato Complexes of Zinc(II), Cadmium(II) and Mercury(II)*

Raman spectra of the C-N and C-S stretching vibrations in the zinc(II), cadmium(II)

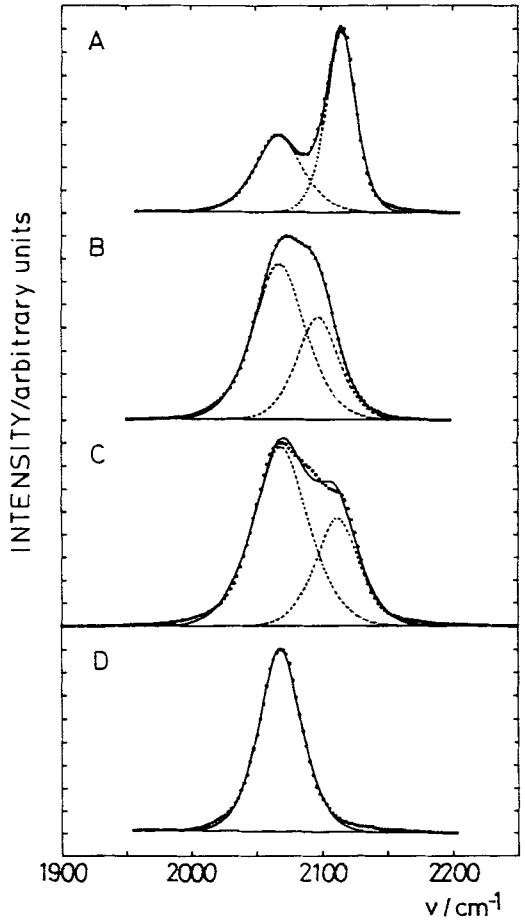

FIGURE 17. Raman spectra of the C-N stretching vibration of SCN^- ion in aqueous solutions of mercury(II) thiocyanate (A), cadmium(II) thiocyanate (B), zinc(II) thiocyanate (C) and ammonium thiocyanate (D). The dots represent the observed intensities and the solid lines show the sum of the components (the broken lines) obtained by the least squares fits.

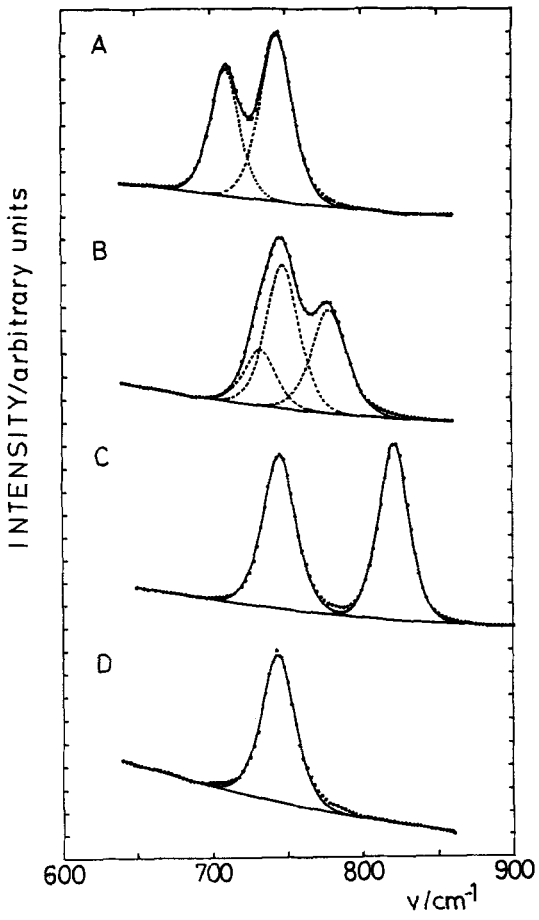

FIGURE 18. Raman spectra of the C-S stretching vibration of SCN^- ion in aqueous solutions of mercury(II) thiocyanate (A), cadmium(II) thiocyanate (B), zinc(II) thiocyanate (C) and ammonium thiocyanate (D). The dots represent the observed intensities and the solid lines show the sum of the components (the broken lines) obtained by the least squares fits.

and mercury(II) solutions which have been used for X-ray scattering measurements, as well as an ammonium thiocyanate solution, are shown by dots in Figures 17 and 18, respectively.

A quantitative analysis of the Raman bands was performed by a nonlinear least-squares method by assuming the Lorentzian-Gaussian function expressed by

$$I(\nu) = I(\nu_0)[\exp\{-4\ln 2((\nu-\nu_0)/\sigma)^2\}\{1+(\nu-\nu_0)/\sigma\}^{-1}]^{1/2} \quad (27)$$

where $I(\nu_0)$ denotes the peak height at the peak position ν_0 and σ represents the half width of the peak. Parameters $I(\nu_0)$, ν_0 and σ were allowed to vary independently in the optimizing procedure.

Resolved peak components are shown by the broken lines in Figures 17 and 18, respectively, for the C-N and C-S bands. The sum of the components thus calculated is

TABLE XI
Raman frequencies of the C-S and C-N stretching bands of the tetrathiocyanato complexes of mercury(II), cadmium(II) and zinc(II) ions in aqueous solutions.

	$[Hg(SCN)_4]^{2-}$	$[Cd(SCN)_2(NCS)_2]^{2-}$	$[Zn(NCS)_4]^{2-}$	free SCN^-	Ref.
C-S band	710	779 732	821	747	67
	717	747	817		55
			823		57
		784			58
C-N band	2117	2105	2114	2068	67
	2114	2098	2110		55
		2102			58

given by the solid lines in the figures, which well agrees with the experimental value. The C-S and C-N stretching vibrational frequencies thus determined are summarized in Table XI, together with those reported previously.[55,57,58]

As seen in Figure 17, the C-N vibrational band at 2068 cm^{-1} observed in all the thiocyanate solutions is assigned to that of free SCN^- ion on the basis of the spectrum of the NH_4SCN solution. The bands around 2100 cm^{-1} appearing in the metal thiocyanate solutions, the frequencies of which well agree with those reported previously (Table XI),[55,58] are ascribed to SCN^- ions bound to a metal ion. As seen in Table XI, in the case of the bonding between a metal ion and an SCN^- ion through its S atom, the C-N band appears at a higher frequency than that of free SCN^- ion. The C-N vibrational frequency also increases when the nitrogen atom of SCN^- ion binds to a metal ion. The frequency shift of the C-N band is thus not indicative of the bonding type of SCN^- ion with a metal ion.

On the other hand, the frequency shift of the C-S band is distinct (see Figure 18 and Table XI) to specify the bonding atom of SCN^- ion with a metal ion. The C-S vibrational band of SCN^- ion bound to a metal ion shifted toward a higher frequency for the zinc(II) thiocyanato complex, but shifted toward a lower frequency for the mercury(II) thiocyanato complex, relative to that of free SCN^- ion. In the case of the cadmium(II) thiocyanate solution, two C-S vibrational bands were observed around 745 and 780 cm^{-1}. These bands have been reported in Refs. 57 and 60. However, a preliminary analysis of the C-S vibrational bands assuming two Lorentzian-Gaussian components failed, and the error-square sum decreased significantly by assuming three peak components and the whole contour of the spectrum was satisfactorily reproduced. The frequencies of the bands finally obtained are listed in Table XI and the corresponding peaks are shown by the broken lines in Figure 18(B). The bands appearing at the lower and higher frequencies than the band of free SCN^- ion may be ascribed to those of SCN^- ion bound to cadmium(II) ion through the N and S atom, respectively, and the result is inconsistent with that revealed by the X-ray diffraction study of the cadmium(II) thiocyanate solution as described in a previous section.

Raman spectra of cadmium(II) thiocyanate aqueous solutions were also measured with varying ratios C_X/C_M where C_X and C_M stand for the total concentrations of SCN^- and cadmium(II) ions, respectively, in a solution. Raman spectra of the C-N and C-S stretching vibrations of SCN^- ion thus measured are shown in Figures 19 and 20, respectively. The Raman bands observed were assigned by taking into account the distribution of species in each cadmium(II) thiocyanate solution.

The Raman spectra in Figure 19 show three peaks at *ca.* 2070, 2105 and 2130 cm^{-1}, the first band being ascribed to the vibration of free SCN^- ion. It was indicated from the result of calorimetric measurements that $[CdX]^+$ and $[Cd_2X]^{3+}$ (X = SCN) were formed in cadmium(II) thiocyanate solutions at $C_X/C_M < 1$ and the $[Cd_2X]^{3+}$ complex

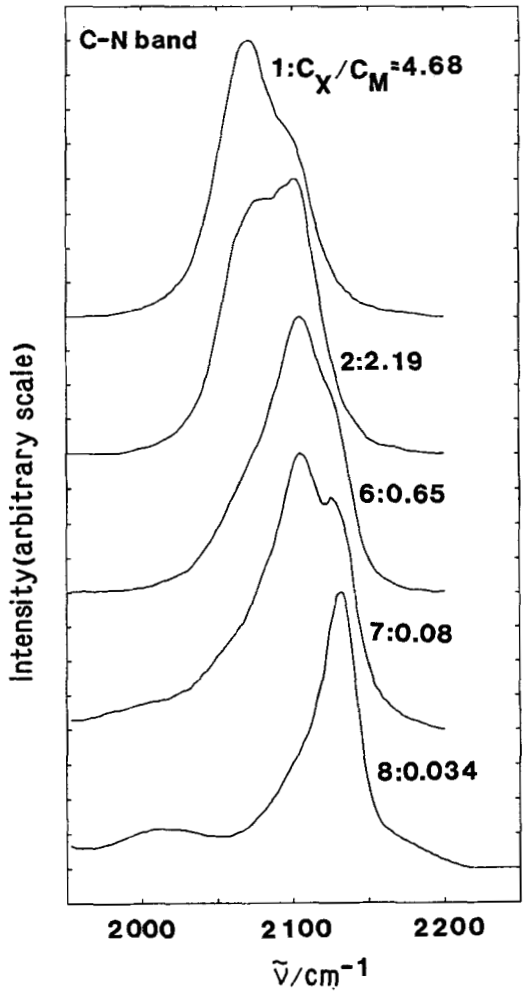

FIGURE 19. Raman spectra of the C-N stretching vibration of SCN^- ion observed in cadmium(II) thiocyanate solutions with varying molar ratios of the metal to ligand ions.

predominated in the solutions with lowering ratios of C_X/C_M. Two peaks at 2105 and 2130 cm^{-1} were observed in the solutions of $C_X/C_M = 0.08$, while the former peak disappeared in the solution of $C_X/C_M = 0.032$. Thus, the 2105 cm^{-1} and 2130 cm^{-1} bands were assigned to the C-N vibrations within $[CdX]^+$ and $[Cd_2X]^{3+}$, respectively.

The Raman spectra in Figure 20 show predominant peaks at *ca.* 720, 740 and 780 cm^{-1}, the second band being attributable to the vibration of free SCN^- ion. In the solutions of $C_X/C_M = 0.65 - 2.19$ examined, the intensity of the 780 cm^{-1} band relative to that of the 720 cm^{-1} band increased with increasing ratios C_X/C_M, and thus, these two bands should be assigned to the vibration of, at least, two different species. Since it was indicated from the distribution of species in the solutions that $[CdX]^+$ was present as the main species and the concentration of the complex increased with increasing ratios

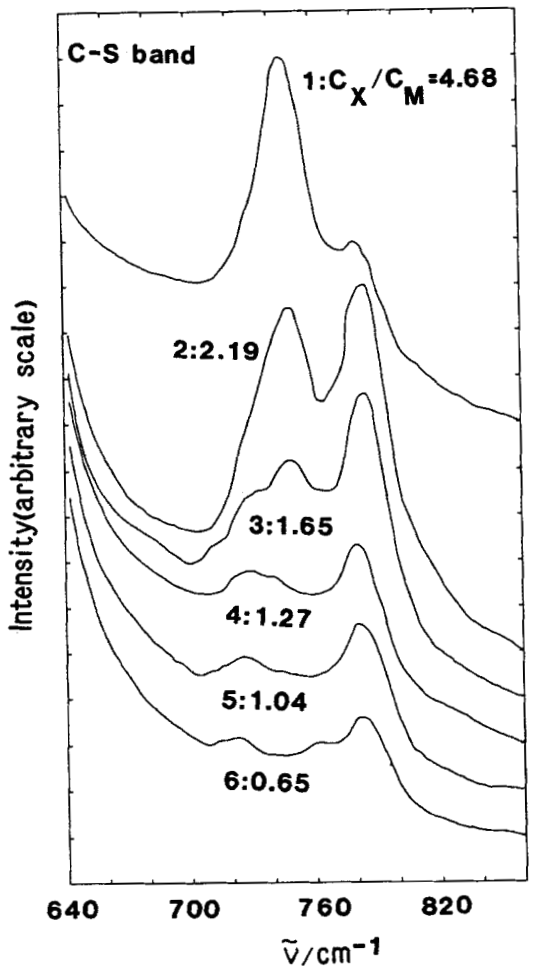

FIGURE 20. Raman spectra of the C-S stretching vibration of SCN^- ion observed in cadmium(II) thiocyanate solutions with varying molar ratios of the metal to ligand ions.

of C_X/C_M in the range 0.65 - 1.65, the 780 cm^{-1} band was assigned to the C-S stretching vibration within $[CdX]^+$. Since it was indicated from the calorimetric measurements that $[Cd_2X]^{3+}$ was appreciably formed in the solutions of C_X/C_M = 0.65 - 1.04 and $[CdX_2]$ in the solutions of C_X/C_M = 1.27 - 2.19, a weak band observed at 720 cm^{-1} may be ascribed to the C-S stretching vibrations of the complexes.

5.5 *Coordination Structure of $[Cd_2X]^{3+}$ and $[CdX_n]^{(2-n)+}$ (X = SCN)*

Within thiocyanato complexes of metal ions, zinc(II) ion is coordinated with N atom of SCN^- ion, but it was suggested that cadmium(II) ion is coordinated with both the N and S atoms of SCN^- ions as discussed in preceding sections.

It has been known that the C-S stretching vibration of SCN^- ion shifts toward the higher and lower frequencies, respectively, within metal complexes than that of the free ion as the result of the coordination of SCN^- ion to a metal ion through the N and S

TABLE XII

Thermodynamic quantities, ΔG_n°/kJ mol^{-1}, ΔH_n°/kJ mol^{-1} and ΔS_n°/J K^{-1} mol^{-1}, for the stepwise formation of $[MX_n]^{(2-n)+}$ (M = Zn or Cd, X = SCN and n = 1-4) in water and in dimethyl sulfoxide at 25°C.

	Cd(II)		Zn(II)	
	Water[a] 3 mol dm^{-3} $NaClO_4$	DMSO[b] 1 mol dm^{-3} NH_4ClO_4	Water[c] 5 mol dm^{-3} $NaClO_4$	DMSO[d] 1 mol dm^{-3} NH_4ClO_4
ΔG_1°	−7.8	−10.3	−5.2	−7.9
ΔG_2°	−2.3	−5.2	−3.8	−8.1
ΔG_3°	−0.3	−1.2	−3.3	−13.7
ΔG_4°	−1.0	–	−2.0	−9.4
ΔH_1°	−10.2	−3.0	−5.0	5.5
ΔH_2°	−20.1	−2.8	2.9	23.5
ΔH_3°	22.6	4.2	−6.3	−17.8
ΔH_4°	−22.8	–	−4.4	−10.7
ΔS_1°	−8	25	1	45
ΔS_2°	−60	8	23	105
ΔS_3°	77	18	−10	−13
ΔS_4°	−73	–	−8	−4

[a]Ref. 66. [b] Ref. 70. [c]Ref. 14. [d]Ref. 71.

atoms.[53–58] The Raman bands observed at *ca.* 720 and 780 cm^{-1} thus indicated the formation of the complexes having the Cd-S and Cd-N bonds.

Thermodynamic quantities, ΔG_n°/kJ mol^{-1}, ΔH_n°/kJ mol^{-1} and ΔS_n°/J K^{-1} mol^{-1}, for the stepwise reaction, $[MX_{n-1}]^{(3-n)+} + X^- = [MX_n]^{(2-n)+}$ (M = Zn and Cd, X = SCN and n = 1-4), in aqueous solutions are summarized in Table XII, together with those in DMSO for comparison.[70,71] The ΔH_n° and ΔS_n° values for the $[CdX_n]^{(2-n)+}$ complexes in aqueous solution irregularly changes with n and they mostly compensated each other to result in a rather smooth change in ΔG_n°. The irregularities of ΔH_n° and ΔS_n° with n might be correlated to the bonding type of SCN^- ions with Cd(II) ion as well as a structural change in cadmium(II) thiocyanato complexes in aqueous solution.

[Cd(SCN)Cd]$^{3+}$. It is expected that two cadmium(II) ions are bridged by an SCN^- ion within the dinuclear complex. A similar bridged structure is found in $Cd(SCN)_2$ crystal. The $[Cd(SCN)Cd]^{3+}$ complex has both Cd-S and Cd-N bonds, and thus, showed the C-S vibrational band at 720 cm^{-1} which is an indicative of the Cd-S bond formation within the complex.

[Cd(NCS)]$^+$. Since the 780 cm^{-1} band is assigned to the C-S stretching vibration arising from Cd-N bonding within the mono(thiocyanato)cadmium(II) complex which predominantly formed in the solutions of C_X/C_M = 0.65-2.19 in Figure 20, the coordination structure $[Cd(NCS)]^+$ is suggested for the complex. The ΔS_1° value for the formation of the mono(thiocyanato)cadmium(II) complex is comparable with that of $[Zn(NCS)]^+$ in aqueous solution. The result may also support the formation of $[Cd(NCS)]^+$, instead of $[Cd(SCN)]^+$.

[Cd(SCN)(NCS)]. In the cadmium(II) thiocyanate solutions of C_X/C_M = 1.27 - 2.19, the mono- and di(thiocyanato)cadmium(II) complexes are formed but the formation of the dinuclear complex is negligible. Therefore, the 720 cm^{-1} band still observed in the solutions may arise from the formation of the Cd-S bond within the di(thiocyanato)-cadmium(II) complex. Consequently, the structure [Cd(SCN)(NCS)] having both Cd-S and Cd-N bonds is suggested. The stepwise ΔH_2° and ΔS_2° values for the reaction, $[Cd(NCS)]^+ + SCN^- = [Cd(SCN)(NCS)]$, are largely negative, which are probably due to the formation of a covalent-type bond between moderately soft cadmium(II) ion and the soft S atom of SCN^- ion.

[Cd(SCN)(NCS)$_2$]$^-$. Although there is no evidence for the structure of the tri(thiocyanato)cadmate(II) complex from Raman spectroscopic data, the structure

$[Cd(SCN)(NCS)_2]^-$ is suggested, because the tetra(thiocyanato)cadmate(II) complex may be formed from the trithiocyanato complex with an SCN^- ion by bonding through the S atom as discussed below.

$[Cd(SCN)_2(NCS)_2]^{2-}$. The ΔH_4° and ΔS_4° values were similar to the ΔH_2° and ΔS_2° values, respectively, the result indicating that the Cd-S bond may be formed at the formation of the tetra(thiocyanato)cadmate(II) complex in aqueous solution. From this result we concluded that the third complex is $[Cd(SCN)(NCS)_2]^-$, from which an additional Cd-S bond is formed to produce $[Cd(SCN)_2(NCS)_2]^{2-}$.

Relatively largely positive ΔH_3° and ΔS_3° values observed at the third step of formation of $[Cd(SCN)(NCS)_2]^-$ suggest the change in the coordination symmetry around cadmium(II) ion from octahedral to tetrahedral.

It is known that cadmium(II) ion is tetrahedrally coordinated with four SCN^- ions and no solvent molecules in the first coordination sphere within the tetra(thiocyanato)-cadmate(II) complex in aqueous solution. On the other hand, aquacadmium(II) ion is octahedrally coordinated with six water molecules in aqueous solution.[8] Thus, the coordination symmetry around cadmium(II) ion changes at a certain step of formaiton of the thiocyanato complex of the metal ion. When the symmetry changes from octahedral to tetrahedral, more than one (three in this case) water molecules should be replaced with an entering SCN^- ion. Such an extensive desolvation process should be accompanied by a relatively large entropy gain. At the same time, a large absorption of heat should result due to the rupture of many metal-solvent bonds. As seen in Table XII, the same trend in the variation of ΔH_n° has been observed in the formation of the thiocyanato complexes of cadmium(II) in DMSO.

It is noted that the ΔH_2° and ΔS_2° values are largely positive in the complex formation reaction of the zinc(II) thiocyanate system both in water and in DMSO (Table XII), and the result suggests that the coordination symmetry around zinc(II) ion may be changed at the second step of the complex formation. The structure change occurring at a different stage of the complex formation in the zinc(II) thiocyanate system from that in the cadmium(II) system may be due to a small ionic size of zinc(II) ion than that of cadmium(II) ion.

6. ENTHALPIES OF TRANSFER OF SINGLE IONS AND COMPLEXES FROM WATER TO A DIOXANE-WATER MIXTURE

6.1 *Introduction*

In the preceding chapter, we discussed solvent effects on complex formation equilibria between some metal ions and ligands in aqueous dioxane solutions. Changes in enthalpies of formation of a metal complex between water and a dioxane-water mixture is represented as the sum of enthalpies of transfer of species pertaining to the complex formation reactions. Therefore, enthalpies of transfer ΔH_t° of single ions and complexes from water to dioxane-water mixture (dioxane content: 0.2 mole fraction or 55.0 w/w%) have been evaluated by using an extrathermodynamic tetraphenylarsonium-tetraphenylborate assumption:[72]

$$\Delta H_t^\circ(Ph_4As^+) = \Delta H_t^\circ(BPh_4^-) \tag{28}$$

for dividing enthalpies of transfer of salts measured into those of each ionic component.

6.2 *Enthalpies of Transfer of Single Ions*

Enthalpies of solution of six salts were measured in water and in the 0.2 mole fraction

TABLE XIII
Enthalpies of solution (ΔH_s°) of some 1:1 electrolytes in water and in dioxane-water mixture (dioxane content: 0.2 mole fraction), and enthalpies of transfer (ΔH_t°) of the electrolytes from water to the mixture at 25°C.

Species	ΔH_s°(w) kJ mol^{-1}	ΔH_s°(mix) kJ mol^{-1}	ΔH_t° kJ mol^{-1}
$NaBPh_4$	−20.0	−39.4	−19.4
Ph_4AsCl	−10.2	5.7	15.9
NaCl	4.4	0.2	−4.2
$NaClO_4$	15.0	−9.4	−24.4
$(C_2H_5)_4NClO_4$	32.2	23.2	−9.0
$(C_2H_5)_4NCl$	−12.4	−1.4	11.0

TABLE XIV
Enthalpies of transfer (ΔH_t°) of single ions from water to the dioxane-water mixture (dioxane content: 0.2 mole fraction) at 25°C.

Ion	ΔH_t°/kJ mol^{-1}
Ph_4As^+	0.4
Bph_4^-	0.4
Na^+	−19.8
Cl^-	15.5
$(C_2H_5)_4N^+$	−14.5
ClO_4^-	−4.6

dioxane-water mixture and the results are summarized in Table XIII. At infinite dilution all the salts in Table XIII were assumed to be fully dissociated both in water and in the dioxane-water mixture, and thus, the enthalpy of transfer of salt i of 1:1 electrolyte (consisting of A^+ and B^-) from water to the mixture was represented as the sum of the enthalpies of transfer of each ionic component as follows:

$$\Delta H_t^\circ(A^+B^-) = \Delta H_t^\circ(A^+) + \Delta H_t^\circ(B^-) \tag{29}$$

Enthalpies of transfer of the six single ions were thus evaluated from those of the salts in Table XIII by applying the extrathermodynamic assumption in Eq. 28 to calculations for minimizing the error-square sum, $U = \Sigma\{\Delta H_{t,obsd}^\circ(i) - \Delta H_{t,calcd}^\circ(i)\}^2$. The enthalpies of transfer of the single ions from water to the 0.2 mole fraction dioxane-water mixture thus obtained are tabulated in Table XIV.

Enthalpies of solution of $NiCl_2$, $CuCl_2$, $AgClO_4$, sodium glycinate, glycine, sodium β-alaninate, β-alanine and ethylenediamine were also measured in these solvents and the values are summarized in Table XV. Sodium glycinate, sodium β-alaninate and ethylenediamine were dissolved in an alkaline solution to prevent protonation of the species. Glycine and β-alanine were dissolved in neutral solutions in which the species form their zwitterions.

It was assumed that $NiCl_2$, $CuCl_2$, $AgClO_4$, sodium glycinate and sodium β-alaninate are completely dissociated in the solvents examined, and the enthalpies of transfer of nickel(II), copper(II), silver(I), glycinate (gly^-) and β-alaninate (ala^-) ions from water to the dioxane-water mixture were thus estimated by subtracting the contribution of their counter ions which had been determined in advance.

TABLE XV

Enthalpies of solution (ΔH_s°) of some compounds in water and in the dioxane-water mixture (dioxane content: 0.2 mole fraction), and their enthalpies of transfer (ΔH_t°) from water to the mixture at 25°C.

Species	ΔH_s°(w) kJ mol^{-1}	ΔH_s°(mix) kJ mol^{-1}	ΔH_t° kJ mol^{-1}
$AgClO_4$	8.6	−17.9	−26.5
$CuCl_2$	−56.3	−61.0	−4.7
$NiCl_2$	−79.9	−90.0	−10.1
$Ni(gly)_2$	−30.5	−18.7	11.8
$Ni(gly)_2(H_2O)_2$	29.5	40.1	10.6
Aggly	33.2	36.3	3.1
Agala	25.6	24.8	−0.8
Hgly	15.0	16.2	1.2
Hala	9.5	16.3	6.8
Nagly[a]	−11.3	−2.4	8.9
Naala[a]	−19.4	−9.2	10.2
en[b]	−34.5(−32.0)	−34.8	−0.3

[a]Dissolved in solutions containing 0.01 mol dm^{-3} NaOH. [b]Dissolved in solutions containing 0.1 mol dm^{-3} LiOH and 3 mol dm^{-3} $LiClO_4$. The value in parentheses was obtained in the same alkaline solution without $LiClO_4$.

6.3 *Enthalpies of Transfer of Proton, Protonated Glycine, Protonated β-Alanine and Protonated Ethylenediamine from Water to an Aqueous Dioxane Solution*

Glycinate and β-alaninate ions react with proton to form zwitterions HL ($L^- = gly^-$ or ala^-) in aqueous solutions. Enthalpies of formation of the [HL] species in water and in the 0.2 mole fraction dioxane-water mixture are given in Table V. The difference between the enthalpies of formation of [HL] in these solvents is given by the enthalpies of transfer of the species participating in the formation reaction as follows:

$$\Delta H_{HL}^\circ(\text{mix}) - \Delta H_{HL}^\circ(\text{w}) = \Delta H_t^\circ(HL) - \Delta H_t^\circ(H^+) - \Delta H_t^\circ(L^-) \quad (30)$$

Since the ΔH_t° values of L^- and HL for glycine and β-alanine were already determined as described in the previous section, the enthalpy of transfer of proton $\Delta H_t^\circ(H^+)$ from water to the 0.2 mole fraction dioxane-water mixture could be evaluated.

By the same procedure as described above, enthalpies of transfer of $[H_2gly]^+$ and $[H_2ala]^+$ from water to the 0.2 mole fraction dioxane-water mixture were obtained by using Eq. (31):

$$\Delta H_{H_2L}^\circ(\text{mix}) - \Delta H_{H_2L}^\circ(\text{w}) = \Delta H_t^\circ(H_2L) - \Delta H_t^\circ(HL) - \Delta H_t^\circ(H^+) \quad (31)$$

where the ΔH_t° values of H^+ and [HL] were known.

Since the ΔH_t°(en) value was directly measured, the $\Delta H_t^\circ(Hen^+)$ and $\Delta H_t^\circ(H_2en^{2+})$ values were successively calculated by knowing the enthalpies of formation of the $[Hen]^+$ and $[H_2en]^{2+}$ in water and in the 0.2 mole fraction dioxane-water mixture and $\Delta H_t^\circ(H^+)$ evaluated above.

The enthalpies of transfer of glycinate and β-alaninate ions, ethylenediamine and their protonated species, together with the value of proton, from water to the 0.2 mole fraction dioxane-water mixture thus evaluated are summarized in Table XVI.

The enthalpy of transfer of proton was -22.7 kJ mol^{-1}, which was close to that of sodium ion (-19.8 kJ mol^{-1}).

The ΔH_t° value of ethylenediamine was practically zero. The ΔH_t° values of $[Hen]^+$ and $[H_2en]^{2+}$ were -20.0 and -41.7 kJ mol^{-1}, respectively, the latter value being double

TABLE XVI
Enthalpies of transfer (ΔH_t°) of single species from water to the dioxane-water mixture (dioxane content: 0.2 mole fraction) at 25°C.

Species	ΔH_t°/kJ mol^{-1}	Species	ΔH_t°/kJ mol^{-1}
H^+	−22.7	$[Ni(en)]^{2+}$	−38.9
Ag^+	−21.9	$[Ni(en)_2]^{2+}$	−35.2
Ni^{2+}	−41.1	$[Ni(en)_3]^{2+}$	−30.2
Cu^{2+}	−35.7	$[Cu(en)]^{2+}$	−35.0
gly^-	28.7	$[Cu(en)_2]^{2+}$	−33.1
β-ala^-	30.0	$[Ni(gly)]^+$	−12.7
en	−0.3	$[Ni(gly)_2]$	12.3
$[Hen]^+$	−20.0	$[Ni(gly)_3]^-$	39.8
$[H_2en]^{2+}$	−41.7	[Ag(gly)]	2.4
[Hgly][a]	1.2	$[Ag(gly)_2]^-$	28.6
$[H_2gly]^+$	−26.3	[Ag(ala)]	1.8
[Hala][a]	6.8	$[Ag(ala)_2]^-$	30.6
$[H_2ala]^+$	−20.8		

[a]Zwitterion, $^+H_3N(CH_2)_nCOO^-$.

of the former. These results suggest that the enthalpies of transfer of the protonated ethylenediamine species are mostly influenced by the change in solvation of charged ammonio groups within the species.

The enthalpies of transfer of $[H_2gly]^+$ and $[H_2ala]^+$ species, which have a charged ammonio group and a noncharged carboxyl group, were -25.6 and -20.8 kJ mol^{-1}, respectively, the values being not significantly different from that of $[Hen]^+$.

Glycinate and β-alaninate ions involving an anionic carboxylato group and a neutral amino group gave positive ΔH_t° values, 28.7 and 30.0 kJ mol^{-1}, respectively.

The enthalpies of transfer of zwitterionic glycine and β-alanine were small (1.2 and 6.8 kJ mol^{-1}, respectively), which might be compared with that of ethylenediamine (−0.3 kJ mol^{-1}). On the other hand, the enthalpy of hydration of glycine zwitterion in water was estimated to be −243 kJ mol^{-1},[73] which was considerably negative compared with those of noncharged molecules such as methylamine (-45.2 kJ mol^{-1}) and neutral acetic acid (-52.7 kJ mol^{-1}), although the value for the glycine zwitterion was less negative than those of $[H_2gly]^+$(-365.4 kJ mol^{-1}) and gly^- (-379.5 kJ mol^{-1}).[73] The result suggests that the glycine zwitterion is strongly hydrated in water through both the ammonio and carboxylate groups. A largely negative enthalpy of transfer of an ammonio group may be cancelled by a largely positive enthalpy of transfer of a carboxylate group within the zwitterionic glycine to lead to the small overall enthalpy of transfer of glycine from water to the dioxane-water mixture.

6.4 *Enthalpy of Transfer of Water*

The enthalpy of transfer of one mole of water molecules from an aqueous solution to the 0.2 mole fraction dioxane-water mixture was determinde by measuring enthalpies of solution of bis(glycinato)nickel(II) and diaquabis(glycinato)nickel(II) complexes in water and in the 0.2 mole fraction dioxane-water mixture. However, the solubilities of the complexes were too low both in water and in the mixture to directly measure heats of solution of the complexes with a sufficient accuracy. Therefore, the complex salts were dissolved in each of the solvents containing sodium or lithium glycinate in which the neutral complexes were expected to be fully converted into the tris(blycinato)-nickelate(II) complex, and thus, the measured enthalpies of dissolution of the bis-(glycinato)nickel(II) and diaquabis(glycinato)nickel(II) complexes in the solvents were respectively given as the sum of the enthalpy of solution ΔH_{s1}° of $[Ni(gly)_2]$ or ΔH_{s2}°

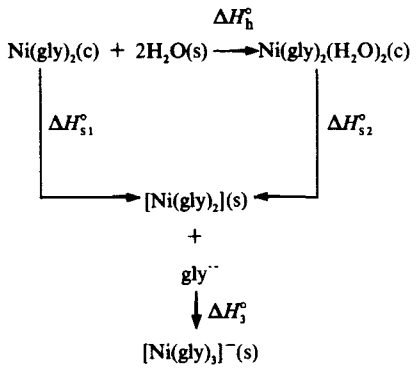

FIGURE 21 Relationship between ΔH°_{s1}, ΔH°_{s2}, ΔH°_h and ΔH°_3.

of $[Ni(gly)_2(H_2O)_2]$ and the enthalpy ΔH°_3 of the reaction, $[Ni(gly)_2] + gly = [Ni(gly)_3]^-$, in the solvents. Since the latter value was already determined (see Table VIII), the former values were obtained.

In a given solvent used, as is shown in Figure 21, enthalpies of solution of $[Ni(gly)_2]$ and $[Ni(gly)_2(H_2O)_2]$ are related to the enthalpy ΔH°_h of the reaction (32) as follows:

$$Ni(gly)_2(c) + 2H_2O(s) = Ni(gly)_2(H_2O)_2(c) \quad (32)$$

$$\Delta H^\circ_h = \Delta H^\circ_{s1} - \Delta H^\circ_{s2} \quad (33)$$

where (c) and (s) denote the crystalline and solution states, respectively. The enthalpy values of ΔH°_{s1}, ΔH°_{s2} and ΔH°_h thus obtained in water and in the 0.2 mole fraction dioxane-water mixture are summarized in Table XVII.

The difference between the enthalpies of reaction (32) in water (ΔH°_h(w)) and in the dioxane-water mixture (ΔH°_h(mix)) is attributable to the enthalpy of transfer of two moles of water molecules from water to the dioxane-water mixture:

$$\Delta H^\circ_t(H_2O) = (\Delta H^\circ_h(w) - \Delta H^\circ_h(mix))/2 \quad (34)$$

The values of ΔH°_h(w) and ΔH°_h(mix) were -60.0 and -48.8 kJ mol^{-1}, respectively, and thus, the $\Delta H^\circ_t(H_2O)$ value was estimated to be -0.6 kJ mol^{-1}. This result is consistent with the fact that the heat of mixing of water with dioxane is only slightly exothermic in a composition of water-rich dioxane-water mixtures.[74] The relatively small $\Delta H^\circ_t(H_2O)$ value suggests that interaction energies between water and dioxane molecules in the dioxane-water mixtures are not significantly different from the energy between water molecules in aqueous solution.

TABLE XVII

Enthalpies of solution,[a] ΔH°_s/kJ mol^{-1}, of anhydrous (ΔH°_{s1}) and dihydrate (ΔH°_{s2}) salts of bis(glycinato)-nickel(II) complex in water and in the dioxane-water mixture (dioxane content: 0.2 mole fraction) and related enthalpies (definition of which is given in Figure 21) at 25°C.

	$\Delta H^\circ_{s1} + \Delta H^\circ_3$	$\Delta H^\circ_{s2} + \Delta H^\circ_3$	ΔH°_3	ΔH°_{s1}	ΔH°_{s2}	ΔH°_h
water	−66.0	−6.0	−35.5	−30.5	29.5	−60.0
mixture	−55.4	3.4	−36.7	−18.7	40.1	−58.8
$\Delta\Delta H^\circ$[a]	10.6	9.4	−1.2	11.8	10.6	1.2

[a] $\Delta\Delta H^\circ = \Delta H^\circ$(mix) - ΔH°(w).

Since the interaction energies between solvent molecules in the two solvents are thus concluded to be similar, the difference in the enthalpies of transfer of ions and complexes from water to the dioxane-water mixture should be ascribed to the different solvation energies of the species in the solvents. Ions and complexes introduced from the gas phase to the solvents first destroy the solvent-solvent bonds and then are coordinated with water molecules liberated from the broken solvent structure in the bulk. The small $\Delta H_t^\circ(H_2O)$ value obtained suggests that an energy for an ion to break the solvent-solvent bonds is not appreciably different in water and in the dioxane-water mixture, and thus, a negative ΔH_t° value of the ion from water to the mixture may indicate that solvation of the ion is more enhanced in the mixture than in water. On the contrary, a positive ΔH_t° value of an ion may indicate that solvation of the ion is more weakened in the mixture than in water.

Proton, sodium, silver(I), nickel(II) and copper(II) ions which have relatively small ionic radii showed negative ΔH_t° values from water to the 0.2 mole fraction dioxane-water mixture, the result suggesting that solvation of the cations is enhanced in the mixture. On the other hand, chloride, glycinate and β-alaninate ions showed positive ΔH_t° values from water to the 0.2 mole fraction dioxane-water mixture, the reverse may show that solvation of the anion and carboxylate group within the ligands is weakened in the mixture.

6.5 *Enthalpies of Transfer of Metal Complexes*

By a similar way of evaluation of ΔH_t° of protonated ethylenediamine, and glycinate and β-alaninate ions, the enthalpies of transfer of ethylenediamine and glycinato complexes of nickel(II), ethylenediamine complexes of copper(II) and glycinato and β-alaninato complexes of silver(I) have been determined. The enthalpies of formation of a complex $[ML_n]$ (charge is omitted) pertaining to the reaction:

$$M + nL = [ML_n] \tag{35}$$

in water ($\Delta H_{\beta n}^\circ(w)$) and in the 0.2 mole fraction dioxane-water mixture ($\Delta H_{\beta n}^\circ(mix)$) are expressed in terms of the enthalpies of transfer of the free metal ion, ligand and complex as follows:

$$(\Delta H_{\beta n}^\circ(mix) - \Delta H_{\beta n}^\circ(w) = \Delta H_t^\circ(ML_n) - \Delta H_t^\circ(M) - n\Delta H_t^\circ(L) \tag{36}$$

The enthalpies of formation of the $[Ni(en_n)^{2+}$ (n = 1-3), $[Cu(en)_n]^{2+}$ (n = 1-2), $[Ni(gly)_n]^{(2-n)+}$ (n = 1-3), $[Ag(gly)_n]^{(1-n)+}$ (n = 1-2) and $[Ag(ala)_n]^{(1-n)+}$ (n = 1-2) complexes have been determined in these solvents (see Table VIII). Since the enthalpies of transfer of free nickel(II), copper(II), silver(I), glycinate and β-alaninate ions and ethylenediamine were already determined in the previous section, the enthalpies of transfer of the relevant complexes can be evaluated by using Eq. 36. Enthalpies of transfer of the metal complexes thus obtained are summarized in Table XVI, together with the enthalpies of transfer of the free metal ions, ligands and protonated ligands.

Plots of the ΔH_t° values of the $[Ni(gly)_n]^{(2-n)+}$, $[Ni(en)_n]^{2+}$ and $[Cu(en)_n]^{2+}$ complexes against n are shown in Figure 22. They linearly increase with n for all the complexes although the changes in ΔH_t° of the latter two which have a constant charge (+2) independent of n are rather insensitive to n.

The ethylenediamine complexes of nickel(II) and copper(II) ions gave relatively large and negative values of ΔH_t°. Since the first coordination shell of the metal ion within the complexes were occupied by ethylenediamine and water molecules except for the tris(ethylenediamine)-complexes, the result showed that solvation of the second coordination shell of the species was enhanced in the mixture than in water.

In the case of glycinato nickel(II) complexes in which the charge of the complexes changes with the number of glycinato ions within the complexes, the variation of ΔH_t°

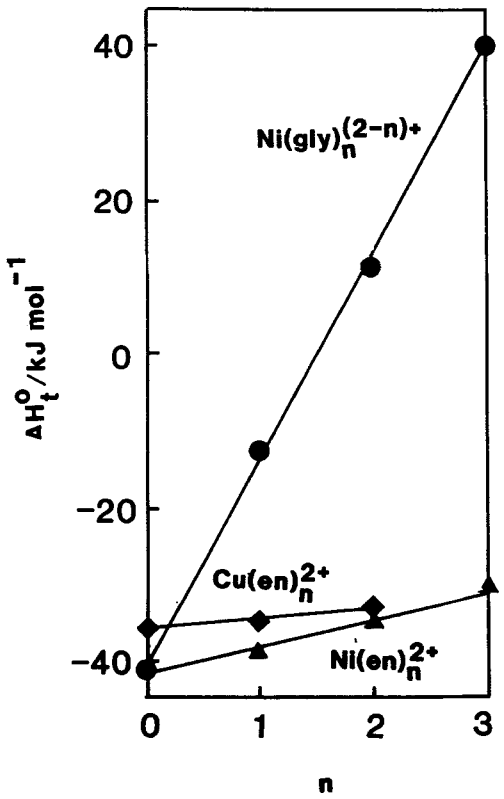

FIGURE 22. Enthalpies of transfer of the (glycinato)nickel(II), (ethylenediamine)nickel(II) and (ethylenediamine)copper(II) complexes plotted against n, the number of ligands within the complexes.

with n was much steeper than those of $[Ni(en)_n]^{2+}$ and $[Cu(en)_n]^{2+}$. Although the ΔH_t° value of the $[Ni(gly)]^+$ complex was still negative, the value was much less negative than the values of H^+, Na^+ and Ag^+ of the same charge. The ΔH_t° values of $[Ni(gly)_2]$ and $[Ni(gly)_3]^-$ were positive, the latter being much larger than that of glycinate or β-alaninate ion.

The linear relationship between ΔH_t° and n for the $[Ni(gly)_n]^{(2-n)+}$ complexes suggests that solvation of glycinate ions coordinated to the central nickel(II) ion is most responsible for the enthalpies of transfer of the complexes from water to the dioxane-water mixture. In the $[Ni(bly)_n]^{(2-n)+}$ complexes, one of oxygen atoms within each carboxylato group of glycinate ions combines with the central metal ions, while the other oxygen atom of the carboxylato group faces to solvent molecules in the second coordination shell to interact with them. Since free glycinate ion has a positive value of ΔH_t°, the interaction between the latter glycinato-oxygen atom and solvent molecules in the second coordination shell may have a positive contribution to the ΔH_t° values of the complexes. The linear change in the ΔH_t° of the $[Ni(gly)_n]^{(2-n)+}$ complexes with n suggests that the interaction between glycinatooxygen atoms and solvent molecules in the second coordination shell may proportionally change with the number of the oxygen atoms.

6.6 *Solvation of Ions in Water and Dioxane-Water Mixtures*

Ions and hydrophilic molecules are exothermically solvated with water. Water molecules are hydrogen-bonded with each other in the bulk, and ions and molecules introduced from the gas phase into water first destroy the water-water bonds and then are coordinated with water molecules liberated from the broken hydrogen-bonded structure in the bulk.

In a dioxane-water mixture, ions introduced into the mixture destroy the dioxane-water and water-water bonds. The bond energies between molecules in the mixture may be different from the water-water bonds in pure water, but the difference may be rather small because the enthalpy of transfer of water from an aqueous solution to the mixture was very small (-0.6 kJ mol^{-1}).

Consequently, a negative enthalpy of transfer of an ion or a molecule from water to a dioxane-water mixture reflects an enhancement of solvation of the species in the dioxane-water mixture than in water. On the other hand, a positive ΔH_t° value of a species indicates that solvation of the species is weakened in the mixture. Free metal ions show negative values of ΔH_t° as seen in Table XVI, but chloride, glycinate and β-alaninate ions exhibit positive enthalpies of transfer.

Solvation of positively charged ions is significantly enhanced in dioxane-water mixtures compared to that in water, while anions have much weaker solvation structures in the mixtures than in water. However, the solvent effect on the enthalpies of formation of various metal complexes and protonated ligands was relatively small. The difference between the enthalpies of stepwise formation of a protonated ligand in the 0.2 mole fraction dioxane-water mixture and in water, $\Delta H_n^\circ(\text{mix})-\Delta H_n^\circ(\text{w})$, is represented in terms of the enthalpies of transfer of the protonated species $\Delta H_t^\circ(H_nL)$ and proton $\Delta H_t^\circ(H^+)$ as follows:

$$\Delta H_n^\circ(\text{mix}) - \Delta H_n^\circ(\text{w}) = \Delta H_t^\circ(H_nL) - \Delta H_t^\circ(H_{n-1}L) - \Delta H_t^\circ(H^+) \quad (37)$$

The enthalpy values of $\Delta\Delta H_n^\circ(\Delta H_n^\circ(\text{mix}) - \Delta H^\circ(\text{w}))$, $\Delta H_t^\circ(H_nL)$ and $\Delta H_t^\circ(H^+)$ for the ethylenediamine and glycinate and β-alaninate ions are summarized in Table XVIII.

It is clearly seen from Table XVIII that the enthalpies of transfer of charged species have significantly large absolute values, but they compensate each other to lead to relatively small values of $\Delta\Delta H_n^\circ$. The same consideration can be made for the value $\Delta H_n^\circ(\text{mix})-\Delta H_n^\circ(\text{w})$ of the stepwise formation of a metal complex, which is given by $\Delta H_t^\circ(ML_n)-\Delta H_t^\circ(ML_{n-1})-\Delta H_t^\circ(L)$. The quantities for the ethylenediamine and glycinato complexes of nickel(II) ion, ethylenediamine complexes of copper(II) ion and glycinato and β-alaninato complexes of silver(I) ion are summarized in Table XIX.

Then questions may arise why solvation of a metal ion is enhanced and why solvation of an anionic species is weakened in dioxane-water mixtures than in water.

TABLE XVIII

Differences between stepwise enthalpies of formation of $[H_nL]$ in water and those in the dioxane-water mixture (dioxane content: 0.2 mole fraction), $\Delta\Delta H_n^\circ$/kJ mol^{-1} ($= \Delta H_n^\circ(\text{mix})-\Delta H_n^\circ(\text{w})$), and enthalpies of transfer, ΔH_t°/kJ mol^{-1}, of H^+, L and $[H_nL]$ from water to the mixture at 25°C

Species	$\Delta\Delta H_n^\circ$	$\Delta H_t^\circ(H_nL)$	$\Delta H_t^\circ(H_{n-1}L)$	$\Delta H_t^\circ(H^+)$
[Hgly]	−4.8	1.2	28.7	−22.7
[Hala]	−0.7	6.8	30.0	−22.5
$[Hen]^+$	3.0	−20.0	−0.3	−22.7
$[H_2gly]^+$	−4.8	−25.6	1.2	−22.7
$[H_2ala]^+$	−5.1	−20.8	6.8	−22.7
$[H_2en]^{2+}$	1.0	−41.7	−20.0	−22.7

TABLE XIX

Differences between stepwise enthalpies of formation of $[ML_n]$ in water and those in the dioxane-water mixture (dioxane content: 0.2 mole fraction), $\Delta\Delta H_n^\circ$/kJ mol^{-1} (= ΔH_n°(mix)-ΔH_n°(w)), and enthalpies of transfer, ΔH_t°/kJ mol^{-1}, of M^{2+}, L and $[ML]_n$ from water to the mixture at 25°C.

Species	$\Delta\Delta H_n^\circ$	$\Delta H_t^\circ(ML_n)$	$\Delta H_t^\circ(ML_{n-1})$	$\Delta H_t^\circ(L)$
$[Ni(en)]^{2+}$	2.5	−38.9	−41.1	−0.3
$[Ni(en)_2]^{2+}$ *3*	4.0	−35.2	−38.9	−0.3
$[Ni(en)_3]^{2+}$	5.3	−30.2	−35.2	−0.3
$[Cu(en)]^{2+}$	1.0	−35.0	−35.7	−0.3
$[Cu(en)_2]^{2+}$	2.2	−33.1	−35.0	−0.3
$[Ni(gly)]^+$	−0.3	−12.7	−41.1	28.7
$[Ni(gly)_2]$	−3.7	12.3	−12.7	28.7
$[Ni(gly)_3]^-$	−1.2	39.8	12.3	28.7
[Ag(gly)]	−4.4	2.4	−21.9	28.7
$[Ag(gly)_2]^-$	−2.5	18.6	2.4	28.7
[Ag(gly)]	−6.3	1.8	−21.9	30.0
$[Ag(ala)_2]^-$	−1.2	30.6	1.8	30.0

A water molecule has an oxygen atom as the electron donor (D_w) and two protons as the electron acceptor (A_w). They interact to form hydrogen-bonds in the bulk water and the equilibrium of the hydrogen-bonding between water molecules may be written as follows:

$$D_w + A_w = D_w{-}A_w \tag{38}$$

It should be noted that free D_w or A_w means not only a free water molecule, but also a terminal oxygen (D_w) or hydrogen (A_w) atom of water within a hydrogen-bonded network chain of water. The equilibrium in Eq. (38) is largely shifted toward the right hand side in pure water at room temperature.

A basic dioxane molecule may act as the donor (D_d) with a comparable donicity with water, because the donor number of dioxane (D_N = 14.8) is not largely different from that of water (D_N = 18.0). The acceptor property of dioxane is much smaller than that of water. Therefore, when dioxane is introduced in water, dioxane molecules may form a hydrogen-bonding associate with protons, *i.e.* the acceptor sites of water, as represented by D_d-A_w:

$$D_d + A_w = D_d{-}A_w \tag{39}$$

Thus, formation of the dioxane-water associates will shift the equilibrium between water molecules given in Eq. (38) to increase the concentration of D_w, while the concentration of A_w decreases due to the formation of the D_d-A_w associate.

A metal ion which is an electron acceptor interacts with oxygen donor atoms within water molecules to form a solvate species and an anionic species is solvated through protons within water molecules in aqueous solution.

$$M^{z+} + m\ D_w = [M(D_w)_m]^{z+} \tag{40}$$

$$L^- + m\ A_w = [L(A_w)_m]^- \tag{41}$$

and solvated metal ions and anionic ligands are in equilibrium with free D_w and A_w of water, respectively. In dioxane-water mixture, metal ions may be preferentially solvated with water molecules in a mixture with relatively low content of dioxane. Anionic

ligands may not be solvated with dioxane molecules because of its poor acceptor property. Threfore, the solvation of cations may be enhanced with the increase in the concentration of donor sites of water (D_w). On the contrary, anions are less solvated in the dioxane-water mixture due to the decrease in the acceptor sites (A_w) in the solvent.

7. COMPLEX FORMATION AND SOLVATION OF $[CuCl_n]^{(2-n)+}$ IN APROTIC SOLVENTS

7.1 *Introduction*

Although a number of studies have so far been carried out for electronic spectra of copper(II) chloro complexes in both crystalline and solution states, only a few quantitative investigations were examined for the formation of the complexes in solutions. Khan and Shwing-Weill[75] reported the formation constants and electronic spectra of $[CuCl_n]^{(2-n)+}$ (n = 1-4) in aqueous solution contining 5 mol dm^{-3} $Na(ClO_4, Cl)$ as a constant ionic medium. Elleb *et al.*[76,77] also spectrophotometrically studied the complex formation reactions in *N,N*-dimethylformamide (DMF) and dimethyl sulfoxide (DMSO) containing 1 mol dm^{-3} $LiClO_4$ and in propylene carbonate containing 0.1 mol dm^{-3} $(C_2H_5)_4NClO_4$. Manahan and Iwamoto[78] investigated the formation and electronic spectra of the copper(II) chloro complexes in acetonitrile (AN) by a combination of spectrophotometric and electrochemical methods. In weaker donor solvents such as acetonitrile and propylene carbonate, a series of four mononuclear complexes, $[CuCl_n]^{(2-n)+}$ (n = 1-4), were found. However, the only formation of $[CuCl]^+$, $[CuCl_3]^-$ and $[CuCl_4]^{2-}$ were concluded in stronger donor solvents such as DMSO and DMF.

Complex formation reactions of metal ions in aprotic solvents are markedly different from this in aqueous solution. It has already been elucidated that formation of copper(II) chloro complexes is enhanced in aprotic solvents with a weaker (acetonitrile[78] and propylene carbonate[77]) or a stronger (dimethyl sulfoxide[77] and *N,N*-dimethylformamide[76]) donicity than water. According to Ahrland,[79] it can be explained in terms of difference in solvation of chloride ion in water and in aprotic solvents. Solvation of chloride ion is enhanced in water, due to hydrogen-bonding with water molecules, compared to aprotic solvents. Ahrland[79] also pointed out that stepwise entropies of formation of metal complexes in aprotic solvents were generally larger than those in water, and thus, the larger entropies led to more favorable formation of the complexes in the former solvents than in the latter. Such a more favorable entropy of complex formation reactions of metal ions in aprotic solvents than in water is interpreted in terms of both different solvation structure of metal ions and different solvent structure between solvent molecules in aprotic solvents from those in water. In water, water molecules leave a hydrate structure and then enter another fairly well-ordered structure of bulk water. The entropy changes at the two stages compensate each other to yield a modest entropy gain, or even a net loss if the entropy changes connected with the coordination of the ligand is not so favourable. In an aprotic solvent, solvent molecules leave a solvate structure which may be more strictly ordered than the corresponding hydrate and then enter a bulk solvent that is fairly unstructured. Thus, a very large entropy gain may result.

A large difference in formation constants of copper(II) chloro complexes was also found in some aprotic solvents which have different donor and acceptor properties. Copper(II) chloro complexes are preferably formed in acetonitrile (AN) compared with those in *N,N*-dimethylformamide (DMF). Some typical physicochemical properties of acetonitrile and *N,N*-dimethylformamide are summarized in Table XX. Acetonitrile may form a weaker solvation structure with copper(II) ion than DMF. The acceptor

TABLE XX
Some physicochemical properties of acetonitrile and *N,N*-dimethylformamide.

	Acetonitrile	*N,N*-Dimethylformamide
Molecular weight	41.053	73.095
Boiling point/°C (1.0132×10^5 Pa)	81.6	153.0
Freezing point/°C	−43.835	−60.43
Density/g cm^{-3}	0.7766 (25°C)	0.94397 (25°C)
Viscosity/Pa s	0.000325 (30°C)	0.000802 (25°C)
Heat of vaporization/J mol^{-1}	33.2 (25°C)	47.5 (25°C) 38.3 (at b.p.)
Heat capacity/J K^{-1} g^{-1}	91.6 (26.84°C)	156.7 (25°C)
Conductivity/S^{-1} cm^{-1}	6×10^{-10} (25°C)	6×10^{-8} (25°C)
Dipole moment/C m	11.5×10^{-30} (3.44 D)	12.9×10^{-30} (3.86 D)
Relative dielectric constant	37.5 (20°C)	36.71 (25°C)
Donor number	14.1	26.6
Acceptor number	19.3	16.0

property of AN may be similar to that of DMF (see Table XX). Although the formation constants of copper(II) chloro complexes have been determined in several aprotic solvents, no enthalpy and entropy values of formation of the complexes have been reported.

Copper(II) ion within its chloro complexes is solvated with AN and DMF in the first solvation shell except for $[CuCl_4]^{2-}$ which may have a distorted T_d structure in the solvents, but solvation of DMF may be much preferable compared with that of AN owing to a larger donicity of the former solvent than the latter. However, a change in the acceptor ability of the central metal ion with varying numbers and kinds of ligands within the complex may also play an important role for solvation of metal ions in the solvents. The acceptor ability of the metal ion within the copper(II) chloro complexes may be decreased with increasing number of chloride ions within the complexes due to the electron donation from the chloride ions to the metal ion. Therefore, the strength of the metal solvent bonds within the chloro complexes of copper(II) may be weakened with the number of chloride ions within the complexes.

We investigated complex formation equilibria between copper(II) and chloride ions in acetonitrile and *N,N*-dimethylformamide by calorimetry and spectrophotometry. Thermodynamic quantities of formation of the complexes are discussed in connection with enthalpies of transfer of the metal ion and complexes from AN to DMF.[80,81]

7.2 *Complex Formation of $[CuCl_n]^{(2-n)+}$ in Acetonitrile and N,N-Dimethylformamide*

Calorimetric titration curves obtained by titrating copper(II) perchlorate solutions with a $(C_2H_5)_4NCl$ solution in acetonitrile containing 0.1 mol dm^{-3} $(C_2H_5)_4NClO_4$ and in *N,N*-dimethylformamide containing 0.2 mol dm^{-3} $(C_2H_5)_4NClO_4$ are depicted in Figures 23 and 24, respectively. Enthalpies ΔH/kJ mol^{-1} of reaction per addition of a unit mole of chloride ions at each titration point were plotted against the ratio C_X/C_M, where C_X and C_M denote the total concentrations of chloride and copper(II) ions, respectively, in the solutions. The titration curves were well explained in terms of formation of a series of mononuclear complexes $[CuCl_n]^{(2-n)+}$ (n = 1-4) in the both solvents, and the formation constants and enthalpies of formation of the complexes were evaluated by the least-squares method. Theoretical curves calculated by using the constants thus optimized are illustrated by the solid lines in Figures 23 and 24, and they well reproduced the experimental points over the whole range of C_X/C_M examined.

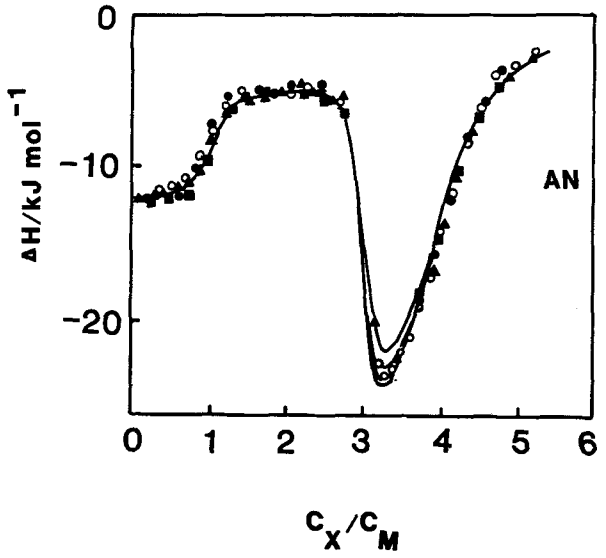

FIGURE 23. Calorimetric titration curves of copper(II) chloride acetonitrile solutions containing 0.1 mol dm^{-3} $(C_2H_5)_4NClO_4$. Initial concentrations of copper(II) perchlorate (C_M/mmol dm^{-3}): 16.06 (○), 11.66 (▲), 9.67 (●) and 6.282 (■). The solid lines were calculated by using the constants in Table XXI.

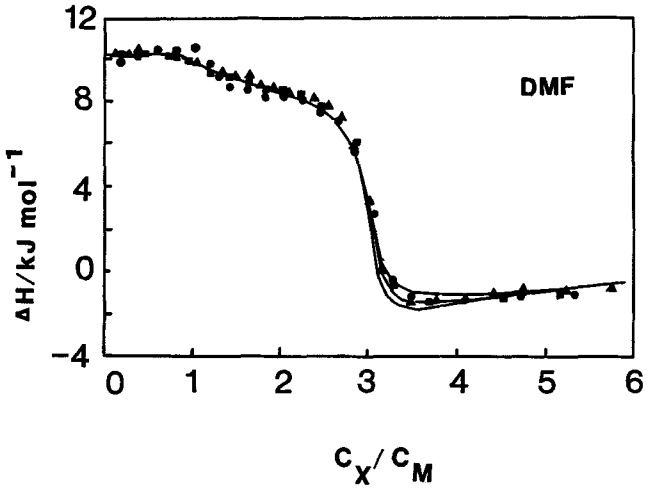

FIGURE 24. Calorimetric titration curves of copper(II) chloride DMF solutions containing 0.2 mol dm^{-3} $(C_2H_5)_4NClO_4$. Initial concentrations of copper(II) perchlorate (C_M/mmol dm^{-3}): 9.80 (●), 14.66 (■) and 19.93 (▲). The solid lines were calculated by using the constants in Table XXI.

Thermodynamic quantities for the stepwise reaction, $[CuCl_{n-1}]^{(3-n)+} + Cl^- = [CuCl_n]^{(2-n)+}$ (n = 1-4) in the 0.1 mol dm^{-3} $(C_2H_5)_4NClO_4$ AN solution and in the 0.2 mol dm^{-3} $(C_2H_5)_4NClO_4$ DMF solution are summarized in Table XXI.

Formation of the chloro complexes of copper(II) ion was more favorable in AN than in DMF, as shown in Figure 25 by the distribution curves of the complexes in the solvents. The enhancement of the formation of the complexes in AN was mainly owing

TABLE XXI

Thermodynamic quantities, $\log(K_n/\text{mol}^{-1}\,\text{dm}^3)$, $\Delta G_n^\circ/\text{kJ mol}^{-1}$, $\Delta H_n^\circ/\text{kJ mol}^{-1}$ and $\Delta S_n^\circ/\text{J K}^{-1}\,\text{mol}^{-1}$, for the stepwise reaction, $CuCl_{n-1}^{(3-n)+} + Cl^- = CuCl_n^{(2-n)+}$ ($n = 1$–4), in acetonitrile and in *N,N*-dimethylformamide at 25°C.

	Acetonitrile	*N,N*-Dimethylformamide
$\log K_1$	9.69	6.79
$\log K_2$	7.95	4.54
$\log K_3$	4.94	4.00
$\log K_4$	2.85	1.52
ΔG_1°	−55.3	−38.8
ΔG_2°	−45.4	−25.9
ΔG_3°	−28.2	−22.8
ΔG_4°	−16.3	−8.7
ΔH_1°	−11.7	10.3
ΔH_2°	−5.0	9.7
ΔH_3°	−4.4	7.3
ΔH_4°	−34.3	−8.1
ΔS_1°	147	165
ΔS_2°	135	120
ΔS_3°	80	101
ΔS_4°	−61	2
$\Delta G_{\beta_4}^{\circ\,a}$	−144.1	−96.2
$\Delta H_{\beta_4}^{\circ\,a}$	−54.5	19.2
$\Delta S_{\beta_4}^{\circ\,a}$	300	387

[a]For the reaction, $Cu^{2+} + 4Cl^- = [CuCl]_4^{2-}$

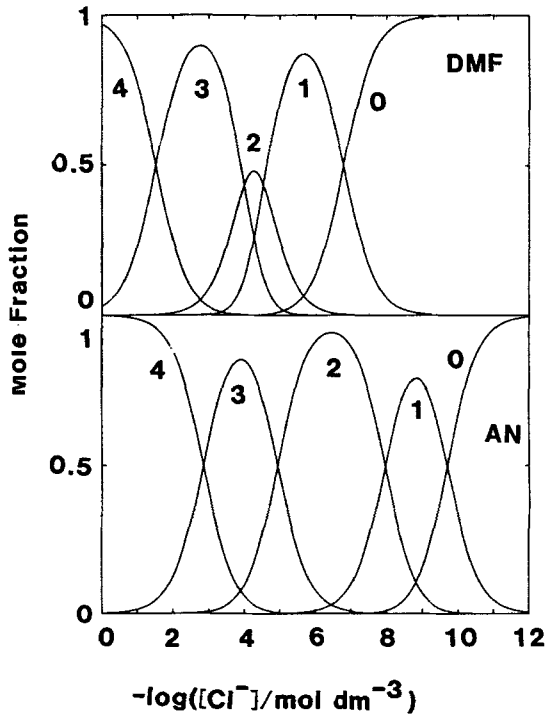

FIGURE 25. Distribution curves of the $[CuCl_n]^{(2-n)+}$ ($n = 1$–4) complexes in the 0.2 mol dm^{-3} $(C_2H_5)_4NClO_4$ AN solution. Numbers represent n of the $[CuCl_n]^{(2-n)+}$ complex.

to the larger negative enthalpies than those in DMF. The entropies of formation of the complexes were not largely different at each consecutive step $n = 1$–3 in these solvents, and the formation of the $[CuCl_4]^{2-}$ complex was entropically less favorable in AN than in DMF. The more negative enthalpies of formation of copper(II) chloride complexes in AN than in DMF may be ascribed to weaker solvation of the metal ion in the former solvent, as is expected from the smaller donor number of AN. The difference in solvation of copper(II) ion in AN and DMF will be discussed in the later section.

Formation of a complex in a solution is accompanied by desolvation of both metal ion and ligand followed by the bond formation between them. The metal-ligand bonds within a series of complexes of a metal ion are usually weaker in a complex formed at a higher consecutive step. Thus, the enthalpies of formation of the $[ML_n]$ complexes may become less negative with an increase in n from the viewpoint of the metal-ligand bonds. However, the ΔH_4° values of formation of the $[CuCl_4]^{2-}$ complex in AN and DMF were more negative than the ΔH_n° values of formation of the $[CuCl_n]^{(2-n)+}$ ($n = 1$–3) complexes in the solvents. The trend was more remarkable in AN than in DMF. Therefore, the more negative ΔH_4° value than the ΔH_n° ($n = 1$–3) values should be ascribed to a weaker solvation in $[CuCl_3]^-$ than in $[CuCl_n]^{(2-n)+}$ ($n = 0$–2) in the solvents. The metal-solvent bonds within the $[CuCl_3]^-$ complex may be weaker than those within the $[CuCl_n]^{(2-n)-}$ ($n = 0$–2) complexes in these solvents, especially in AN as indicated by a largely negative ΔH_4° value, and thus, a relatively less energy for removing solvent molecules from the coordination sphere of the $[CuCl_3]^-$ complex might be needed in the course of formation of $[CuCl_4]^{2-}$.

A largely positive ΔS_n° ($n = 1$–3) value indicated that desolvation of solvent molecules also played an important role in the course of formation of the $[CuCl_n]^{(2-n)+}$ complexes in AN and in DMF. On the other hand, a negative ΔS_4° value in AN suggested that desolvation of the $[CuCl_3]^-$ complex did not play an essential role, and thus, the complex might not be strongly solvated in the solvent. The ΔS_4° value in DMF was much smaller than the ΔS_n° ($n = 1$–3) values, although the ΔS_4° value was still slightly positive. Therefore, the $[CuCl_3]^-$ complex may not be strongly solvated in DMF. Thus, we concluded that the $[CuCl_4]^{2-}$ complex has practically no solvent molecules in the primary coordination sphere of the metal ion within the complex in both AN and DMF. This conclusion is supported by the electronic spectra of $[CuCl_4]^{2-}$ in AN and in DMF which are very similar in both the solvents.

7.3 *Enthalpies of Transfer of Cu^{2+} Ion*

Enthalpies of transfer of Cu^{2+} from water to AN and to DMF were determined by measuring enthalpies of solution of anhydrous $CuCl_2$ crystals in the solvents. Copper(II) chloride dissolved was expected to be compeltely dissociated into copper(II) and chloride ions in water as noted in Chapter 6, but it was mostly associated in AN and in DMF.

Enthalpies of solution of $CuCl_2$ crystals for the following processes were determined in AN and in DMF:

$$CuCl_2(c) = Cu^{2+}(s) + 2Cl^-(s);\ \Delta H_s^\circ(Cu^{2+}, 2Cl^-) \tag{42}$$

$$CuCl_2(c) = [CuCl_2](s);\ \Delta H_s^\circ(CuCl_2) \tag{43}$$

by measuring the enthalpy of solution ΔH_{obsd}° and by using Eqs. (44) and (45):

$$\Delta H_s^\circ(Cu^{2+}, 2Cl^-) = \Delta H_{s,obsd}^\circ - \sum_n \alpha_n \Delta H_{\beta n}^\circ \tag{44}$$

TABLE XXII
Enthalpies of solution ΔH_s° of anhydrous $CuCl_2$ and enthalpies of transfer ΔH_t° of copper(II) and chloride ions from water to acetonitrile and to *N,N*-dimethylformamide at 25°C

	ΔH/kJ mol^{-1}		
	Water	AN	DMF
$\Delta H^\circ_{s,obsd}$	−56.3	−15.9	−55.3
$\Delta H^\circ_s(CuCl_2)$	−	−15.9	−54.7
$\Delta H^\circ_s(Cu^{2+}, 2Cl^-)$	−56.3	0.6	−74.5
$\Delta H^\circ_t(Cl^-)$	−	19.0[a]	21.3[a]
$\Delta H^\circ_t(Cu^{2+})$	−	18.9	−60.8

[a]Ref. 7.

$$\Delta H^\circ_s(CuCl_2) = \Delta H^\circ_s(Cu^{2+}, 2Cl^-) + \Delta H^\circ_{\beta 2} \tag{45}$$

where (c) and (s) stand for the crystalline and solution states, respectively, and α_n denotes the mole fraction of the $[CuCl_n]^{(2-n)+}$ complex. The α_n value was calculated in each measurement by knowing the formation constants of the copper(II) chloride complexes and the total concentration of $CuCl_2$ dissolved in a solvent. The results are listed in Table XXII.

The enthalpy of transfer $\Delta H^\circ_t(Cu^{2+}, 2Cl^-)$ from water (W) to another solvent (S) was represented as the sum of enthalpies of transfer of each ionic component as follows:

$$\Delta H^\circ_t(Cu^{2+}, 2Cl^-) = \Delta H^\circ_{s,S}(Cu^{2+}, 2Cl^-) - \Delta H^\circ_{s,W}(Cu^{2+}, 2Cl^-)$$
$$= \Delta H^\circ_t(Cu^{2+}) + 2\Delta H^\circ_t(Cl^-) \tag{46}$$

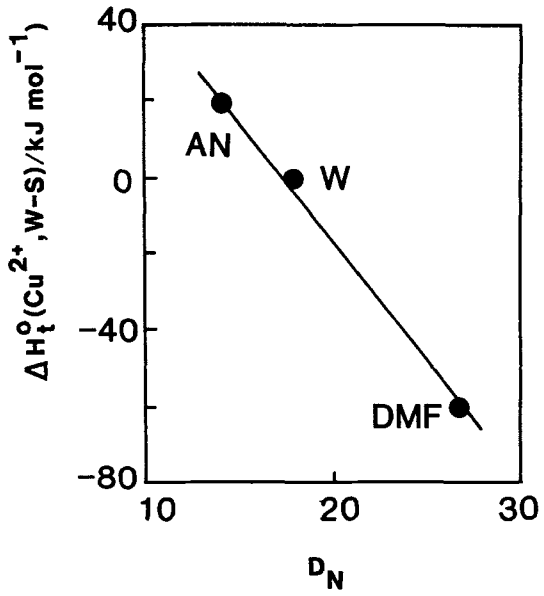

FIGURE 26. Enthalpies of transfer of Cu^{2+} from water to AN and to DMF plotted against the donor number D_N of the solvents.

The $\Delta H_t^\circ(Cl^-)$ values from water to AN and to DMF have been reported by Cox *et al.*[82] on the basis of the extrathermodynamic assumption, $\Delta H_t^\circ(Ph_4As^+) = \Delta H_t^\circ(BPh_4^-)$, and thus, the $\Delta H_t^\circ(Cu^{2+})$ values from water to the aprotic solvents were calculated by subtracting the contribution of Cl^- ions from $\Delta H_t^\circ(Cu^{2+}, 2Cl^-)$. The results are also given in Table XXII. The $\Delta H_t^\circ(Cu^{2+})$ values thus obtained were plotted against the donor number (D_N) of the solvents in Figure 26, which showed a very good linear relationship. Figure 26 indicates that copper(II) ion is more strongly solvated in DMF than in water, and much more than in AN.

7.4 *Enthalpies of Transfer of $[CuCl_n]^{(2-n)+}$ from Acetonitrile to N,N-Dimethyl formamide*

The difference in overall enthalpies of formation of the copper(II) chloride complexes in AN and in DMF is related to enthalpies of transfer of species pertaining to the complex formation reaction as follows:

$$\Delta H_{\beta n}^\circ(DMF) - \Delta H_{\beta n}^\circ(AN) = \Delta H_t^\circ(CuCl_n^{(2-n)+}) - \Delta H_t^\circ(Cu^{2+}) - n\Delta H_t^\circ(Cl^-) \qquad (47)$$

The $\Delta H_t^\circ(CuCl_n^{(2-n)+})$ value can be calculated, since all other values in Eq. (47) have been determined. The $\Delta H_t^\circ(CuCl_n^{(2-n)+})$ (n = 1-4) values thus calculated are summarized in Table XXIII and are also plotted against n in Fig. 27.

Although the absolute values of formal charges of the $[CuCl_n]^{(2-n)+}$ (n = 0-4) complexes vary with n from 2 (n = 0) to 0 (n = 2) and then again to 2(n = 4), the $\Delta H_t^\circ(CuCl_n^{(2-n)+})$ values monotonously changed with n from the $\Delta H_t^\circ(Cu^{2+})$ value of -79.7 kJ mol^{-1} to the $\Delta H_t^\circ(CuCl_4^{2-})$ value of 4.1 kJ mol^{-1}. The dielectric constant of AN (36.0) is not different from that of DMF (36.7). Therefore, it is obvious that simple electrostatic theories (such as Born's equation and its derivatives with respect to temperature) are not applicable to explain the change in enthalpies of transfer of the complexes between the solvents. Such a monotonous variation of ΔH_t° values has also been observed in enthalpies of transfer of mercury(II) halide complexes $[HgX_n]^{(2-n)+}$ (n = 1-4) from dimethyl sulfoxide to pyridine,[83] the solvents having largely different dielectric constants.

Accordingly, the enthalpy of transfer of $[CuCl_n]^{(2-n)+}$ from AN to DMF should be ascribed to different solvation of the both metal and ligand ions within the complexes between the solvents. It is expected that solvation of Cl^- ion within $[CuCl_n]^{(2-n)+}$ may

TABLE XXIII

Thermodynamic quantities of transfer, ΔG_t°/kJ mol^{-1}, ΔH_t°/kJ mol^{-1} and ΔS_t°/J K^{-1} mol^{-1}, of copper(II)chloro complexes from acetonitrile to *N,N*-dimethylformamide at 25°C

Species	ΔG_t°	ΔH_t°	ΔS_t°	$\Delta\Delta G_n^\circ$	$\Delta\Delta H_n^\circ$	$\Delta\Delta S_n^\circ$
Cu^{2+}	-77.4[a]	-79.7	-8			
Cl^-	3.7[b]	2.3[b]	-5[b]			
$[CuCl]^+$	-57.7	-55.4	6	16.5	22.0	18
$[CuCl_2]$	-34.0	-38.4	-15	19.5	14.7	-15
$[CuCl_3]^-$	-25.3	-24.4	3	5.0	11.7	21
$[CuCl_4]^{2-}$	-14.0	4.1	61	7.6	26.2	63

$\Delta\Delta G_n^\circ = \Delta G_n^\circ(DMF) - \Delta G_n^\circ(AN)$, $\Delta\Delta H_n^\circ(DMF) - \Delta H_n^\circ(AN)$, $\Delta\Delta S_n^\circ = \Delta S_n^\circ(DMF) - \Delta S_n^\circ(AN)$, for the reaction, $[CuCl_{n-1}]^{(3-n)+} + Cl^- = [CuCl_n]^{(2-n)+}$ (n = 1-4).

[a]Ref. 84, [b]Ref. 7.

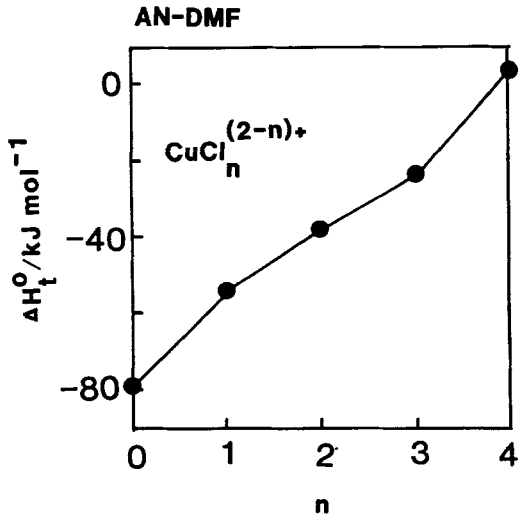

FIGURE 27. Enthalpies of transfer of the $[CuCl_n]^{(2-n)+}$ (n = 1-4) complexes plotted against n, the number of Cl^- ions bound per metal ion within a complex.

not be significantly different in AN and DMF, since the $\Delta H_t^\circ(Cl^-)$ value from AN to DMF is only slightly positive (see Table XXII). The enthalpy of transfer of $[CuCl_n]^{(2-n)+}$ should thus be mainly attributed to the difference in solvation of the metal ion within the complexes in the solvents.

The $\Delta H_t^\circ(CuCl_n^{(2-n)+})$ (n = 1-3) values from AN to DMF were negative as well as $\Delta H_t^\circ(Cu^{2+})$, indicating that the metal ion within the $[CuCl_n]^{(2-n)+}$ (n = 1-3) complexes was more strongly solvated with DMF than with AN. The ΔH_t° values increased in the sequence $[CuCl]^+ < [CuCl_2] < [CuCl_3]^-$, and the result indicates that solvation of the complexes weakened in this sequence.

$\Delta H_t^\circ(CuCl_4^{2-})$ value was only slightly positive, similar to $\Delta H_t^\circ(Cl^-)$, indicating that the metal ion within the complex was probably not primarily solvated with solvent molecules in both AN and DMF, and thus, the enthalpy of transfer of the $[CuCl_4]^{2-}$ complex was mainly determined by the change in secondary solvation of the complex in the solvents.

7.5 *Gibbs Energies and Entropies of Transfer of* $[CuCl_n]^{(2-n)+}$ *from Acetonitrile to N,N-Dimethylformamide*

The Gibbs energy of transfer ΔG_t° of Cu^{2+} has been reported by Coetzee and Istone[84] to be 59.4 and -18.0 kJ mol^{-1} from water to AN and to DMF, respectively, and thus, the $\Delta G_t^\circ(Cu^{2+})$ value from AN to DMF is −77.4 kJ mol^{-1}. The $\Delta G_t^\circ(Cl^-)$ value has also been reported to be 3.7 kJ mol^{-1} from AN to DMF.[7]

By using the ΔG_t° values of copper(II) and chloride ions from AN to DMF, we calculated Gibbs energies of transfer of $[CuCl_n]^{(2-n)+}$ (n = 1-4) by the same procedure as that used for evaluation of ΔH_t° of the complexes in a previous section.

The entropies of transfer ΔS_t° of $[CuCl_n]^{(2-n)+}$ (n = 1-4) from AN to DMF could thus be calculated from the Gibbs energies and enthalpies of transfer of the complexes. The results are summarized in Table XXIII.

All the $[CuCl_n]^{(2-n)+}$ (n = 1-4) complexes were more stable in DMF than in AN, as indicated by the negative ΔG_t° values of the complexes, which were predominantly

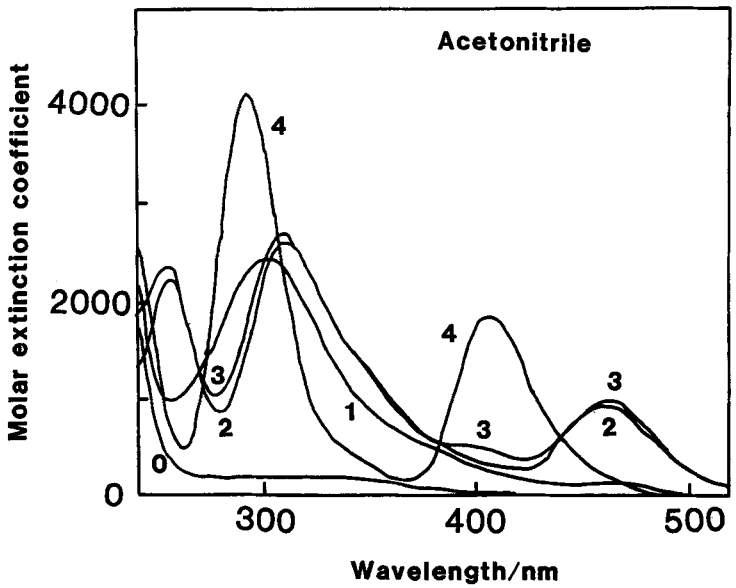

FIGURE 28 Molar extinction coefficients, absorbance/$[Cu^{2+}]_{tot}^{-1}$ cm^{-1}, of individual copper(II) chloro complexes at various wavelengths in the 0.1 mol dm^{-3} $(C_2H_5)_4NClO_4$ AN solution. Numbers represent n of the $[CuCl_n]^{(2-n)+}$ complex.

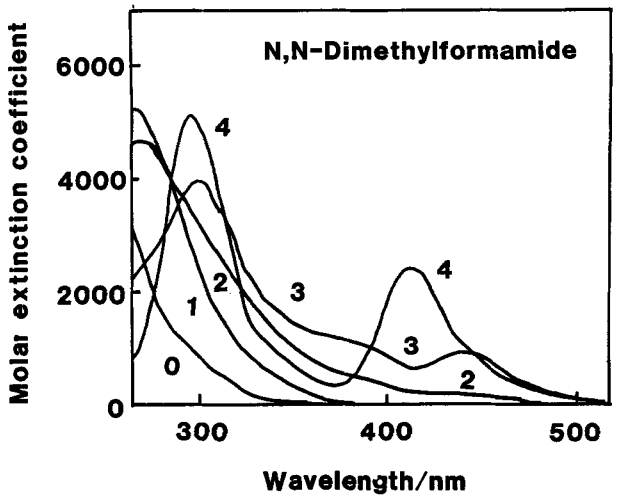

FIGURE 29 Molar extinction coefficients, absorbance/$[Cu^{2+}]_{tot}^{-1}$ cm^{-1}, of individual copper(II) chloro complexes at various wavelengths in the 0.2 mol dm^{-3} $(C_2H_5)_4NClO_4$ AN solution. Numbers represent n of the $[CuCl_n]^{(2-n)+}$ complex.

ascribed to by the enthalpy term except for the $[CuCl_4]^{2-}$ complex. As to the $[CuCl_4^2]^{2-}$ complex, the largely positive ΔS_t° value led to the negative ΔG_t° value, the ΔH_t° value being even slightly positive. However, the reason why the $\Delta S_t^\circ(CuCl_4^{2-})$ value was so largely positive compared with the $\Delta S_t^\circ(CuCl_n^{(2-n)+})$ (n = 1-3) values still remained unknown.

TABLE XXIV
Absorption maxima, λ_{max}/nm, of electronic spectra of copper(II) chloro complexes in acetonitrile and *N,N*-dimethylformamide

Species	AN	DMF
$[CuCl]^+$	300	265
$[CuCl_2]$	255	265
	308	
	460	
$[CuCl_3]^-$	255	
	308	300
	460	440
$[CuCl_4]^{2-}$	290	296
	405	410

7.6 *Electronic Spectra of Chloro Complexes of Copper(II) Ion*

Electronic spectra of copper(II) chloride solutions at various concentrations of chloride ions were measured in the 0.1 mol dm^{-3} $(C_2H_5)_4NClO_4$ AN solution and in the 0.2 mol dm^{-3} $(C_2H_5)_4NClO_4$ DMF solution. Each spectrum obtained was resolved into spectra of individual chloro complexes of copper(II) by knowing the formation constants of the complexes in each solvent. Molar extinction coefficients of the individual complexes at various wavelengths thus obtained in AN and in DMF are depicted in Figures 28 and 29, respectively.

The absorption maxima of the individual chloro complexes of copper(II) obtained in AN and in DMF are given in Table XXIV. An absorption maximum of $[CuCl]^+$ was found at slightly longer wavelength by *ca.* 35 nm in AN than in DMF. Three absorption maxima of the complex were found at *ca.* 255, 308 and 460 nm in AN, while only one absorption maximum was found at *ca.* 265 nm in DMF. The $[CuCl_3]^-$ complex showed three absorption maxima at almost the same wavelengths as those of $[CuCl_2]$ in AN, but only two maxima were found in DMF within the wavelength region examined here. The absorption spectrum of the $[CuCl_4]^{2-}$ complex with two absorption maxima at *ca.* 290 and 405 nm in AN was very similar to that in DMF in which two absorption maxima were observed at 296 and 410 nm.

It has been indicated from thermodynamic considerations in previous sections that the $[CuCl_4]^{2-}$ complex may have no solvent molecules in the first coordination sphere of the metal ion within the complex. Although the structure of the $[CuCl_4]^{2-}$ complex has not yet been determined by a diffraction method, it should be the same in AN and in DMF, as indicated by the similar absorption spectra in both the solvents.

According to Fergusson,[85] the presence of an absorption maximum between 435 and 455 nm of a chloro complex of copper(II) ion was indicative of the D_{2d} form of the complex. Therefore, it is plausible that the $[CuCl_2]$ and $[CuCl_3]^-$ complexes in AN and the $[CuCl_3]^-$ complex in DMF have the D_{2d} form, since their spectra have an absorption maximum at the wavelength region. On the other hand, the $[CuCl_2]$ complex in DMF has no maximum in the wavelength region 400–500 nm, and thus, the different structures of the solvated $[CuCl_2]$ complex were expected in AN and in DMF.

8. SOLVATION OF Cu(II) ION AND COMPLEX FORMATION OF $[CuCl_n]^{(2-n)+}$ IN ACETONITRILE-*N,N*-DIMETHYLFORMAMIDE MIXTURES

8.1 *Introduction*

As discussed in a preceding chapter, a large difference is found between the

thermodynamic quantities of formation of $[CuCl_n]^{(2-n)+}$ ($n = 1$–4) in acetonitrile and in *N,N*-dimethylformamide. This is well interpreted in terms of a stronger solvation of copper(II) ion with DMF than with AN, as indicated by a largely negative enthalpy of transfer of the metal ion from AN to DMF, which leads to a weaker complexation of copper(II) ion with chloride ions in the former solvent than in the latter. The result indicates that copper(II) ion may preferentially be solvated with DMF molecules in AN-DMF mixtures, and DMF molecules may stepwise coordinate to the metal ion as ligands with increasing concentration of DMF in the mixtures.

In this chapter, therefore, we aim at elucidating solvation phenomena of copper(II) ion and complex formation of the metal ion with chloride ions in AN-DMF mixtures. Thermodynamic quantities of formation of a series of copper(II)-DMF solvates and the structures of the solvated copper(II) ion are determined in the mixtures. Thermodynamic quantities of formation of $[CuCl_n]^{(2-n)+}$ determined in the AN-DMF mixtures are discussed on the basis of the thermodynamic quantities and the structures of copper(II)-DMF solvates thus obtained.

8.2 *Preferential Solvation of Copper(II) Ion with DMF in Acetonitrile-rich AN-DMF Mixtures*

Calorimetric titration curves obtained by titrating copper(II) perchlorate acetonitrile solutions with an AN-DMF mixture containing 1 mol dm^{-3} DMF are illustrated in Figure 30. Enthalpies ΔH° per addition of a unit mole of DMF, calculated according to $\Delta H^\circ = -q/(vC_{X,tit})$ where v and $C_{X,tit}$ stand for the volume of an aliquot of the titrant added and the concentration of DMF in the mixture, respectively, were plotted against the ratio C_X/C_M in the test solution at each titration point, where C_X and C_M denote total concentrations of DMF and Cu(II) ion in the test solution, respectively. Experimental

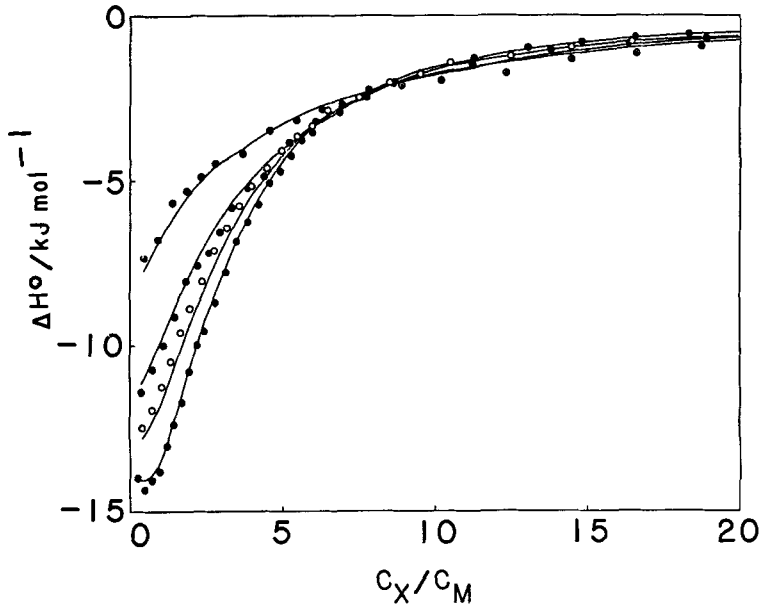

FIGURE 30. Calorimetric titration curves for the formation of copper(II)-DMF solvates in acetonitrile containing 0.1 mol dm^{-3} $(C_2H_5)_4NClO_4$ at 25°C. Initial concentrations of copper(II) perchlorate (C_M/mmol dm^{-3}): 24.72 (●), 17.70 (○), 10.47 (◎) and 6.11 (⊙).

TABLE XXV

The least-squares refinement of formation constants, β_n/mol^{-n} dm^{3n}, and enthalpies, $\Delta H^\circ_{\beta_n}$/kJ mol^{-1}, of formation of copper(II)-*N,N*-dimethylformamide solvate species in acetonitrile-*N,N*-dimethylformamide mixtures containing 0.1 mol dm^{-3} $(C_2H_5)_4NClO_4$ at 25°C.

	(1, 2, 3, 4)[a]	(1, 2, 3, 4, 6)[a]
$\log \beta_1$	2.64 (0.07)	2.64 (0.07)
$\log \beta_2$	4.44 (0.08)	4.46 (0.08)
$\log \beta_3$	5.97 (0.12)	6.12 (0.11)
$\log \beta_4$	6.73 (0.18)	7.21 (0.14)
$\log \beta_6$	—	7.90 (0.31)
$\Delta H^\circ_{\beta_1}$	−16.1 (0.4)	−15.8 (0.4)
$\Delta H^\circ_{\beta_2}$	−40.4 (2.8)	−42.0 (3.2)
$\Delta H^\circ_{\beta_3}$	−50.6 (4.0)	−42.8 (3.9)
$\Delta H^\circ_{\beta_4}$	−81.6 (0.7)	−73.6 (2.3)
$\Delta H^\circ_{\beta_6}$	—	−77.8 (1.8)
U[b]	1.055	0.916

Values in parentheses refer to standard deviations. [a]The number of dmf molecules within $[Cu(dmf)_n]^{2+}$ assumed to be formed. [b]The error-square sum of the least-squares refinement of 111 calorimetric data points.

points in Figure 30 show negative ΔH° values, which indicate that copper(II) ion is exothermically coordinated with DMF molecules in AN.

The calorimetric data were analyzed by taking into account the formation of $[Cu(dmf)_n]^{2+}$ with plausible combinations of n's. Among various sets of the complexes examined, the set (1-4) assuming the complexes with $n = 1, 2, 3$ and 4, and the set (1-4, 6) assuming $[Cu(dmf)_6]^{2+}$ in addition to $[Cu(dmf)_n]^{2+}$ (n = 1-4) gave relatively small error-square sums as shown in Table XXV. The formation of $[Cu(dmf)_5]^{2+}$ was uncertain. The $\Delta H^\circ_{\beta_4}$ value is largely negative and the $\Delta H^\circ_{\beta_6}$ value evaluated in the set (1-4, 6) is only −4.2 kJ mol^{-1} more negative than the $\Delta H^\circ_{\beta_4}$ value as expected from weak interactions between the metal ion and ligands at the axial position. Finally, we propose the formation of $[Cu(dmf)_n]^{2+}$ (n = 1-4, 6) and the thermodynamic quantities for the stepwise formation of the complexes are given in Table XXVI. The distribution

TABLE XXVI

Thermodynamic quantities, $\log(K_n$/mol^{-1} dm$^3)$, ΔG°_n/kJ mol^{-1}, ΔH°_n/kJ mol^{-1} and ΔS°_n/J K^{-1} mol^{-1}, for the stepwise formation of $[Cu(dmf)_n]^{2+}$ (n = 1-4, 6) in acetonitrile-*N,N*-dimethylformamide mixture containing 0.1 mol dm^{-3} $(C_2H_5)_4NClO_4$ at 25°C.

$\log K_1$	2.64	ΔH°_1	−15.8
$\log K_2$	1.82	ΔH°_2	−26.2
$\log K_3$	1.66	ΔH°_3	−0.8
$\log K_4$	1.09	ΔH°_4	−30.8
$\log K_5K_6$	0.69	$\Delta H^\circ_5 + \Delta H^\circ_6$	−4.2
ΔG°_1	−15.1	ΔS°_1	−2
ΔG°_2	−10.4	ΔS°_2	−53
ΔG°_3	−9.5	ΔS°_3	29
ΔG°_4	−6.2	ΔS°_4	−83
$\Delta G^\circ_5 + \Delta G^\circ_6$	−3.9	$\Delta S^\circ_5 + \Delta S^\circ_6$	−1

For overall formation of $[Cu(dmf)_6]^{2+}$: $\Delta G^\circ_{\beta_6}$ = −45.1 kJ mol^{-1}, $\Delta H^\circ_{\beta_6}$ = −77.8 kJ mol^{-1} and $\Delta S^\circ_{\beta_6}$ = −110 J K^{-1} mol^{-1}.

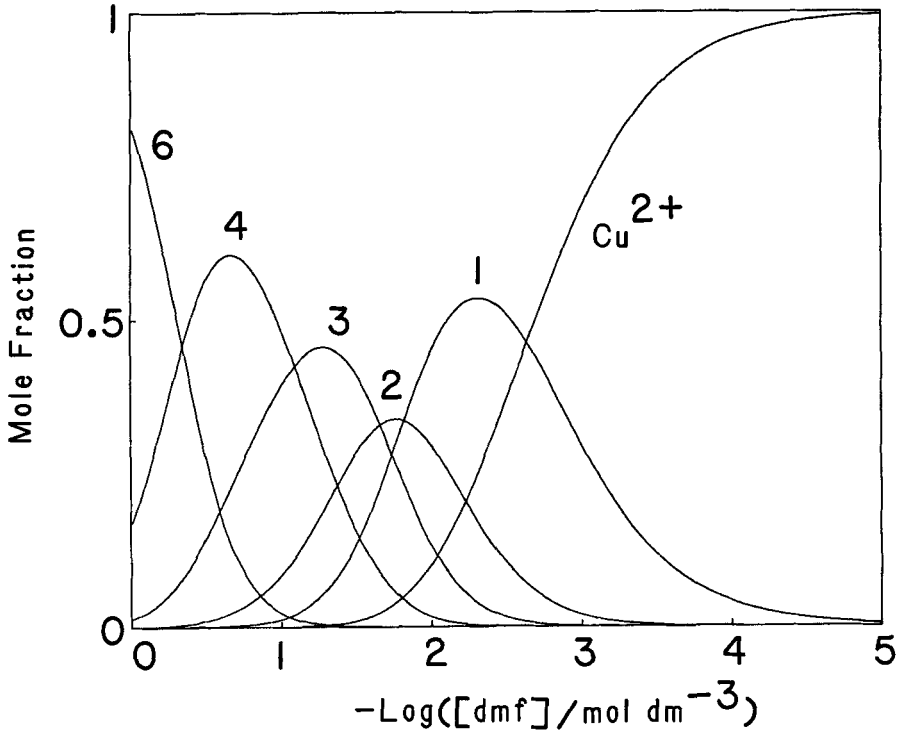

FIGURE 31. Distribution of copper(II)-DMF solvates in acetonitrile. The numbers represent n within $[Cu(dmf)_n]^{2+}$.

of species for the complexes is shown in Figure 31. As illustrated by the solid lines in Figure 30, theoretical curves calculated by using the constants of the set (1-4, 6) in Table XXV well reproduced experimental points.

It is well known that copper(II) ion is hexa-coordinated with water molecules to form a distorted octahedral structure in aqueous solution.[8] Similarly, copper(II) ion may be hexa-coordinated with solvent molecules in acetonitrile, which are replaced with DMF molecules in AN-DMF mixtures.

Although the stepwise ΔH_n° and ΔS_n° values irregularly varied with n, they compensate each other to result in the smooth change in ΔG_n°, and thus, in K_n. The ΔH_3° value is very small negative compared with other ΔH_n° ($n = 1, 2$ and 4) values, and the corresponding ΔS_3° value is significantly positive. The result suggests that more than one acetonitrile molecule in the first coordination sphere of copper(II) ion may be liberated at this step. One acetonitrile molecule at the corner of the square plane of $[Cu(dmf)_3]^{2+}$ may be replaced at the fourth stage of complexation where ΔH_4° and ΔS_4° values are both largely negative. The result indicates that the acetonitrile molecule within $[Cu(dmf)_3]^{2+}$ may be rather weakly combined with the central metal ion.

X-ray diffraction measurements have been carried out in an AN-DMF mixture, which contains about 1 mol dm^{-3} $Cu(ClO_4)_2$ and 5 mol dm^{-3} DMF, as will be discussed in a later section. It elucidates that copper(II) ion is coordinated with four DMF molecules in the AN-DMF mixture. Thus, the result from the present calorimetric measurements is supported by the X-ray diffraction measurements.

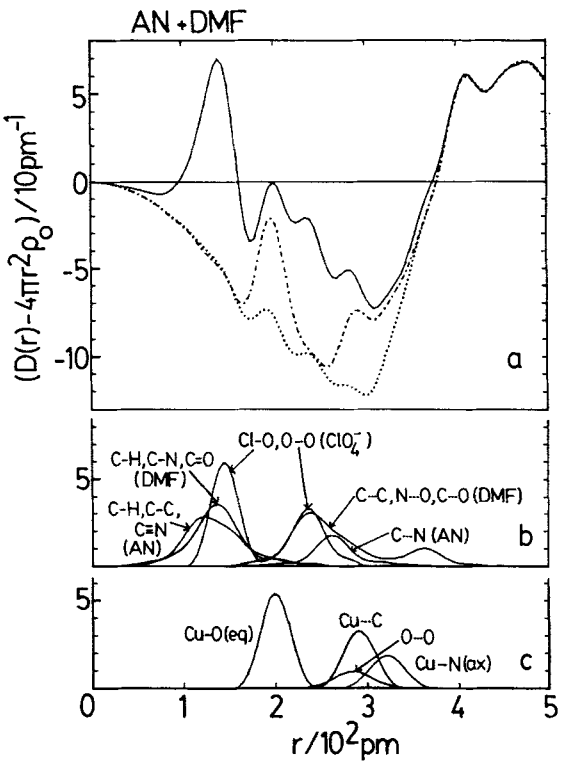

FIGURE 32. (a); The $D(r)-4\pi r^2\rho_0$ curve for copper(II) perchlorate in an AN-DMF mixture ($C_{DMF}/C_{Cu} = 5$). The chain line shows the residual curve after subtraction of the theoretical peaks shown in b. After subtraction of the theoretical peaks due to the Cu-O(eq), Cu···C(eq), Cu-N(ax) (or Cu-O(ax)) and O···O interactions, the dotted line is obtained. (b) and (c); The theoretical peak shapes of each atom pair.

8.3 *Solvation Structures of Cu(II) Ion in N,N-Dimethylformamide and in an Acetonitrile-N,N-Dimethylformamide Mixture*

X-ray diffraction measurements were carried out for copper(II) perchlorate solutions in pure DMF containing 0.551 mol dm^{-3} $Cu(ClO_4)_2$ and in an AN-DMF mixture containing 0.939 mol dm^{-3} $Cu(ClO_4)_2$ and 5 mol dm^{-3} DMF. The $D(r) - 4\pi r^2\rho_0$ curves against r obtained in the AN-DMF mixture and in pure DMF are illustrated by the solid lines in Figures 32(a) and 33(a), respectively.

The $D(r) - 4\pi r^2\rho_0$ curve in Figure 32(a) showed four peaks at about 150, 200, 240 and 290 pm in the region 100 - 300 pm. The first peak at about 150 pm was attributed to the C-H, C-N and C=O bonds within DMF molecules, the C-H, C-C and C-N bonds within AN molecules and the Cl-O bond within perchlorate ions. The third peak at about 240 pm was mainly ascribed to the nonbonding C···C, N···O and C···O pairs within DMF and the O···O pairs of perchlorate ions. Since these interactions within DMF and AN molecules and perchlorate ions have been known, the theoretical peaks of these interactions shown in Figure 32(b) were subtracted from the $D(r) - 4\pi r^2\rho_0$ curve, and then the curve expressed by the chain line was obtained. The residual curve showed two peaks at about 200 and 290 pm and no peak was found in the region 230 - 270 pm. The two peaks were well explained by assuming the interactions within $[Cu(dmf)_4]^{2+}$ with the planar structure, in which the Cu-O(eq) bond distance was assumed to be 200 pm and the nonbonding Cu···C(eq) and O···O pairs were assumed to be 290 pm. Although no peak was found in the region 300 - 350 pm, the analysis by the least-squares method

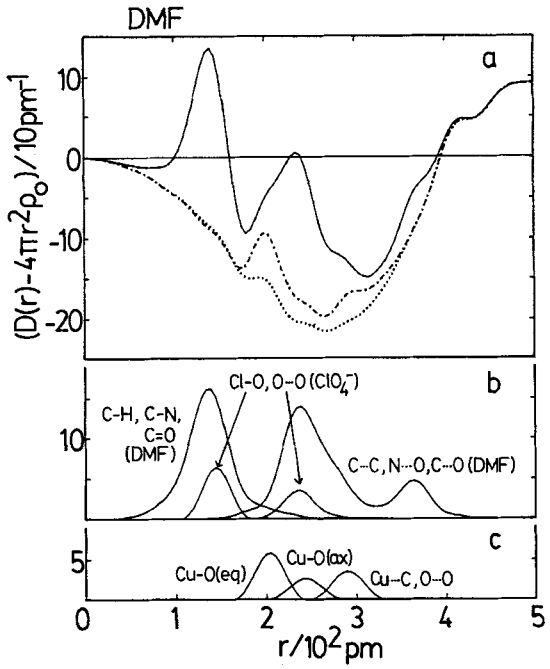

FIGURE 33. (a); The $D(r)-4\pi r^2\rho_0$ curve for copper(II) perchlorate DMF solution. The chain line shows the residual curve after subtraction of the theoretical peaks shown in b. After subtraction of the theoretical peaks due to the Cu-O(eq), Cu···C(eq), Cu-O(ax) and O···O interactions, the dotted line is obtained. (b) and (c); the theoretical peak shapes of each atom pair.

indicated the Cu-N(ax) or Cu-O(ax) interaction at 322 pm. The Cu-O(eq), Cu-N(ax) (or Cu-O(ax)), Cu-C(eq) and O-O interactions are shown in Figure 32(c). After subtraction of these peaks, no significant peak remained as shown by the dotted line in Figure 32(a). The bond distances were finally refined by the least-squares method by using s·i(s) data.

An analytical procedure similar to that employed above was applied to the scattering data of copper(II) perchlorate solution in pure DMF. After subtraction of the intramolecular interactions within DMF molecules and perchlorate ions shown in Figure 33(b) from the $D(r) - 4\rho r^2\rho_0$ curve illustrated by the solid line in Figure 33(a), the chain line was obtained, which showed two peaks at about 200 and 290 pm. These peaks may be attributed to the Cu-O(eq) bonds and the nonbonding Cu···C(eq) pairs within copper(II)-DMF solvate species. After subtraction of the four Cu-O(eq) and Cu···C(eq) interactions, a significant peak remained at about 240 pm, which may be ascribed to the Cu-O(ax) bonds, and thus, the $s \cdot i(s)$ data were finally refined by assuming the distorted octahedral structure for the copper(II)-DMF solvate species. The interactions within $[Cu(dmf)_6]^{2+}$ is shown in Figure 33(c). Subtraction of the theoretical curve for the interactions within $[Cu(dmf)_6]^{2+}$ from the chain line led to an almost smooth background curve shown by the dotted line. The bond distances finally obtained for the copper(II)-DMF solvate species in the AN-DMF mixture and in pure DMF are summarized in Table XXVII.

Copper(II) ion in pure DMF is coordinated with six DMF molecules, four of which have the Cu-O bond length of 203 pm. The other two DMF molecules have a longer bond length of 243 pm. The interaction between copper(II) ion and the latter two DMF molecules within $[Cu(dmf)_6]^{2+}$ should be much weaker than that between copper(II) ion and the other four DMF molecules.

TABLE XXVII

Bond lengths, r/pm, and coordination number, n, within the copper(II)-DMF solvates in *N,N*-dimethylformamide and in an acetonitrile-*N,N*-dimethylformamide mixture of 0.1 mole fraction DMF

		DMF	AN-DMF mixture
Cu-O(eq)	r	203(3)	200(1)
	n	4	4
Cu-O(ax)	r	243(5)	330(10)
	n	2	2
Cu···C(eq)	r	290(5)	290(2)
	n	4	4

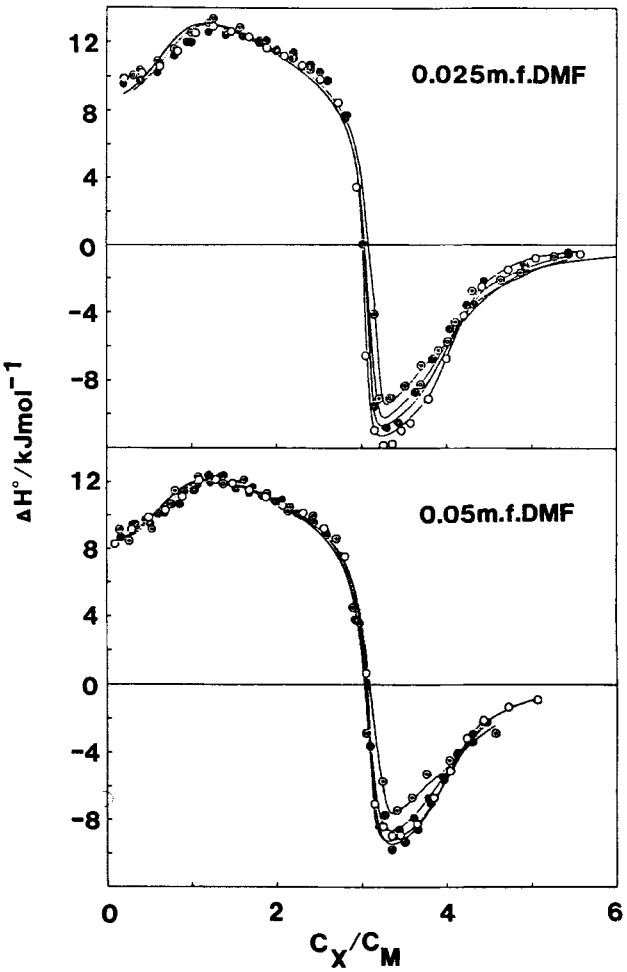

FIGURE 34. Calorimetric titration curves of copper(II) chloride solutions in the AN-DMF mixtures of 0.025 and 0.05 mole fraction DMF containing 0.2 mol dm^{-3} $(C_2H_5)_4NClO_4$. Initial concentrations of copper(II) perchlorate (C_M/mmol dm^{-3}): 4.55 (⊙), 7.14 (⊙), 10.19 (●) and 19.25 (○) in the 0.025 mole fraction DMF mixture, and 6.05 (⊙), 11.83 (●), 20.48 (○) and 26.37 (⊙) in the 0.05 DMF mole fraction.

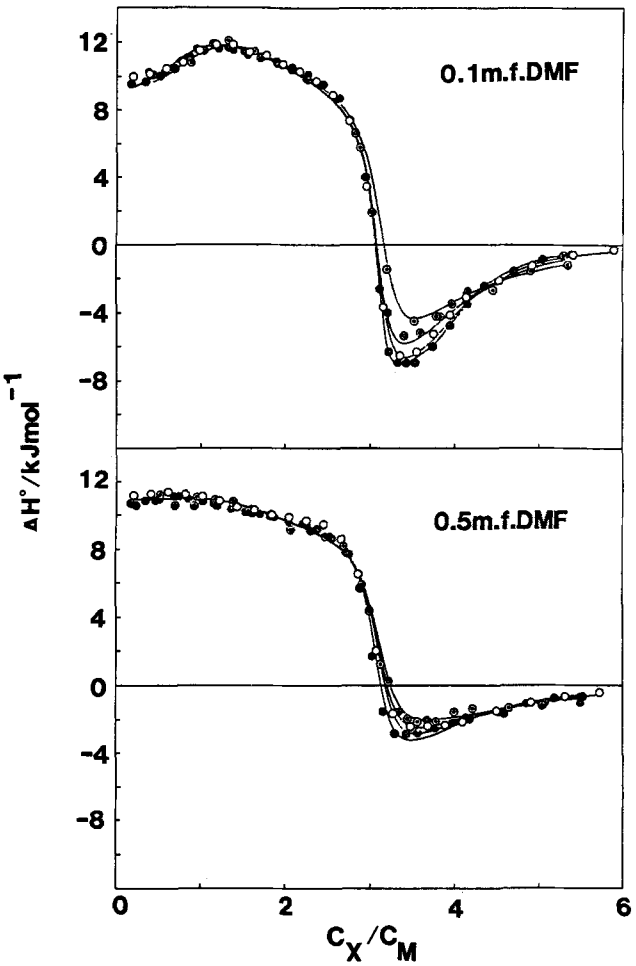

FIGURE 35. Calorimetric titration curves of copper(II) chloride solutions in the AN-DMF mixtures of 0.1 and 0.5 mole fraction DMF containing 0.2 mol dm^{-3} $(C_2H_5)_4NClO_4$. Initial concentrations of copper(II) perchlorate (C_M/mmol dm^{-3}): 4.59 (⊙), 10.69 (⊙), 20.50 (○) and 29.23 (●) in the 0.1 mole fraction DMF mixture, and 8.87 (⊙), 13.35 (●), 19.81 (⊙) and 29.94 (●) in the 0.5 mole fraction DMF.

In an AN-DMF mixture of 0.1 mole fraction DMF, copper(II) ion is coordinated with four DMF molecules. The Cu-O bond length is 200 pm, which is close to that in pure DMF. However, further solvation of copper(II) ion with AN and/or DMF molecules may not occur, because no other interactions between the metal ion and the solvent molecules have been observed in the region of about 240 pm. Therefore, the solvated species of copper(II) ion should be $[Cu(dmf)_4]^{2+}$ in the AN-DMF mixture of 0.1 mole fraction DMF. The conclusion is consistent with that derived from the thermodynamic consideration in a previous section.

8.4 *Complex Formation of $[CuCl_n]^{(2-n)+}$ in Acetonitrile-N,N-Dimethylformamide Mixtures*

Complex formation equilibria between copper(II) and chloride ions have been investigated in various AN-DMF mixtures, DMF contents in the mixtures examined

TABLE XXVIII

The least-squares refinement of formation constants, β_n/mol^{-n} dm^{3n}, and enthalpies, $\Delta H^\circ_{\beta n}$/kJ mol^{-1}, of formation of copper(II) chloro complexes in acetonitrile-*N,N*-dimethylformamide mixtures containing 0.2 mol dm^{-3} $(C_2H_5)_4NClO_4$ at 25°C

	DMF content/mole fraction			
	0.025	0.05	0.1	0.5
log β_1	6.7(0.4)	6.2(0.2)	5.9(0.1)	6.0(0.1)
log β_2	12.2(0.7)	11.4(0.4)	10.8(0.3)	10.9(0.1)
log β_3	18.4(1.2)	16.9(0.5)	15.8(0.4)	15.2(0.4)
log β_4	21.4(1.2)	19.7(0.5)	18.4(0.4)	17.3(0.3)
$\Delta H^\circ_{\beta 1}$	8.7(0.3)	8.3(0.2)	9.2(0.1)	10.9(0.1)
$\Delta H^\circ_{\beta 2}$	37.1(5)	29.9(2)	26.7(1)	22.2(0.2)
$\Delta H^\circ_{\beta 3}$	31.2(0.2)	29.9(0.2)	30.2(0.1)	30.0(0.2)
$\Delta H^\circ_{\beta 4}$	18.8(0.3)	18.8(0.2)	20.9(0.2)	23.5(0.2)

being 0.025, 0.05, 0.1 and 0.5 mole fractions, containing 0.2 mol dm^{-3} $(C_2H_5)_4NClO_4$ as a constant ionic medium at 25°C.

Calorimetric titration curves in the AN-DMF mixtures examined are illustrated in Figures 34 and 35. The ΔH° value observed was positive in the range $C_X/C_M < 3$ but turned to negative in the range $C_X/C_M > 3$ in all the AN-DMF mixtures examined. The trend in the variation of ΔH° is similar to that in pure DMF, but different from that in pure AN where the ΔH° value is negative over the whole range of C_X/C_M as described in Chapter 7. Calorimetric titration curves in the 0.5 mole fraction DMF mixture were essentially the same as those in pure DMF. However, a noticeable change was observed in the titration curves in the mixtures with decreasing DMF content, *i.e.*, the ΔH° value became more positive in the range $C_X/C_M = 1$–2, but more negative in the range $C_X/C_M = 3$–4, in the AN-DMF mixtures of lower DMF contents.

Calorimetric data in any AN-DMF mixture examined were well explained in terms of the formation of $[CuCl_n]^{(2-n)+}$ ($n = 1$–4), as well as those in pure AN and DMF, and their formation constants, enthalpies and entropies were obtained. The results are summarized in Table XXVIII. As illustrated by the solid lines in Figures 34 and 35, theoretical curves calculated by using the constants in Table XXIII well reproduced the experimental points in each AN-DMF mixture examined.

Thermodynamic quantities, log(K_n/mol dm^{-3}), ΔG°_n/kJ mol^{-1}, ΔH°_n/kJ mol^{-1} and ΔS°_n/J K^{-1} mol^{-1}, for the stepwise formation of $[CuCl_n]^{(2-n)+}$ ($n = 1$–4) are summarized in Table XXIX. Distribution of species calculated by using the formation constants in each AN-DMF mixture examined are depicted in Figure 36 together with those in the pure solvents for comparison.

In the AN-DMF mixtures, copper(II) ion is coordinated with four DMF molecules, and the four DMF molecules are stepwise replaced with chloride ions in the course of formation of $[CuCl_n]^{(2-n)+}$. Therefore, thermodynamic quantities of stepwise formation of the copper(II) chloro complexes may reflect the coordination structure of the complexes.

The ΔH°_1 and ΔS°_1 values were both positive and practically kept constant in all the AN-DMF mixtures examined. The ΔH°_1 value in any AN-DMF mixture was more positive by *ca.* 20 kJ mol^{-1} than that in pure AN, the magnitude is about one fourth of the overall enthalpy of formation of $[Cu(dmf)_4]^{2+}$. It is thus plausible that one DMF molecule within $[Cu(dmf)_4]^{2+}$ is replaced with a chloride ion and $[CuCl(dmf)_3]^+$ is formed.

The ΔH°_2 and ΔS°_2 values became markedly positive in the AN-DMF mixtures of low DMF contents. The result indicates that the desolvation of DMF molecules from

TABLE XXIX

Thermodynamic quantities, $\log(K_n/\text{mol}^{-1}\ \text{dm}^3)$, ΔG_n°/kJ mol^{-1}, ΔH_n°/kJ mol^1 and ΔS_n°/J K^{-1} mol^{-1}, for the stepwise reaction, $[CuCl_{n-1}]^{(3-n)+} + Cl^- = [CuCl_n]^{(2-n)+}$ (n = 1-4), in acetonitrile-*N,N*-dimethylformamide mixtures containing 0.2 mol dm^{-3} $(C_2H_5)_4NClO_4$ at 25°C

	DMF content/mole fraction					
	0.0	0.025	0.05	0.1	0.5	1.0
$\log K_1$	9.7	6.7	6.2	5.9	6.0	6.8
$\log K_2$	8.0	5.5	5.2	4.9	4.9	4.5
$\log K_3$	4.9	6.1	5.5	5.0	4.3	4.0
$\log K_4$	2.9	3.0	2.9	2.6	2.2	1.5
ΔG_1°	−55.3	−38.3	−35.5	−33.8	−34.5	−38.8
ΔG_2°	−45.4	−31.5	−29.5	−28.1	−27.8	−25.9
ΔG_3°	−28.2	−35.0	−31.3	−28.5	−24.3	−22.8
ΔG_4°	−16.3	−17.3	−16.4	−14.9	−12.3	−8.8
ΔH_1°	−11.7	8.8	8.3	9.2	10.9	10.3
ΔH_2°	−5.0	28.4	21.6	17.5	11.3	9.7
ΔH_3°	−4.4	−5.9	0.0	3.5	7.8	7.3
ΔH_4°	−34.3	−12.5	−11.1	−9.3	−6.5	−8.1
ΔS_1°	147	158	147	144	152	165
ΔS_2°	135	201	171	153	131	120
ΔS_3°	80	98	105	107	107	101
ΔS_4°	−61	16	18	19	20	2

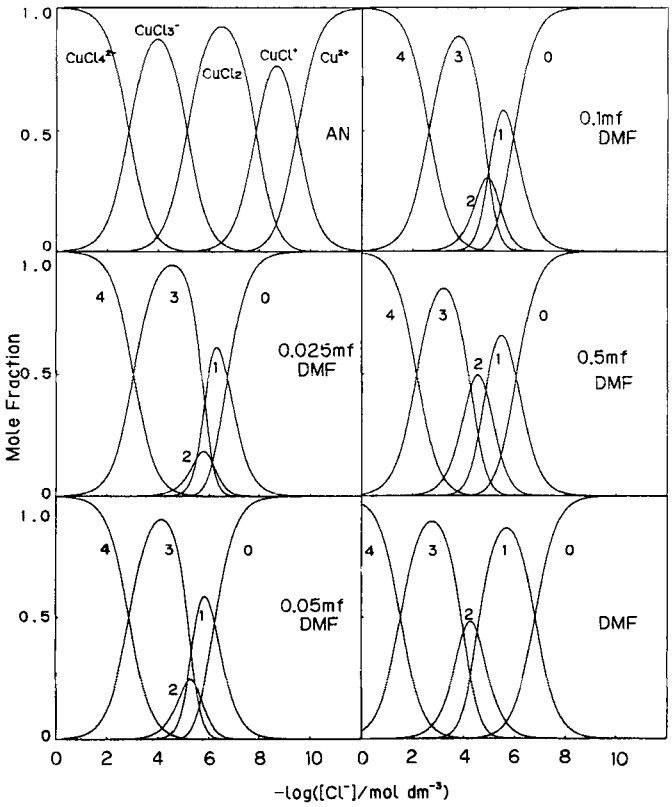

FIGURE 36. Distribution of the copper(II) chloro complexes in various acetonitrile-*N,N*-dimethylformamide mixtures containing 0.2 mol dm^{-3} $(C_2H_5)_4NClO_4$ at 25°C.

$[CuCl(dmf)_3]^+$ takes place in a different manner in each mixture depending on the solvent composition. On the other hand, the ΔH_3° value became less positive with lowering DMF contents in the mixtures and the $(\Delta H_2^\circ + \Delta H_3^\circ)$ value was practically independent of the solvent composition. The result indicates that total number of DMF molecules desolvating at the second and third steps may be kept constant in all the mixtures examined. As will be discussed later, the $[CuCl_3(dmf)]^-$ species is expected to be present in all the AN-DMF mixtures examined. Therefore, two DMF molecules may be liberated at the second and third consecutive steps, but the desolvating scheme depends on the solvent composition in the mixtures. We propose:

$$[CuCl(dmf)_3]^+ + Cl^- = [CuCl_2(dmf)_2] + dmf \quad (48)$$

$$[CuCl_2(dmf)_2]^+ + Cl^- = [CuCl_3(dmf)]^- + dmf \quad (49)$$

in a mixture of a high DMF content, while in a mixture of a relatively low DMF content,

$$[CuCl(dmf)_3]^+ + Cl^- = [CuCl_2(dmf)] + 2dmf \quad (50)$$

$$[CuCl_2(dmf)] + Cl^- = [CuCl_3(dmf)] \quad (51)$$

Accordingly, the dichlorocopper(II) complex may be solvated with one or two DMF molecules in the first coordination sphere of the metal ion, and thus, an equilibrium as represented by reaction (52) is established between the two solvate species of the dichloro complex,

$$[CuCl_2(dmf)] + dmf = [CuCl_2(dmf)_2] \quad (52)$$

and the equilibrium shifts depending on the DMF content in the AN-DMF mixtures.

The ΔH_4° value was negative in any AN-DMF mixture examined and became slightly more negative with lowering DMF contents in the mixtures, but it remained much less negative than that in pure AN. The ΔS_4° value was positive and was practically independent of the solvent composition in all the mixtures examined, while the ΔS_4° value in AN was largely negative by *ca.* -60 J K^{-1} mol^{-1}. The result suggests that one DMF molecule still coordinates to copper(II) ion within the trichlorocuprate(II) complex and $[CuCl_3(dmf)]^-$ is formed in all the mixtures.

8.5 *Enthalpies of Solution of Anhydrous $CuCl_2$ Crystal*

Copper(II) chloride dissolved in an AN-DMF mixture is mostly associated to form various chloro complexes of Cu(II), the distribution of which can be calculated by knowing the formation constants of the complexes and the total concentration of $CuCl_2$ dissolved in a solution. Therefore, by using the procedure described in Section 7.3, the enthalpies $\Delta H_5^\circ(Cu^{2+}, 2Cl^-)$ and $\Delta H_5^\circ(CuCl_2)$ of solution have been determined in various AN-DMF mixtures, the former being the sum of enthalpies of solution of relevant ions and the latter the enthalpy of solution of the neutral complex. The results are summarized in Table XXX and also depicted in Figure 37.

Although the enthalpies of transfer of both copper(II) and chloride ions from AN to any AN-DMF mixture have not been known, the change in $\Delta H^\circ(Cu^{2+}, 2Cl^-)$ with varying solvent compositions may mainly reflect the change in enthalpy of solvation of copper(II) ion because the acceptor properties (the solvating property to anions) of AN and DMF are weak and not appreciably different.

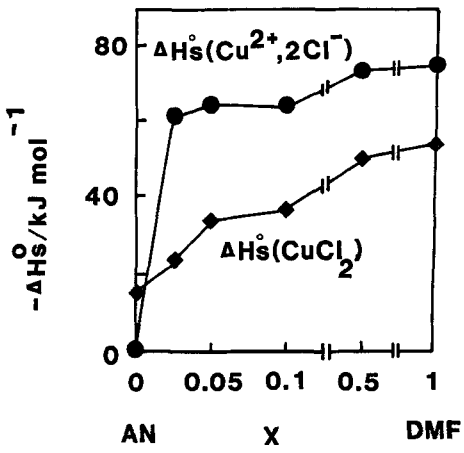

FIGURE 37 Variations of $\Delta H_s^\circ(Cu^{2+}, 2Cl^-)$ and $\Delta H_s^\circ(CuCl_2)$ with mole fraction x of DMF in the AN-DMF mixtures.

As seen in Table XXX, the $\Delta H_s^\circ(Cu^{2+}, 2Cl^-)$ values in all the mixtures examined were largely negative. They are compared with the value in pure DMF, but are very different from the value in pure AN. This also indicates that copper(II) ion is preferentially solvated with DMF molecules in a wide range of the solvent composition of the AN-DMF mixtures.

The $\Delta H_s^\circ(CuCl_2)$ value in the 0.025 mole fraction DMF mixture was close to the value in pure AN, but the value in the 0.5 mole fraction DMF mixture was close to that in pure DMF as seen in Table XXX. The values in the 0.05 and 0.1 mole fraction DMF mixtures were laid just in the middle of the values in AN and in DMF. The variation of $\Delta H_s^\circ(CuCl_2)$ with solvent composition indicates that solvation of $[CuCl_2]$ with DMF molecules markedly weakens in an AN-DMF mixture of a low DMF content. Therefore, we concluded that the $[CuCl_2]$ complex was not markedly preferentially solvated with DMF molecules in contrast to copper(II) ion in the AN-DMF mixtures. This is not unexpected, because electron donation from the ligands to the central metal ion within $[CuCl_2]$ may reduce the acceptor ability of copper(II) ion to lead to weakened interaction of the metal ion with DMF molecules. The conclusion obtained here is also consistent with the result obtained in a preceding section that the ΔH_2° value of stepwise formation of $[CuCl_2]$ became more positive with lowering DMF contents in the AN-DMF mixtures.

TABLE XXX

Enthalpies of solution, ΔH_s°/kJ mol^{-1}, of anhydrous copper(II) chloride salt in various acetonitrile-*N,N*-dimethylformamide mixtures at 25°C

DMF content	$\Delta H_{s,obsd}^\circ$	$\Delta H_s^\circ(CuCl_2)$	$\Delta H_s^\circ(Cu^{2+}, 2Cl^-)$
mole fraction			
0.0	−15.9	−15.9	0.6
0.025	−38.0	−24.3	−61.3
0.05	−41.9	−34.2	−64.1
0.1	−42.5	−37.0	−63.7
0.5	−51.5	−50.5	−72.7
1.0	−55.3	−54.7	−74.6

9. CONCLUDING REMARKS

Solution chemistry, as well as chemistry in any other fields, may include the following four major knowldges concerning (1) structure of species in a given system, (2) reactivities of the species, (3) their physicochemical properties, and (4) ways for producing new materials on the basis of the above three knowledges. In solution chemistry, in the historical point of view, part (3) was the most investigated one, and part (2) has recently been rapidly developed to be another major field of solution chemistry. Part (1), which may be recognized to be the most fundamental field in any chemistry, has not been well established until recent years. Although a remarkable accumulation of structural data has been achieved for species in solution by efforts of many solution chemists, it is still extremely less than a huge amount of data in the gas and solid states. Part (4) may be the most widely extended one in preparative chemistry by selecting good solvents for chemical syntheses, although reasons why a specific solvent is suitable to a specified reaction are even not well known.

In this article we have attempted to combine structural information of complexes in solution with the thermodynamic quantities for reactions of these species. Solvent effects on the reactions have also been discussed, although structural information of these solvents used in the present study has not been given so much and only parameterized information of solvent properties, as well as bulk properties, are available.

In this point of view, the role of solvent molecules in chemical reactions in solution is not well elucidated: we do not know bond energies between ions or molecules and solvent molecules in solution systems, we do not know how many solvent molecules interact with the central species, we do not know what orientation the solvent molecules take in the solvation shells, and we do not know how long the solvent molecules can stay in the solvation shells, except for very limited cases.

Information about the intermediate stage of chemical reactions may be most lacked. A few attempts have been made to determine some thermodynamic quantities of intermediates such as enthalpies, entropies and volumes of activation of reacting species, but no reliable structural data for the intermediates have been known. Further investigations for intermediates by using new methods must be expected.

The lack of leading theories in solution chemistry is also a serious problem. After Debye-Hükel's theory we have not obtained new theories for interpreting ion-ion and ion-solvent interactions. Statistical thermodynamics did not sufficiently work in complicated systems in which most of the solution chemists are interested. Molecular orbital calculations are not applicable in solution systems, in which many molecules are concerned, without extreme simplifications of the systems. Molecular dynamics simulation may be useful to some extent to elucidate solute-solute and solute-solvent interactions in some simple cases, although it is not applicable yet to complexation reactions.

These problems still remain unsolved and much efforts must be needed in order to clarify situations of solution. Nevertheless, many interesting and attractive subjects in solution chemistry have already spread in front of our view. Some of them may be pointed out as follow: (1) solution chemistry under high pressure and temperature, which relates to, for instance, geology of the earth, (2) investigations of liquids and solutions of small clusters, in which we may not be able to consider them as bulk systems; these subjects may be better treated with established theories and may be related to microscopically heterogeneous but macroscopically homogeneous systems such as mixed solvents, (3) investigations for quickly frozen solutions, in which the instantaneous structure of liquids and solutions may be quenched to some extent, (4) investigations of biologically related substances without isolating them from living materials, (5) direct observations of liquid molecules in solution, *etc.* These problems

will hopefully be investigated in more detail in the near future, and some of them have already been touched by some people.

ACKNOWLEDGEMENT

The authors are grateful to Prof. I. Okada, Drs. T. Yamaguchi, K. Ozutsumi, T. Fujita, A.K. Basak and B.G. Jeliazkova, Mr's. Y. Oka, M. Zama, H. Wada, K. Yamamoto and H. Suzuki, and Miss T. Pithprecha for their helpful discussion and contributions to this article. The work has been financially supported by the Grant-in-Aid for Scientific Research No. 57470054 and for Specific Project Research No. 60540389 from the Ministry of Education, Science and Culture of Japan. A part of the computer calculations carried out in the present work has been performed at the Institute for Molecular Science in Okazaki.

REFERENCES

1. R. Yamdagni and P. Kebarle, *Can. J. Chem.*, **52,** 861 (1974); J.B. Cumming and P. Kebarle, *Can. J. Chem.*, **56,** 1 (1978); E.M. Arnett, L.E. Small, R.T. McIver, Jr. and J.S. Miller, *J. Am. Chem. Soc.*, **96,** 5638 (1974).
2. V. Gutmann, *"The Donor-Acceptor Approach to Molecular Interactions"*, Prenum, New York (1978).
3. S. Ahrland, *Pure & Appl. Chem.*, **54,** 1451 (1982).
4. D. Eisenberg and W. Kauzmann, *"The Structure and Properties of Water"*, Oxford, London (1969); W.A.P. Luck Ed., *"Structure of Water and Aqueous Solutions"*, Verlag Chemie and Physik Verlag, Weinheim/ Bergstr., 1974.
5. B.G. Cox, R. Natarajan and W.E. Waghorne, *J. Chem. Soc. Faraday Trans. I,* **1979,** 86.
6. B.G. Cox and A.J. Parker, *J. Am. Chem. Soc.*, **95,** 402 (1973); I.J. Kim, *J. Phys. Chem.*, **82,** 191 (1978).
7. Y. Marcus, *Rev. Anal. Chem.*, **5,** 53 (1980), *Pure & Appl. Chem.*, **55,** 977 (1983) and **57,** 1103 (1985); B.G. Cox, G.R. Hedwig, A.J. Parker and D.M. Watts, *Aust. J. Chem.*, **27,** 477 (1974).
8. H. Ohtaki, *Rev. Inorg. Chem.*, **4,** 103 (1982).
9. S. Sabatini, A. Vacca and P. Gans, *Talanta,* **21,** 53 (1974).
10. R. Karlsson and K. Kullerg, *Chem. Ser.*, **9,** 54 (1976).
11. T. Kawai, S. Ishiguro and H. Ohtaki, *Bull. Chem. Soc. Jpn.*, **53,** 2221 (1980).
12. S. Ishiguro and H. Ohtaki, *Bull. Chem. Soc. Jpn.*, **52,** 3198 (1979).
13. S. Ishiguro and H. Ohtaki, *Bull. Chem. Soc. Jpn.*, **57,** 2622 (1984).
14. S. Ishiguro, K. Yamamoto and H. Ohtaki, *Anal. Sci.*, **1,** 263 (1985).
15. L.S. Frankel, T.R. Stengle and C.H. Langford, *Can. J. Chem.*, **46,** 3183 (1968).
16. T.S. Lee, I.M. Kolthoff and D.L. Leussing, *J. Am. Chem. Soc.*, **70,** 2348 (1948).
17. M.J. Fahsel and C.V. Banks, *J. Am. Chem. Soc.*, **88,** 878 (1966).
18. P. Paoletti, A. Dei and A. Vacca, *J. Chem. Soc. (A),* **1971,** 2656.
19. A.A. Schilt and W.E. Dunbar, *Tetrahedron,* **30,** 401 (1974).
20 R.D. Alexandar, A. William, L. Dudeney and R.J. Irving, *J. Chem. Soc. Faraday Trans. I,* **74,** 1075 (1978).
21. J.V. Rund and P.C. Keller, *J. Chem. Soc. (A),* **1970,** 2827.
22. S. Bandyopadhyay, A.K. Mandel and S. Aditya, *J. Indian Chem. Soc.*, LVIII, 467 (1981).
23. P.R. Mitchell, *J. Chem. Soc. Dalton,* **1980,** 1079.
24. S.L. Fornili and G. Sgroi, *J. Chem. Soc. Faraday Trans. I,* **79,** 1085 (1983).
25. V.I. Korsunskii and Y.I. Naberukin, *Zh. Struct. Khim.*, **18,** 587 (1977).
26. J. Burgess and R. Sherry, *J. Chem. Soc. Perkin Trans. II,* **1981,** 366.
27. P.R. Michell, *J. Am. Chem. Soc.*, **102,** 1180 (1980).
28. L.G. Sillén and A.E. Martell, *"Stability Constants"*, Supplement No. **1,** Spec. Publ. No. **25,** Chemical Society, London, 1971.
29. A.E. Martell and R.M. Smith, *"Critical Stability Consants"*, Vol. **1**, Prenum, New York, 1974.
30. S. Ishiguro, Y. Oka and H. Ohtaki, *Bull. Chem. Soc. Jpn.*, **56,** 2426 (1983).
31. S. Ishiguro, T. Pithprecha and H. Ohtaki, *Bull. Chem. Soc. Jpn.*, **59,** 1487 (1986).
32. S. Ishiguro, Y. Oka and H. Ohtaki, *Bull. Chem. Soc. Jpn.*, **57,** 391 (1984).
33. S. Ishiguro, H. Fujita and H. Ohtaki, unpublished data.
34. T. Fujita and H. Ohtaki, *Bull. Chem. Soc. Jpn.*, **55,** 455 (1982).
35. K. Ozutsumi and H. Ohtaki, *Bull. Chem. Soc. Jpn.*, **56,** 3635 (1983).
36. T. Fujita and H. Ohtaki, *Bull. Chem. Soc. Jpn.*, **56,** 3274 (1983).
37. K. Ozutsumi and H. Ohtaki, *Bull. Chem. Soc. Jpn.*, **57,** 2605 (1984).
38. T. Fujita, T. Yamaguchi and H. Ohtaki, *Bull. Chem. Soc. Jpn.*, **52,** 3539 (1979).
39. K. Ozutsumi and H. Ohtaki, *Bull. Chem. Soc. Jpn.*, **58,** 1651 (1985).
40. K. Ozutsumi, T. Yamaguchi, H. Ohtaki, K. Tohji and Y. Udagawa, *Bull. Chem. Soc. Jpn.*, **58,** 2786 (1985).

41. H.C. Freeman and J.M. Guss, *Acta Crystallogr., Sect. B,* **24,** 1133 (1968).
42. H. Ohtaki, T. Yamaguchi and M. Maeda, *Bull. Chem. Soc. Jpn.,* **49,** 701 (1976).
43. G. Davies, K. Kustin and R.F. Pasternack, *Inorg. Chem,* **8,** 1535 (1969).
44. A.F. Pearlmutter and J. Stuehr, *J. Am. Chem. Soc.,* **90,** 858 (1968).
45. P. Gerding, *Acta Chem. Scand.,* **20,** 2771 (1966).
46. P. Gerding, *Acta Chem. Scand.,* **22,** 1283 (1968).
47. S. Ahrland and L. Kullberg, *Acta Chem. Scand.,* **25,** 3692 (1971).
48. L. Ciavatta and M. Grimaldi, *Inorg. Chim. Acta,* **4,** 312 (1970).
49. Ts. Ruzhitski, V.V. Blokhin and V.E. Mironov, *Russ. J. Phys. Chem.,* **48,** 282 (1974).
50. S. Ahrland and N.-O. Björk, *Acta Chem. Scand. Ser. A,* **30,** 249 (1976).
51. S. Ahrland, I. Persson and R. Portanova, *Acta Chem. Scand. Ser. A,* **35,** 49 (1981).
52. L.H. Jones, *J. Chem. Phys.,* **25,** 1069 (1956).
53. S. Fronaeus and R. Larsson, *Acta Chem. Scand.,* **16,** 1447 (1962).
54. A. Tramer, *J. Chim. Phys.,* **59,** 232 (1962).
55. K.A. Taylor, T.V. Lond II and R.A. Plane, *J. Chem. Phys.,* **47,** 138 (1967).
56. R.E. Hester and K. Krishnan, *J. Chem. Phys.,* **48,** 1825 (1968).
57. D.P. Strommen and R.A. Plane, *J. Chem. Phys.,* **60,** 2643 (1974).
58. A. Antić-Jovanović, M. Jeremić and D.A. Long, *J. Raman Spectrosc.,* **12,** 91 (1982).
59. O.W. Howarth, R.E. Richards and L.M. Venazi, *J. Chem. Soc.,* 1964, 3335.
60. L.N. Mazalov, A.A. Voityuk and G.K. Parygina, *Russ. J. Struct. Chem.,* **23,** 364 (1982).
61. A.L. Beauchamp and D. Goutier, *Can. J. Chem.,* **50,** 977 (1972).
62. M. Cannas, G. Carta, A. Cristini and G. Marongiu, *J. Chem. Soc. Dalton Trans.,* 1976, 300.
63. L.A. Aslanov, V.M. Zonov and K. Kynev, *Sov. Phys. Crystallogr.,* **21,** 693 (1976).
64. H. Scouloudi, *Acta Crystallogr.,* **6,** 61 (1953).
65. I. Persson, Å. Iverfelt and S. Ahrland, *Acta Chem. Scand. Ser. A,* **30,** 270 (1976); K. Brodersen and H.-U. Hummel, *Z. anorg. allg. Chem.,* **491,** 34 (1982), **499,** 15 (1983), **500,** 171 (1983), *Z. Naturforsch.,* **38b,** 911 (1983), **40b,** 347 (1985); K. Brodersen, M. Cygan and H.-U. Hummel, *Z. Naturforsch.,* **39b,** 582 (1984).
66. S. Ishiguro, K. Yamamoto and H. Ohtaki, *Bull. Chem. Soc. Jpn.,* **59,** 1009 (1986).
67. T. Yamaguchi, K. Yamamoto and H. Ohtaki, *Bull. Chem. Soc. Jpn.,* **58,** 3235 (1985).
68. L. Pauling, *"The Nature of Chemical Bond"*, 3rd ed., Cornell University Press, Ithaca, New York (1960).
69. R.D. Shannon, *Acta Crystallogr. Ser. A,* **32,** 751 (1976).
70. S. Ahrland and N.O. Björk, *Acta Chem. Scand. Ser. A,* **30,** 257 (1976).
71. S. Ahrland, N.O. Björk and R. Portanova, *Acta Chem. Scand. Ser. A,* **30,** 270 (1976).
72. B.G. Cox, R. Natarajan and W.E. Waghorne, *J. Chem. Soc. Faraday Trans. I,* **75,** 1780 (1979); N. Bhatnager and A.O. Cambell, *Can. J. Chem.,* **52,** 203 (1974).
73. M.J. Loche and R.J. Sullivan, *J. Am. Chem. Soc.,* **105,** 4226 (1983).
74. J.R. Goates and R.J. Sullivan, *J. Phys. Chem.,* **62,** 188 (1958).
75. M.A. Khan and M.J. Swing-Weill, *Inorg. Chem.,* **15,** 2202 (1976).
76. M. Elleb, J. Meullemeestre, M.J. Swing-Weill and F. Vierling, *Inorg. Chem.,* **19,** 2699 (1980).
77. M. Elleb, J. Meullemeestre, M.J. Swing-Weill and F. Vierling, *Inorg. Chem.,* **21,** 1477 (1982).
78. S.E. Manahan and R.T. Iwamoto, *Inorg. Chem.,* **4,** 1409 (1965).
79. S. Ahrland, *Pure & Appl. Chem.,* **55,** 977 (1983).
80. S. Ishiguro, B.G. Jeliazkova and H. Ohtaki, *Bull. Chem. Soc. Jpn.,* **58,** 1143 (1985).
81. S. Ishiguro, B.G. Jeliazkova and H. Ohtaki, *Bull. Chem. Soc. Jpn.,* **58,** 1749 (1985).
82. B.G. Cox, *Ann. Rev. Chem. Soc.,* **70,** 249 (1973).
83. S. Ahrland and S. Ishiguro, unpublished data.
84. J.F. Coetzee and W.K. Istine, *Anal. Chem.,* **52,** 53 (1980).
85. J. Fergusson, *J. Chem. Phys.,* **40,** 3406 (1964).